LHC Physics Results and Prospects

Opportunities at Future High Energy Colliders
IFT, Madrid - June 11 - July 05 2019

Marco Sessa
University of Science and Technology of China

Outline

- Higgs boson searches and properties with up to 140 fb^{-1} of data
  - Overview of each single decay channel
  - Combination
  - Properties: mass and width measurements
- Di-Higgs searches
- Prospects in view of High Luminosity LHC
- Comparison with CMS results

All ATLAS and CMS public results are available here:
https://twiki.cern.ch/twiki/bin/view/AtlasPublic
http://cms.web.cern.ch/news/cms-physics-results

Main motivations for the Higgs searches

- The Higgs boson plays an important role in the SM: it provides mass to the elementary particles, through the electroweak spontaneous symmetry breaking (EWSB)

- It is a fantastic new tool to test the Standard Model of particle physics

- Several studies investigating the Higgs boson are possible:
  - Cross-section measurements
  - Couplings with SM particles
  - Improving of the precision on the Higgs mass
  - Measuring the Higgs width
  - Di-Higgs production
  - BSM Higgs bosons?

LHC and ATLAS operations

- LHC accelerator performance during Run-2 was outstanding!
  - LHC delivered ~156 fb^{-1} of proton-proton collisions
  - Record of instantaneous luminosity: 2.1*10^{34} $\text{cm}^{-2}\text{s}^{-1}$

- Very good ATLAS data-taking efficiency
  - ~147 fb^{-1} recorded and ~139 fb^{-1} good for physics (95%)
  - Luminosity uncertainty for the full Run-2 dataset: 1.7%

- Maximum average number of events per Bunch Crossing

$<\mu>$ = 33.7 in Run 2 @ 13 TeV

$<\mu>$ = 20.7 in Run 1 @ 8 TeV

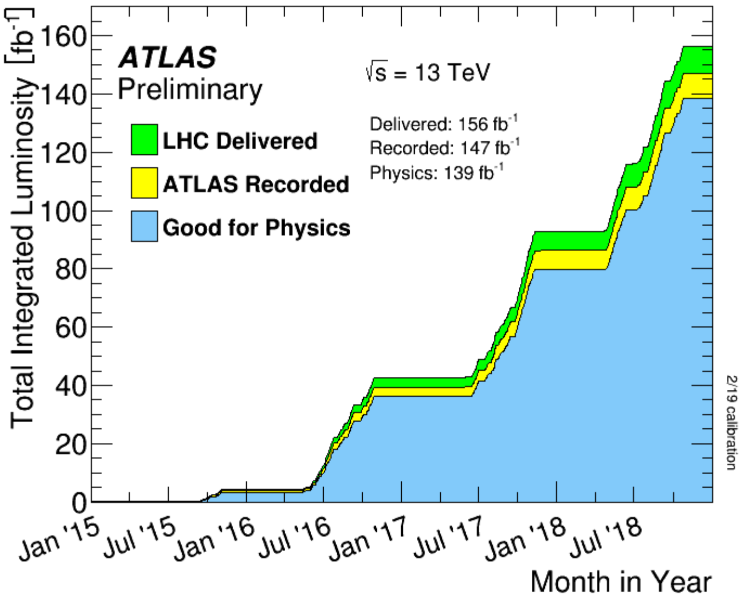

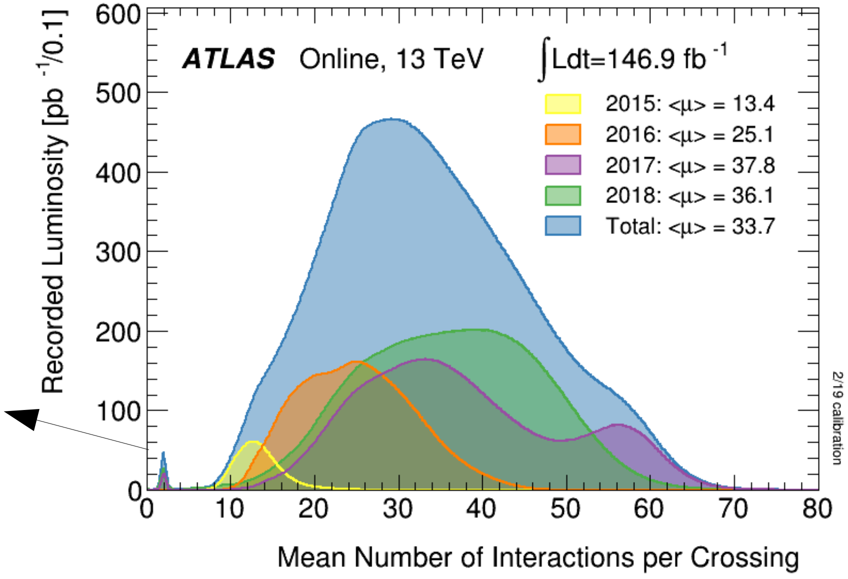

Low-μ data-taking peak provided special samples for precision W physics!

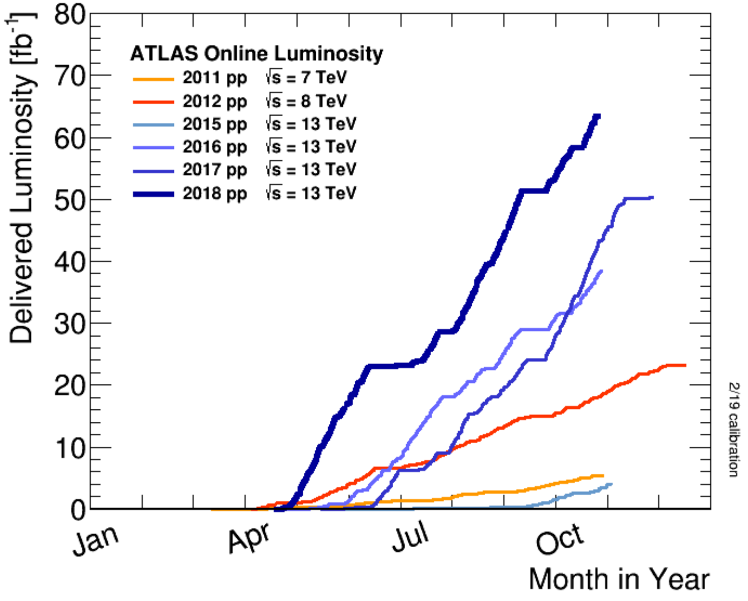

ATLAS detector overview

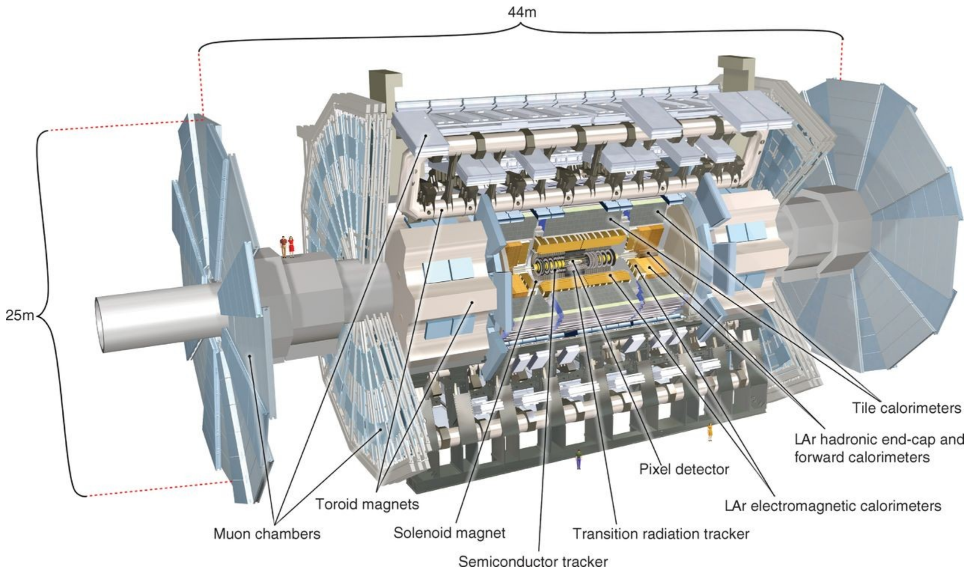

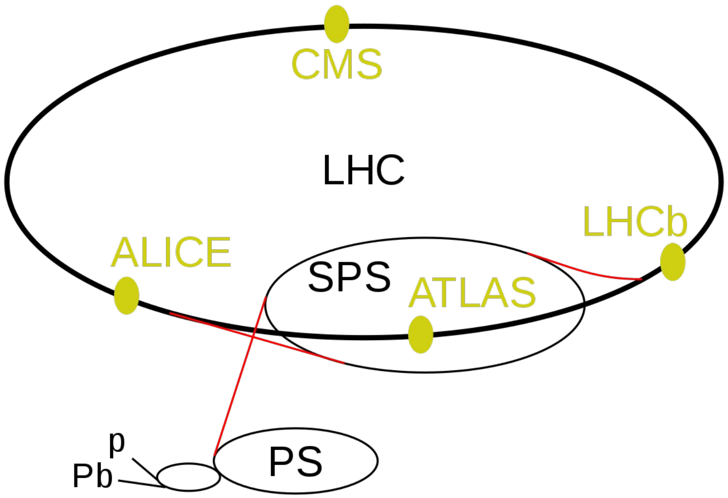

- General purpose detector with 4π coverage

- Sub-detectors optimized to reconstruct final states as produced by SM processes: jets, charged leptons, neutrinos. Four major components :
  - Inner Detector, Calorimeter, Muon Spectrometer and magnet system

- Integrated with the detector components → Trigger and Data Acquisition System, a specialized multi-level computing system, which selects physics events with distinguishing characteristics
  - Collision rate: 40 MHz
  - Accepted event rate: ~1 kHz

Detector performance

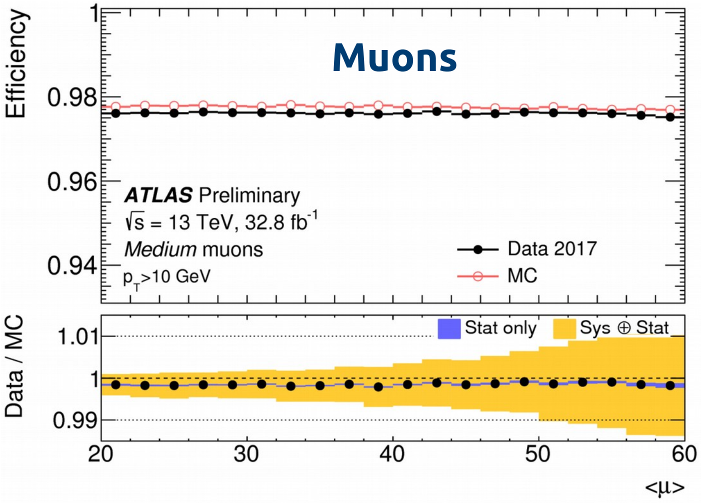

Muons

Photons

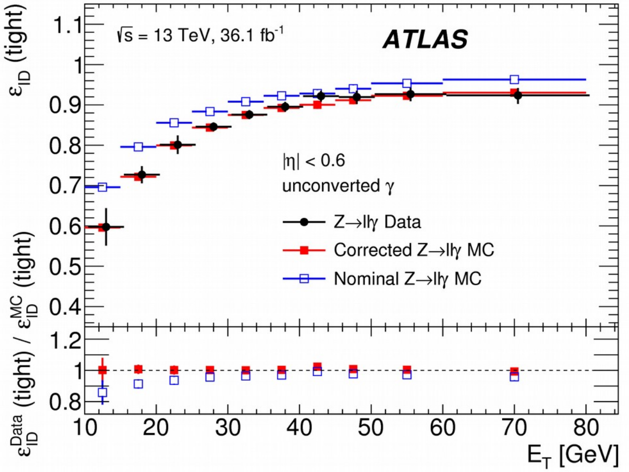

b-tagging scale factor

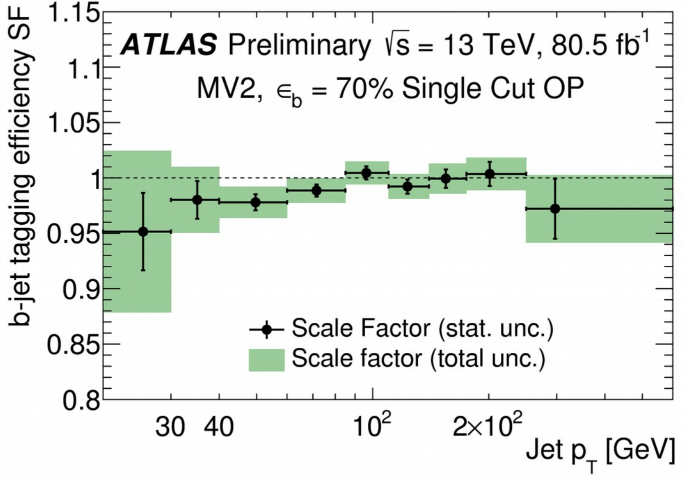

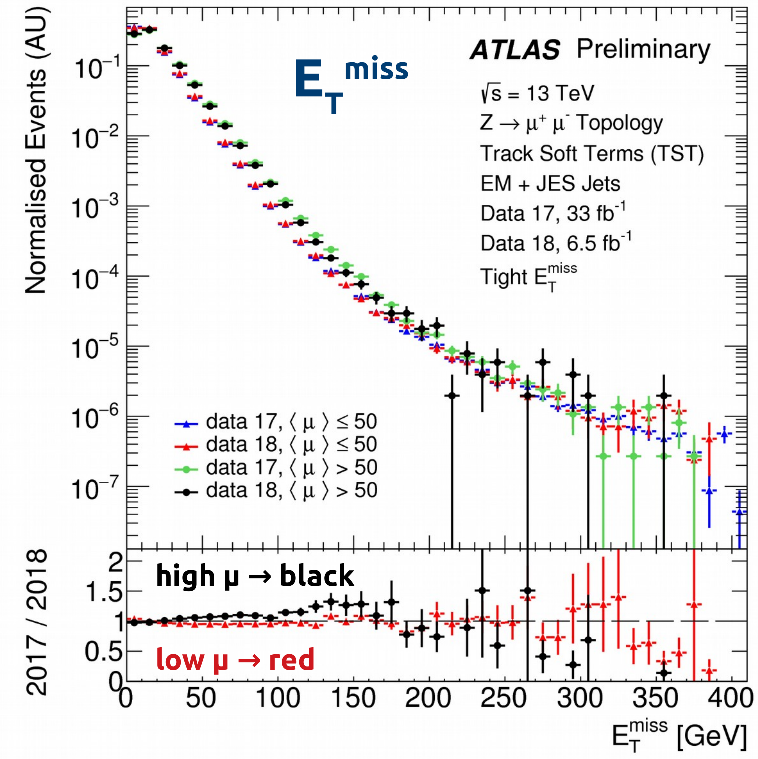

E_T^{miss}

high μ → black

low μ → red

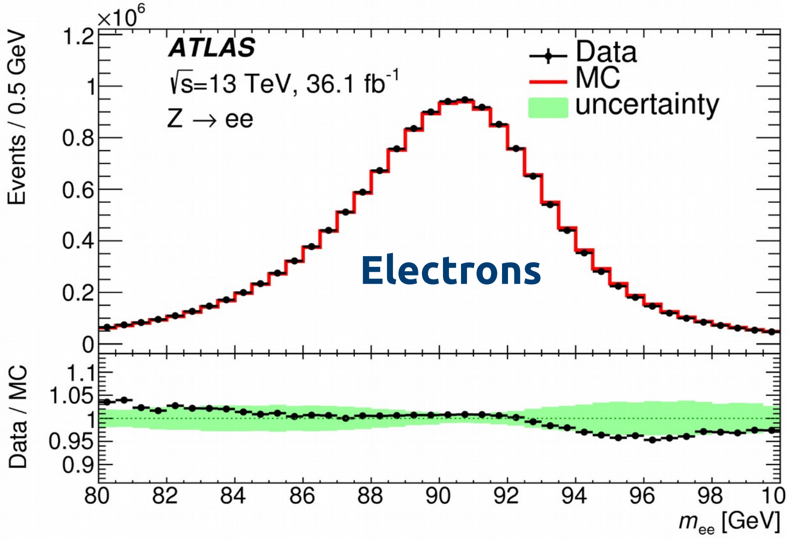

Electrons

Higgs boson production at LHC

Main

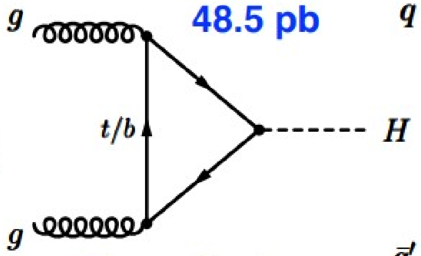

48.5 pb

Gluon-fusion ggF (~87%)

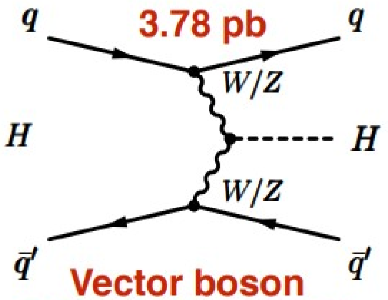

3.78 pb

Vector boson fusion (VBF) (~7%)

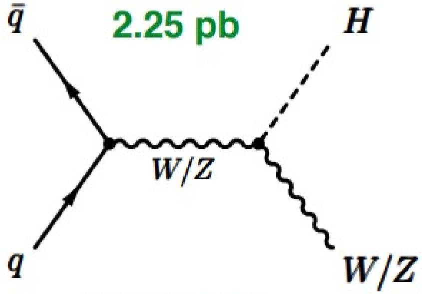

2.25 pb

VH (~4%)

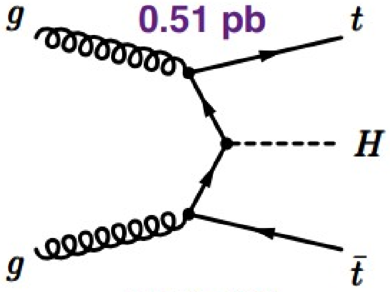

0.51 pb

ttH (~1%)

Rare

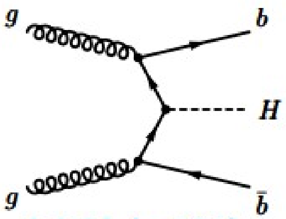

bbH (~1%)
0.49 pb

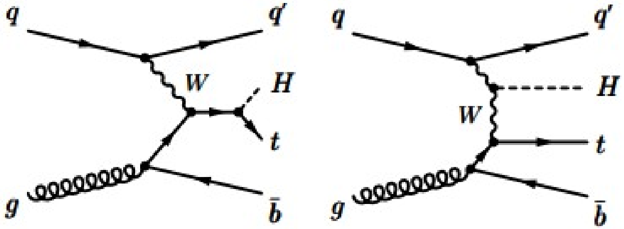

tH (~0.1%) 0.09 pb

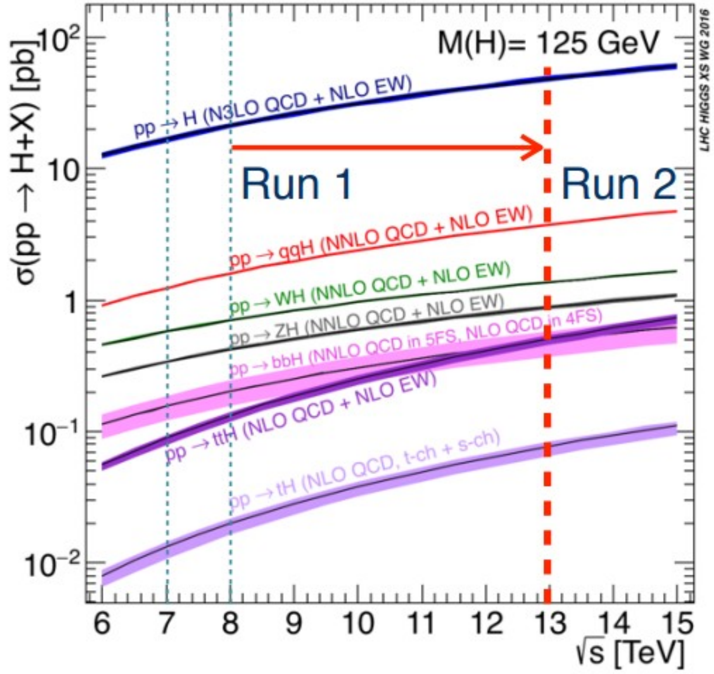

- Distinct topology from each production mode
- Rare production modes difficult to probe, but important for beyond the SM (BSM) scenarios
- Improved accuracy from theory calculations: inclusive σ(ggF) now calculated at N3LO in QCD and NLO in EW, with 5% uncertainty (still dominated by QCD scale and PDF+ α_S)

Higgs boson decays

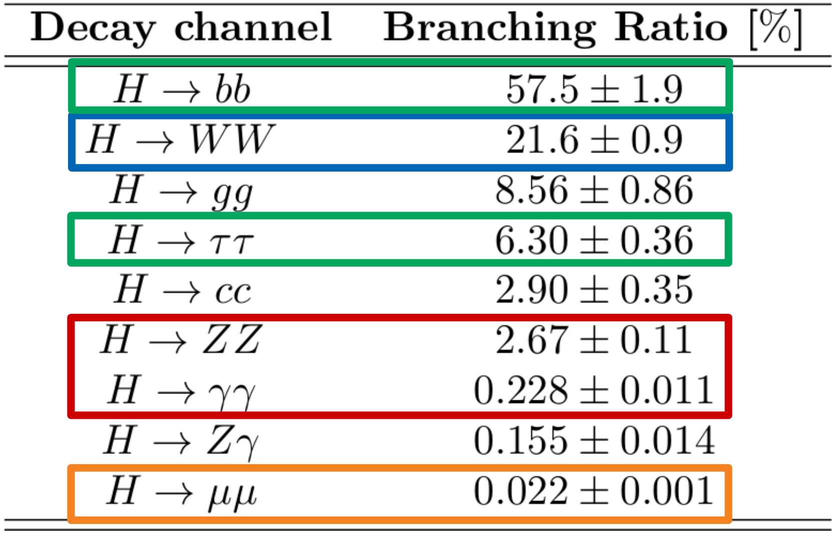

Decay channel	Branching Ratio [%]
$H \to bb$	57.5 ± 1.9
$H \to WW$	21.6 ± 0.9
$H \to gg$	8.56 ± 0.86
$H \to \tau\tau$	6.30 ± 0.36
$H \to cc$	2.90 ± 0.35
$H \to ZZ$	2.67 ± 0.11
$H \to \gamma\gamma$	0.228 ± 0.011
$H \to Z\gamma$	0.155 ± 0.014
$H \to \mu\mu$	0.022 ± 0.001

$H \to ZZ^* \to 4l$ and $H \to \gamma\gamma$: high resolution channels and precise differential measurements

$H \to WW^*$: high BR, but low mass resolution

$H \to \mu\mu$: very small BR, but access to couplings to 2nd generation fermions

$H \to \tau\tau$, $H \to b\bar{b}$: high BR, but low S/B, important to directly probe Higgs boson coupling to fermions

$H \to ZZ^* \to 4\ell$

ATLAS-CONF-2018-018

- Low branching fraction: BR(H→ ZZ*) ~2.7%
  further reduced by $[BR(Z \to ee,\mu\mu)]^2 = [6\%]^2$ ➡ $BR(H \to ZZ^* \to 4l) \sim 0.01\%$
- Non-resonant ZZ* background is the only relevant background in the analysis (irreducible background, estimated from MC simulations)
- Reducible backgrounds (Z+jets and top mainly) strongly suppressed with the event selection
- 12% of uncertainty on combined fiducial cross-section
  - Uncertainty still statistical dominated

$$\sigma_{\text{fid}} = 4.04 \pm 0.41(\text{stat.}) \pm 0.22(\text{syst.})\ \text{fb}$$
$$\sigma_{\text{fid,SM}} = 3.35 \pm 0.15\ \text{fb}$$

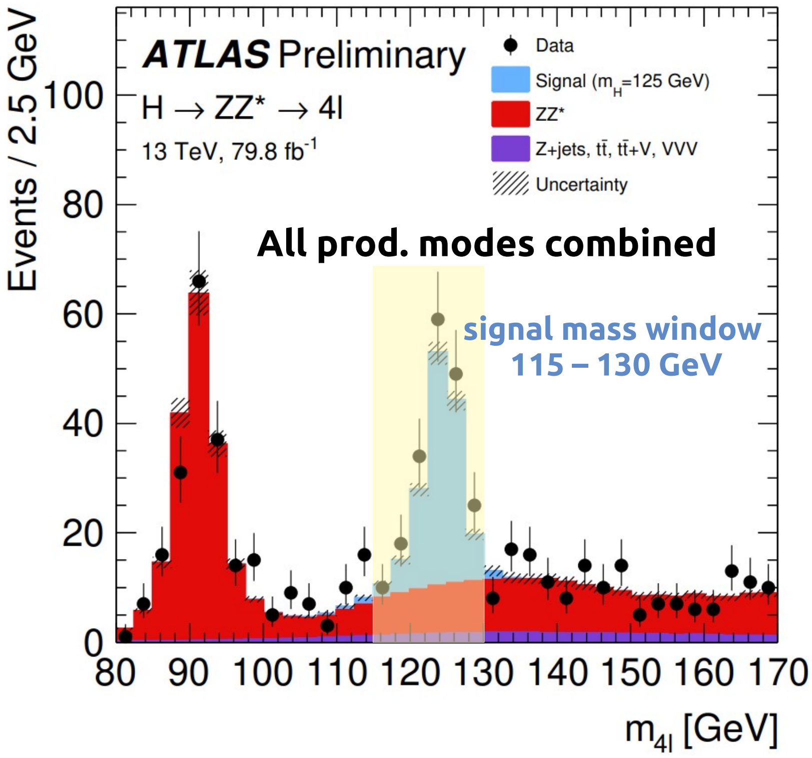

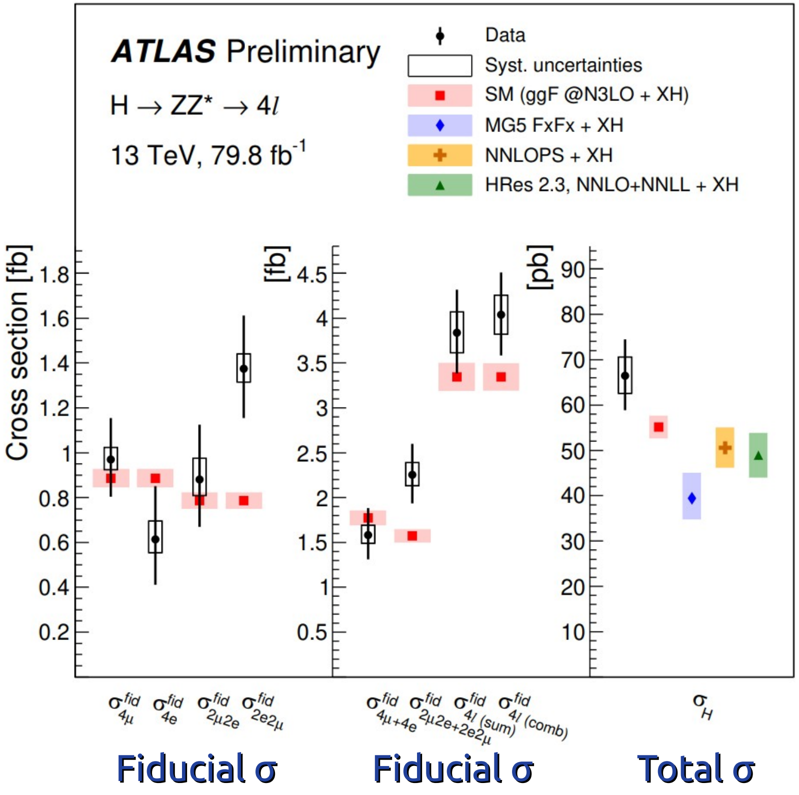

H→γγ

ATLAS-CONF-2018-028

BR(H->γγ) ~ 0.23%

- Clean experimental signature and good invariant mass resolution
- Analysis performed exploiting an event categorization to target the main Higgs production modes
- Signal yield extracted from a simultaneous signal+background fit of the $m_{\gamma\gamma}$ distribution
- Background function chosen as the one that minimizes the fitted signal yield in signal+background fits in a background control sample. Double-sided Crystal Ball function for the signal modeling

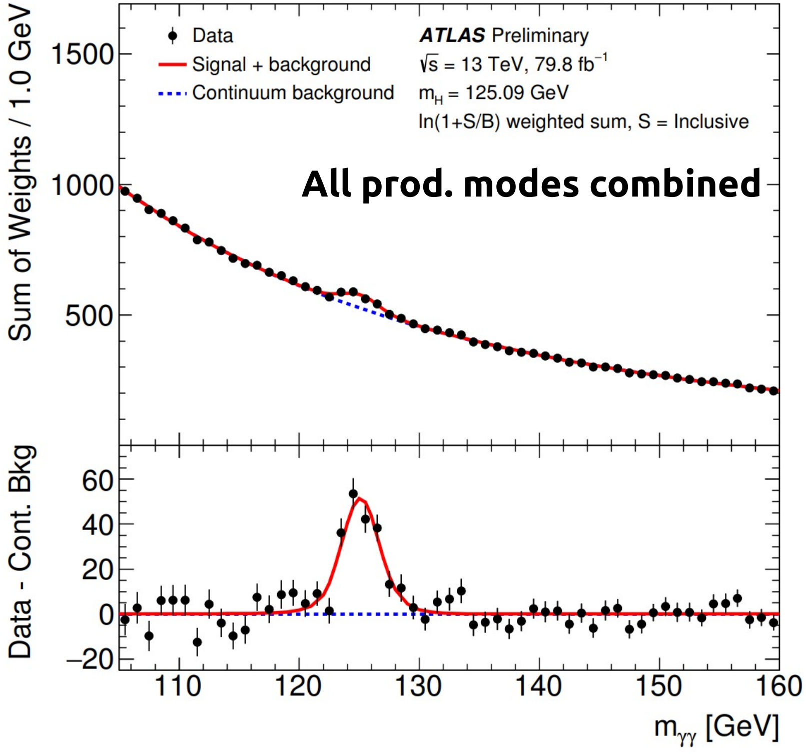

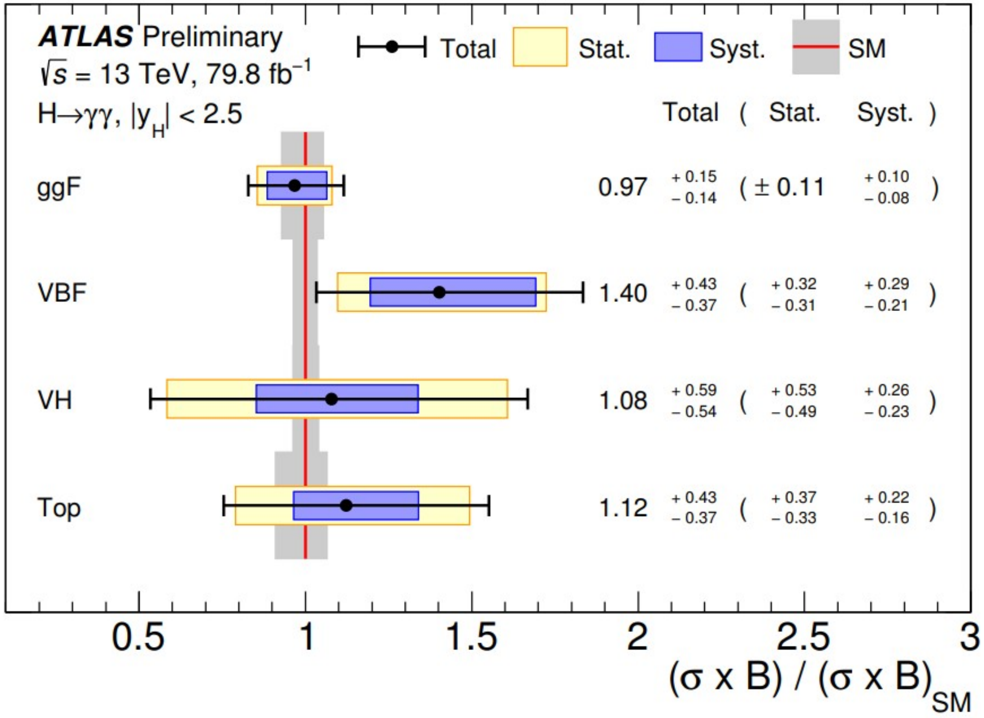

H→WW*

ggF+VBF Phys. Lett. B 789 (2019) 508
WH+ZH arXiv:1903.10052v1

- 2^{nd} largest Higgs branching fraction → BR(H→WW*) ~ 22%
- Access for measurement of the Higgs boson couplings with vectors bosons (W and Z) and fermions (Top mainly)
- Two analyses targeting different Higgs production modes: ggF+VBF and WH+ZH, both with ~$36fb^{-1}$ at 13 TeV

ggF + VBF

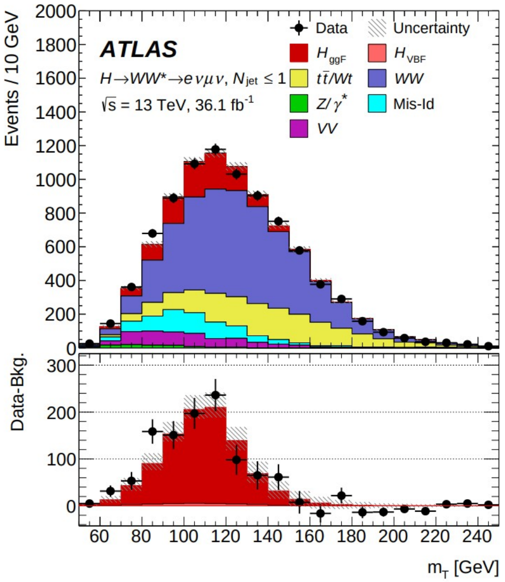

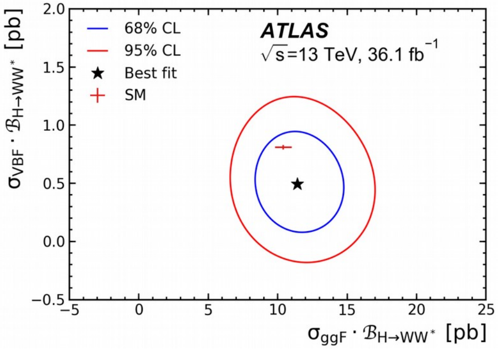

Events split in 3 major Signal Regions on Njets

- **Njet = 0 and Njet = 1 (ggF dominated)**
  - m_T used as discriminant
- **Njet ≥ 2 (VBF dominated)**
  - BDT used as discriminant

$$\mu_{\rm ggF} = 1.10^{+0.10}_{-0.09}({\rm stat.})^{+0.13}_{-0.11}({\rm theo\ syst.})^{+0.14}_{-0.13}({\rm exp\ syst.}) = 1.10^{+0.21}_{-0.20}$$

$$\mu_{\rm VBF} = 0.62^{+0.29}_{-0.27}({\rm stat.})^{+0.12}_{-0.13}({\rm theo\ syst.}) \pm 0.15({\rm exp\ syst.}) = 0.62^{+0.36}_{-0.35}$$

- ggF XSec uncertainty dominated by systematics (10% from theoretical predictions on ggF, WW and Top)
- VBF analysis still suffers of low statistics
- Observed (expected) ggF and VBF significances: 6.0 (5.3) and 1.8 (2.6) standard deviations, respectively

WH+ZH

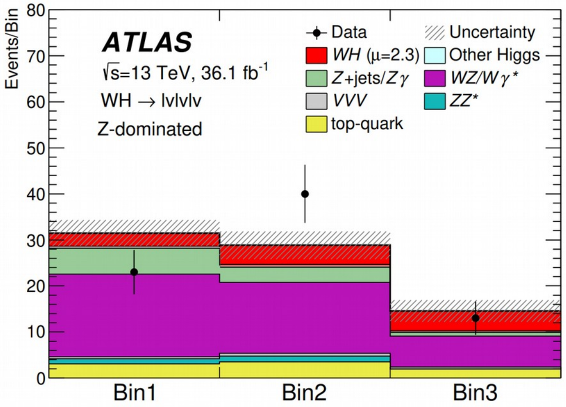

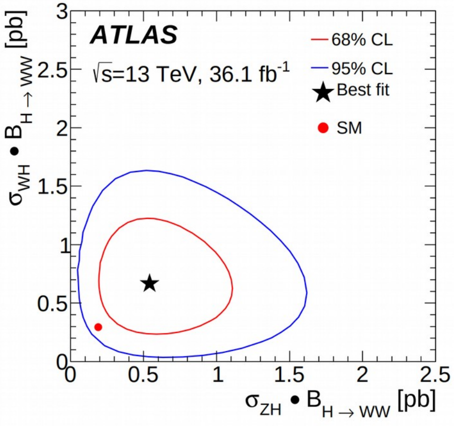

$$\mu_{WH} = 2.3^{+1.1}_{-0.9}({\rm stat.})^{+0.41}_{-0.33}({\rm theo\ syst.})^{+0.49}_{-0.36}({\rm exp\ syst.}) = 2.3^{+1.2}_{-1.0}$$

$$\mu_{ZH} = 2.9^{+1.7}_{-1.3}({\rm stat.})^{+0.66}_{-0.27}({\rm theo\ syst.})^{+0.54}_{-0.28}({\rm exp\ syst.}) = 2.9^{+1.9}_{-1.3}$$

- Events split according the lepton multiplicity (3 and 4) and charge/flavour composition → 4 Signal Regions
- ZH analysis: cut-based. For WH, a BDT discriminant is also used
- The combination leads to an observed (expected) significance for the combined VH production mode of 4.1 (1.9) standard deviations
- Uncertainty still statistically dominated

H→bb

Phys. Lett. B 786 (2018) 59

- Dominant decay of SM Higgs boson: BR(H → bb) ~ 58%
- Analysis targeting the VH production mode
- Boosted decision trees trained in eight signal regions and outputs used as the final discriminating variables in the analysis
- **Double observation:** Higgs decay to bottom quarks and VH production mode
- For H→ bb : Run 2 results combined with the Run 1 results, including also ggF, VBF and ttH categories
- For VH: results combined with γγ and ZZ decay results at 13 TeV

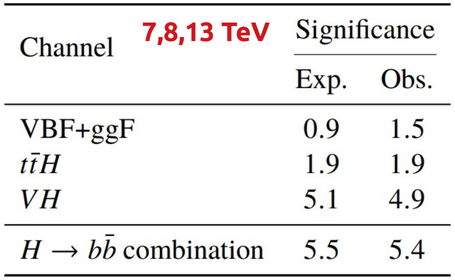

Channel	7,8,13 TeV Significance	
	Exp.	Obs.
VBF+ggF	0.9	1.5
$t\bar{t}H$	1.9	1.9
VH	5.1	4.9
$H \to b\bar{b}$ combination	5.5	5.4

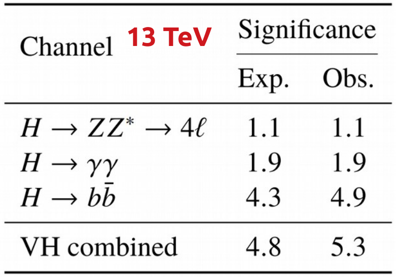

Channel	13 TeV Significance	
	Exp.	Obs.
$H \to ZZ^* \to 4\ell$	1.1	1.1
$H \to \gamma\gamma$	1.9	1.9
$H \to b\bar{b}$	4.3	4.9
VH combined	4.8	5.3

VH (H→bb) with 13 TeV data

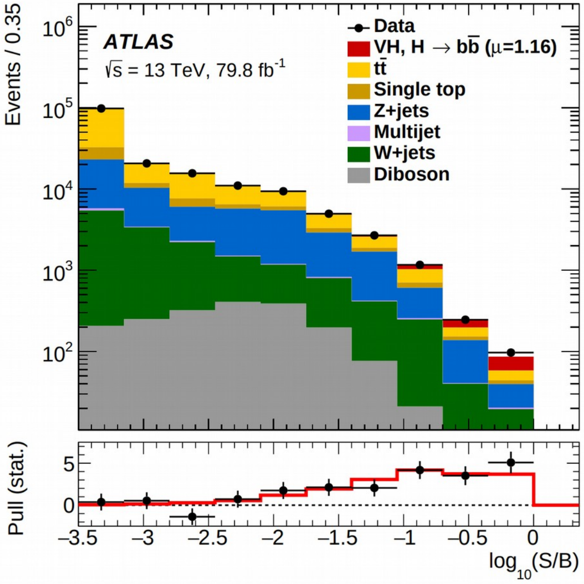

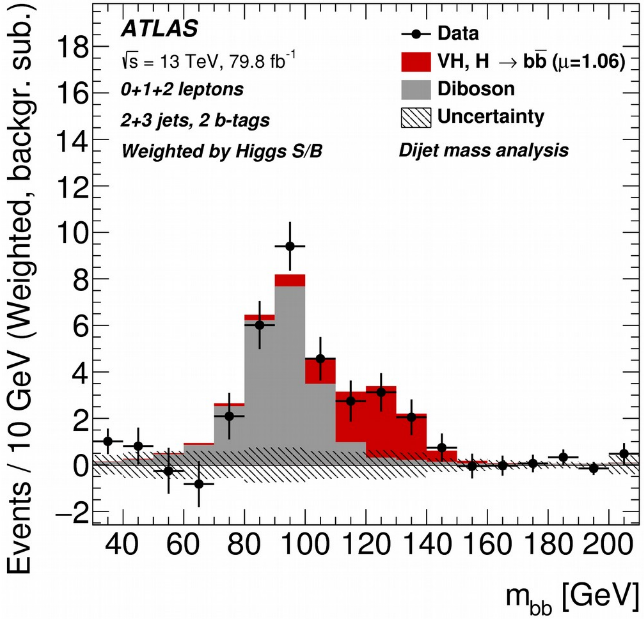

Run 1 + Run 2 H→ bb combination

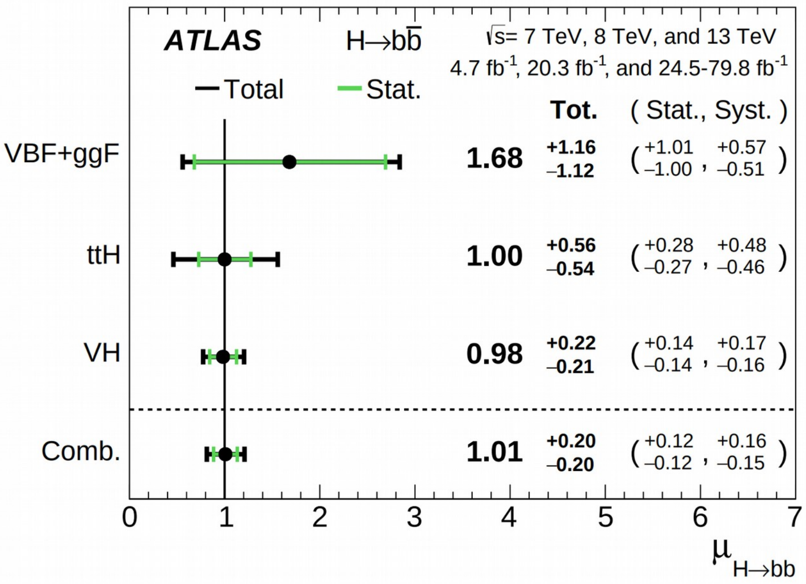

H→ττ

Phys. Rev. D 99 (2019) 072001

- Higgs boson decay to pair of τ-leptons is most promising channel to explore Yukawa-couplings to fermions
- Smaller BR than H → bb, but better experimental accessibility
- Events are categorized into exclusive signal regions
- SM Z → ττ is the major background in all the regions
- Measured cross-section times BR in agreement with SM

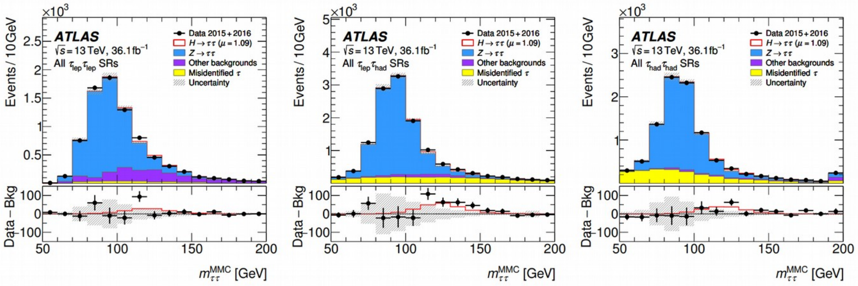

$$\sigma_{H\to\tau\tau} \text{ is } 3.77\,^{+0.60}_{-0.59}\,(\text{stat.})\,^{+0.87}_{-0.74}\,(\text{syst.})\,\text{pb} \qquad \sigma^{\text{SM}}_{H\to\tau\tau} \;=\; 3.46 \pm 0.13\,\text{pb}$$

- Observed (expected) significance at 13 TeV 4.4 σ (4.1 σ)
- Combining with 7 and 8 TeV results → 6.4 σ (5.4 σ)
- Main systematics from theory uncertainty on signal, statistics in Control Regions for bkg estimation, jet Energy Sale/Resolution, E_t^{miss} resolution

Source of uncertainty	Impact $\Delta\sigma/\sigma_{H\to\tau\tau}$ [%] Observed	Expected
Theoretical uncert. in signal	+13.4 / −8.7	+12.0 / −7.8
Background statistics	+10.8 / −9.9	+10.1 / −9.7
Jets and E_T^{miss}	+11.2 / −9.1	+10.4 / −8.4
Background normalization	+6.3 / −4.4	+6.3 / −4.4
Misidentified τ	+4.5 / −4.2	+3.4 / −3.2
Theoretical uncert. in background	+4.6 / −3.6	+5.0 / −4.0
Hadronic τ decays	+4.4 / −2.9	+5.5 / −4.0
Flavor tagging	+3.4 / −3.4	+3.0 / −2.3
Luminosity	+3.3 / −2.4	+3.1 / −2.2
Electrons and muons	+1.2 / −0.9	+1.1 / −0.8
Total systematic uncert.	+23 / −20	+22 / −19
Data statistics	±16	±15
Total	+28 / −25	+27 / −24

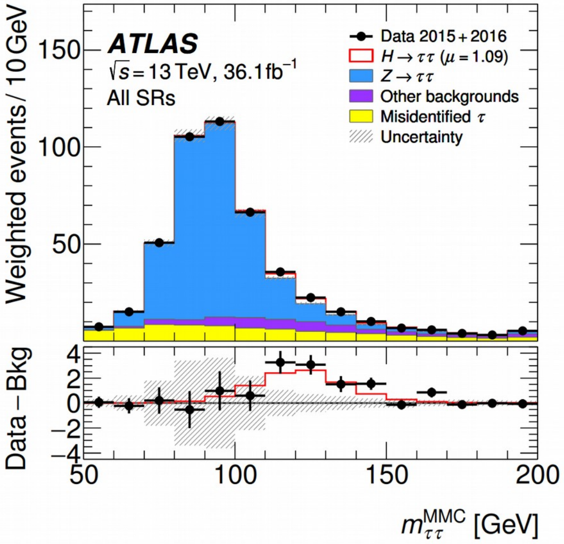

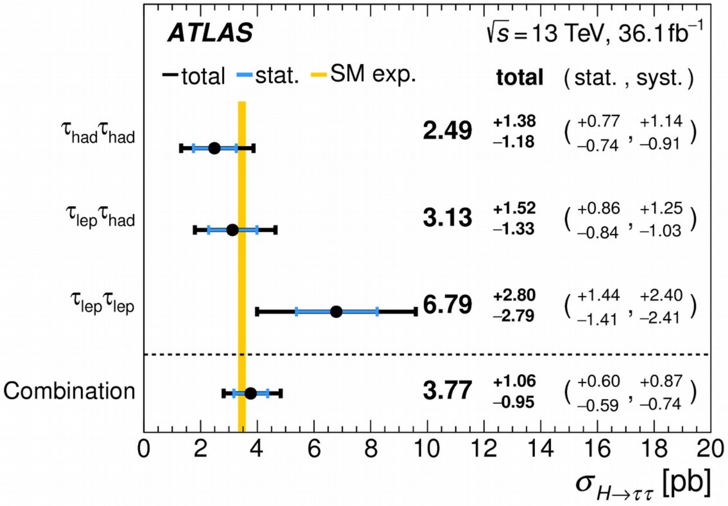

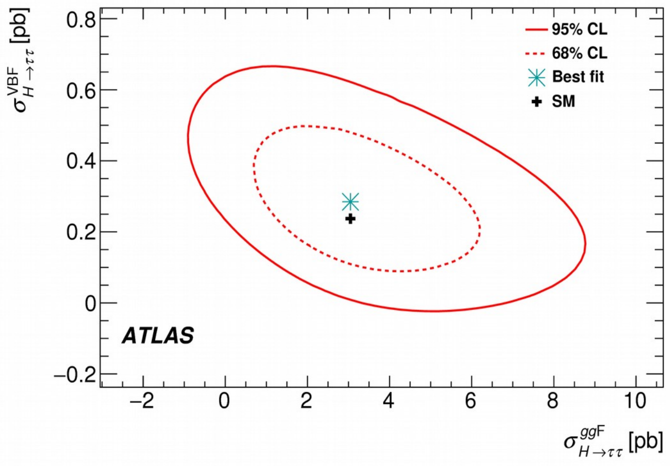

H→μμ

- Most sensitive channel to investigate couplings to 2nd generation fermions
- Very rare process, but high di-muon mass resolution makes channel accessible
- Signal would appear as narrow resonance over smoothly falling background
  - primarily Drell-Yan, but also diboson and leptonic top decays
- Events split in category according to muon pseudo-rapidity and di-muon pair transverse momentum
- Analysis sensitive to two Higgs production mechanisms: ggF and VBF
- A boosted-decision-tree (BDT) is used to maximize the separation between the VBF signal and background

- Best fit value of the H → μμ signal strength: $\mu = 0.1^{+1.0}_{-1.1}$
- Observed (expected) significance 0.0σ (0.9σ)
- Below the most sensitive categories

~ all from statistics

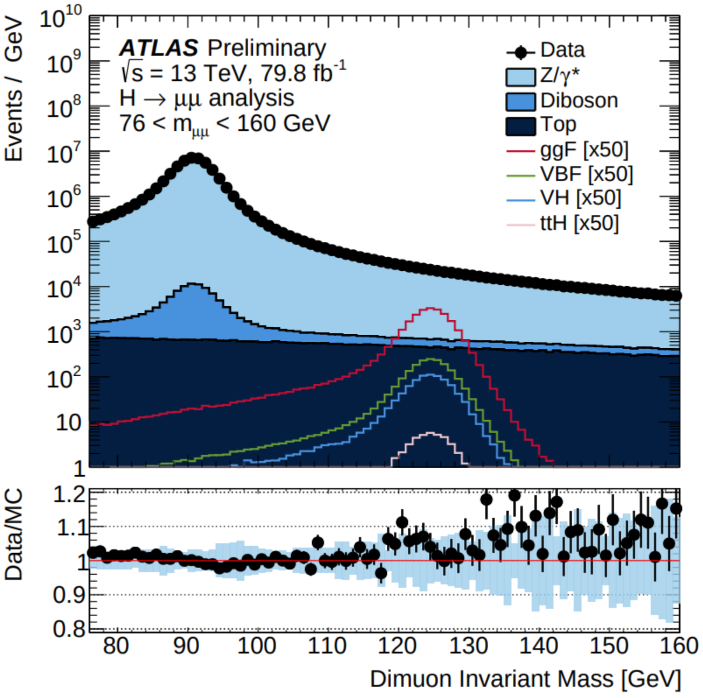

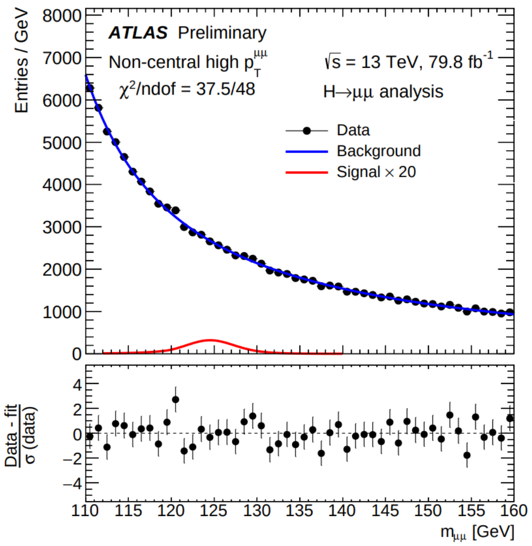

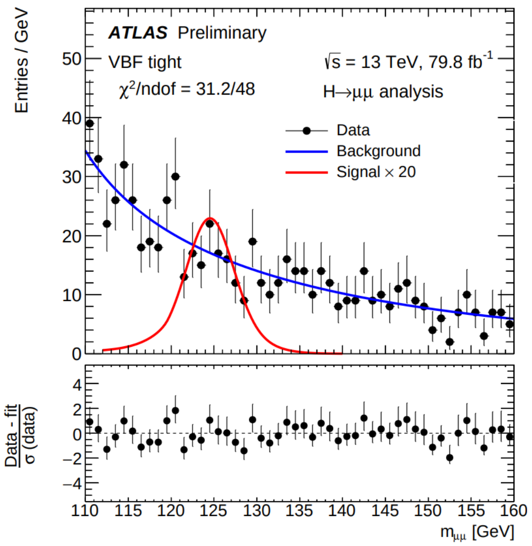

Higgs production with Top quark pair (ttH)

- First ATLAS observation of ttH production mode → lowest cross-section among the main Higgs production modes
- All the main Higgs decay channels involved in this search

Phys. Lett. B 784 (2018) 173

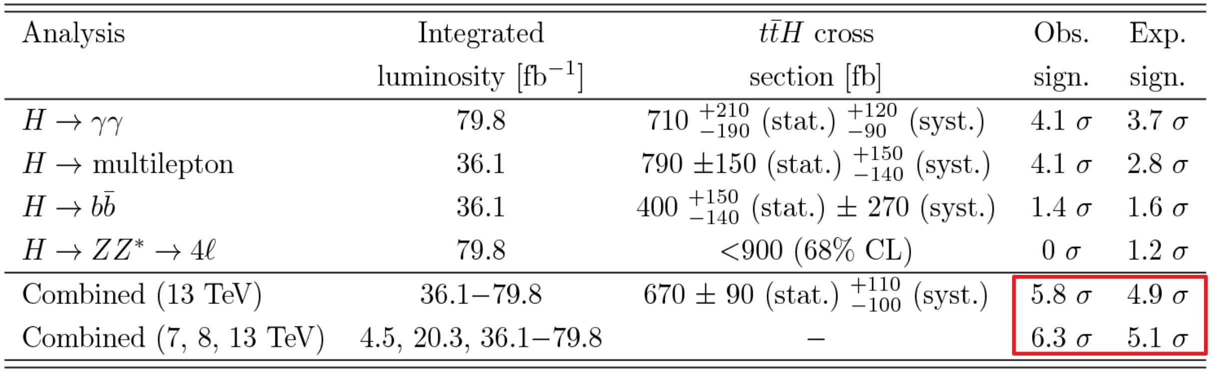

Analysis	Integrated luminosity [fb^{-1}]	$t\bar{t}H$ cross section [fb]	Obs. sign.	Exp. sign.
$H \to \gamma\gamma$	79.8	$710\ ^{+210}_{-190}$ (stat.) $^{+120}_{-90}$ (syst.)	4.1 σ	3.7 σ
$H \to$ multilepton	36.1	790 ± 150 (stat.) $^{+150}_{-140}$ (syst.)	4.1 σ	2.8 σ
$H \to b\bar{b}$	36.1	$400\ ^{+150}_{-140}$ (stat.) $\pm$ 270 (syst.)	1.4 σ	1.6 σ
$H \to ZZ^* \to 4\ell$	79.8	<900 (68% CL)	0 σ	1.2 σ
Combined (13 TeV)	36.1−79.8	670 ± 90 (stat.) $^{+110}_{-100}$ (syst.)	5.8 σ	4.9 σ
Combined (7, 8, 13 TeV)	4.5, 20.3, 36.1−79.8	−	6.3 σ	5.1 σ

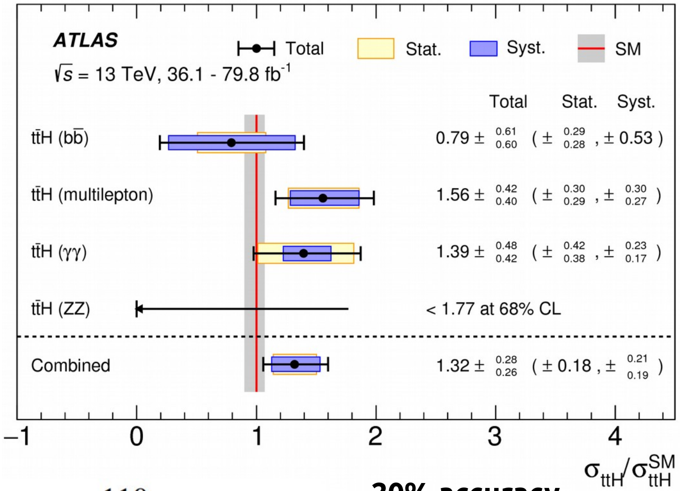

20% accuracy on combination

- The measured total cross-section is found to be: $\sigma_{t\bar{t}H} = 670 \pm 90\ (\text{stat.})\ ^{+110}_{-100}\ (\text{syst.})\ \text{fb}$

  in agreement with SM prediction: 507^{+35}_{-50} fb

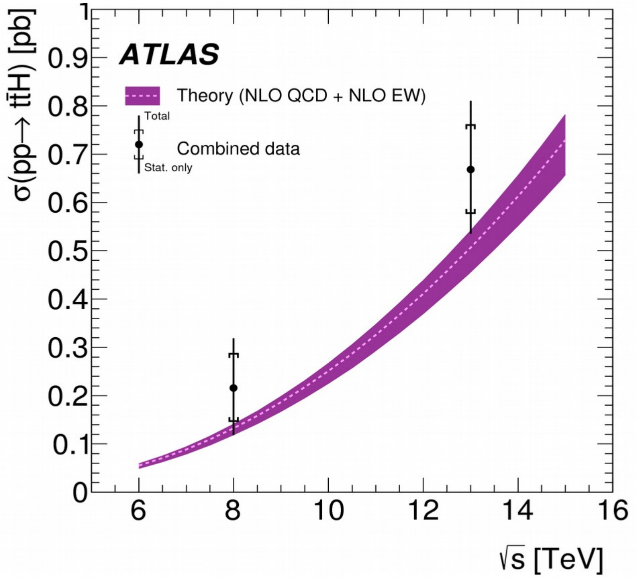

- Statistical and systematic uncertainties comparable
- Main systematic errors come from:
  - Theory uncertainties on ttbar + heavy flavour and ttH signal
  - Experimental uncertainties on non-prompt backgrounds
  - Jet energy scale + jet and E_T^{miss} resolution

Update on ttH(H→γγ)

ATLAS-CONF-2019-004

- First ATLAS Higgs results with full Run-2 dataset (~140 fb^{-1})
- Observed (expected) significance of 4.9 (4.2) standard deviations w.r.t. the background-only hypothesis
- The analysis is performed using a simultaneous fit in seven signal-enriched event categories
    - 3 leptonic categories + 4 hadronic categories, based on BDT score
- Measured cross-section times BR(H→ γγ)

$$\sigma_{t\bar{t}H} \times B_{\gamma\gamma} = 1.59^{+0.43}_{-0.39}\ \text{fb} = 1.59^{+0.38}_{-0.36}\ (\text{stat.})\ ^{+0.15}_{-0.12}\ (\text{exp.})\ ^{+0.15}_{-0.11}\ (\text{theo.})\ \text{fb}$$

25% single measurement accuracy !

in agreement with the Standard Model prediction

$$t\bar{t}H(\rightarrow \gamma\gamma) = 1.15^{+0.09}_{-0.12}\ \text{fb}$$

- Analysis limited by statistical uncertainties (~23%)
- Main systematic uncertainties below:

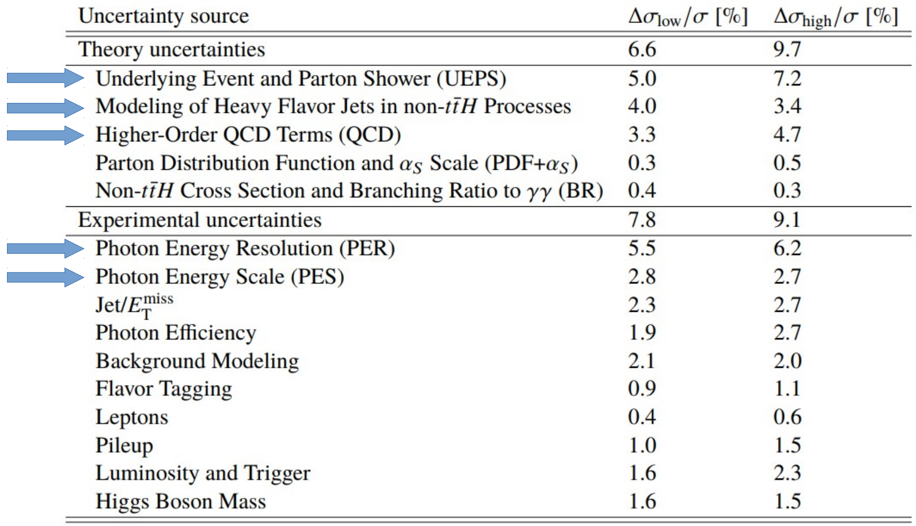

Uncertainty source	$\Delta\sigma_{\text{low}}/\sigma$ [%]	$\Delta\sigma_{\text{high}}/\sigma$ [%]
Theory uncertainties	6.6	9.7
Underlying Event and Parton Shower (UEPS)	5.0	7.2
Modeling of Heavy Flavor Jets in non-$t\bar{t}H$ Processes	4.0	3.4
Higher-Order QCD Terms (QCD)	3.3	4.7
Parton Distribution Function and α_S Scale (PDF+α_S)	0.3	0.5
Non-$t\bar{t}H$ Cross Section and Branching Ratio to $\gamma\gamma$ (BR)	0.4	0.3
Experimental uncertainties	7.8	9.1
Photon Energy Resolution (PER)	5.5	6.2
Photon Energy Scale (PES)	2.8	2.7
Jet/$E_{\text{T}}^{\text{miss}}$	2.3	2.7
Photon Efficiency	1.9	2.7
Background Modeling	2.1	2.0
Flavor Tagging	0.9	1.1
Leptons	0.4	0.6
Pileup	1.0	1.5
Luminosity and Trigger	1.6	2.3
Higgs Boson Mass	1.6	1.5

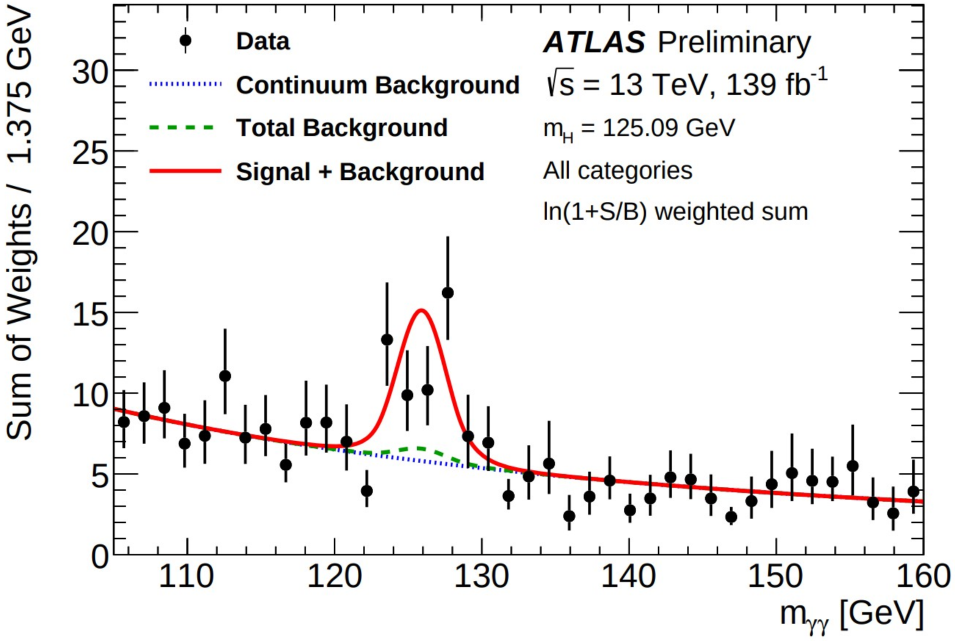

Higgs differential cross-sections

H→ZZ*→4ℓ

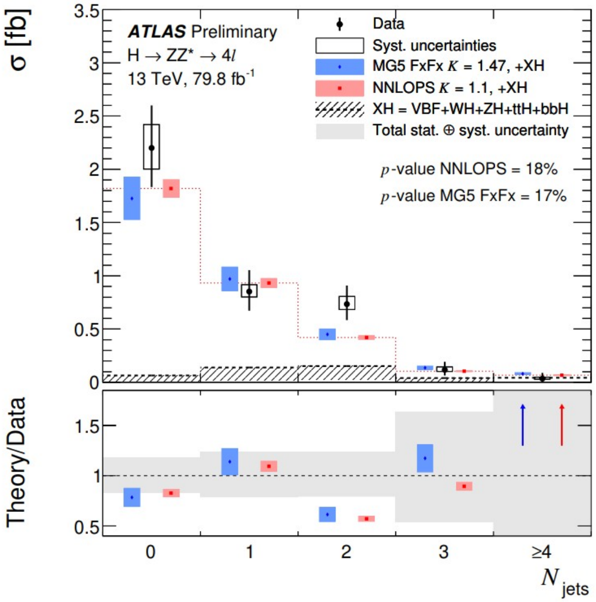

ATLAS-CONF-2018-018

H→ γγ

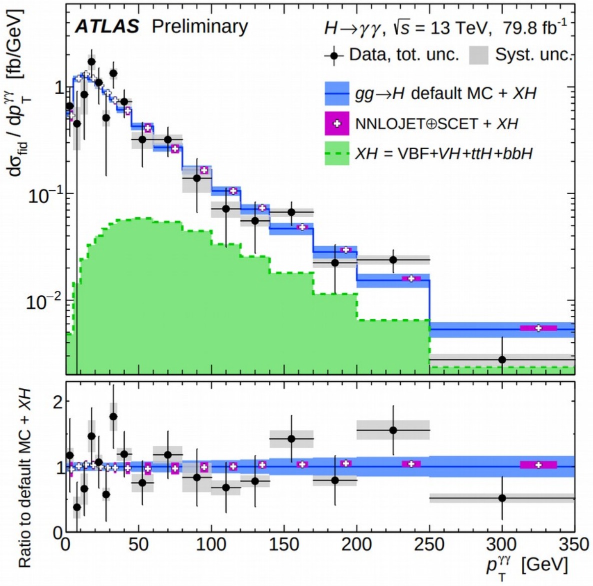

ATLAS-CONF-2018-028

H→ZZ*→4ℓ

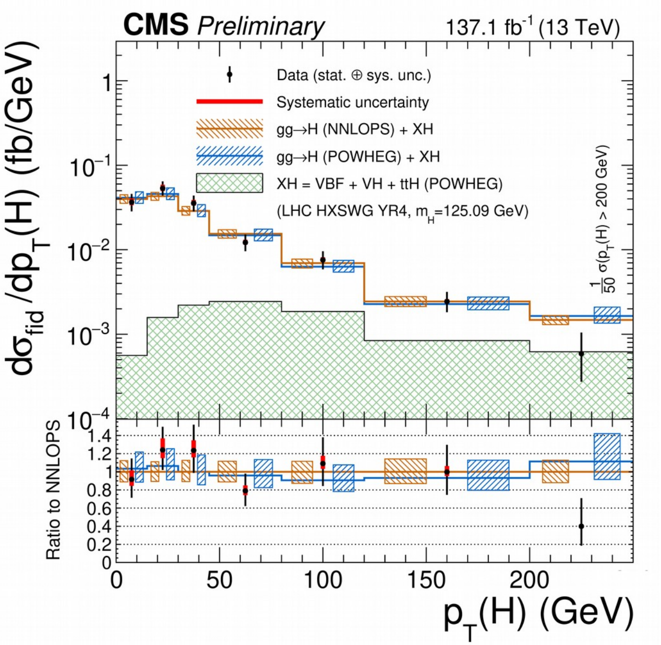

CMS-PAS-HIG-19-001

- ATLAS: H→γγ and H→ZZ* measurements with 80 fb^{-1}
- CMS: H→ZZ* measurements with full Run-2 dataset → unprecedented precision
- Many differential observables measured (including Higgs rapidity and leading jet p_T) → all in good agreement with SM expectation → no evidence of new physics
- Precision still dominated by statistics (~20%) → more data and channels will further improve it!
- Systematics uncertainties ~10% (larger for Njets > 2)

Higgs combination

ATLAS Higgs combination

ATLAS-CONF-2019-005

- ATLAS combined results are based on the combination of the below analyses:

Analysis	Integrated luminosity (fb^{-1})
$H \to \gamma\gamma$ (including $t\bar{t}H$, $H \to \gamma\gamma$)	79.8
$H \to ZZ^* \to 4\ell$ (including $t\bar{t}H$, $H \to ZZ^* \to 4\ell$)	79.8
$H \to WW^* \to e\nu\mu\nu$	36.1
$H \to \tau\tau$	36.1
VH, $H \to b\bar{b}$	79.8
VBF, $H \to b\bar{b}$	24.5 – 30.6
$H \to \mu\mu$	79.8
$t\bar{t}H$, $H \to b\bar{b}$ and $t\bar{t}H$ multilepton	36.1
$H \to$ invisible	36.1
Off-shell $H \to ZZ^* \to 4\ell$ and $H \to ZZ^* \to 2\ell 2\nu$	36.1

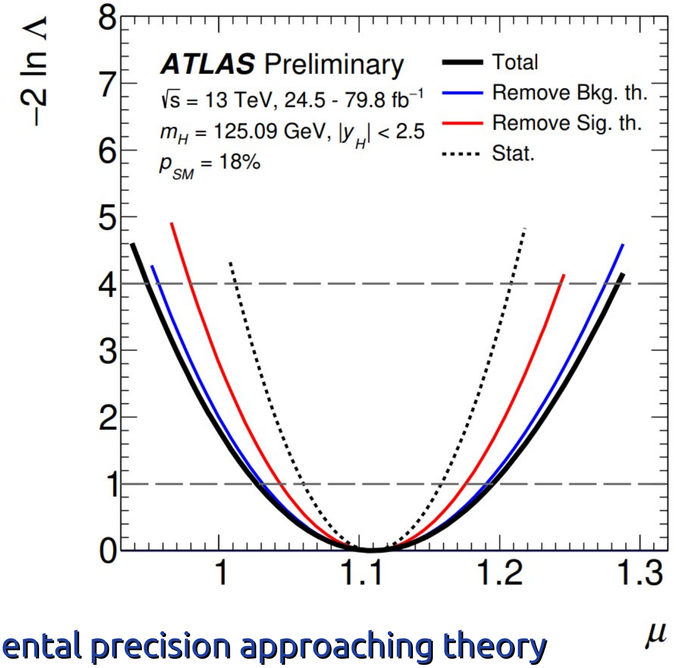

Experimental precision approaching theory precision even before using the full Run 2 statistics

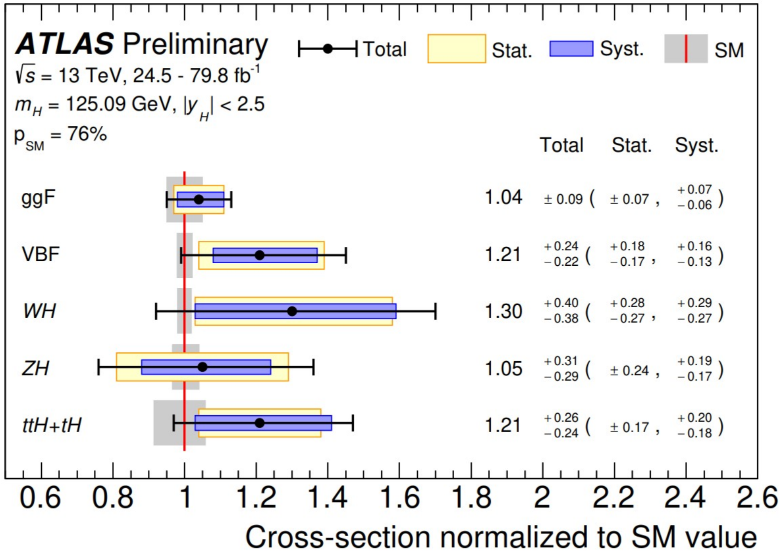

All major production modes are now observed with a significance > 5σ

- Dominant syst. uncertainties:
  - signal theory (4.2%)
  - background theory (2.6%)
  - Electron/photon energy scale and resolution (2.2%)
  - luminosity (2%)

Uncertainty source	$\Delta\mu/\mu$ [%]
Statistical uncertainty	4.4
Systematic uncertainties	6.2
Theory uncertainties	4.8
Signal	4.2
Background	2.6
Experimental uncertainties (excl. MC stat.)	4.1
Luminosity	2.0
Background modeling	1.6
Jets, $E_{\mathrm{T}}^{\mathrm{miss}}$	1.4
Flavour tagging	1.1
Electrons, photons	2.2
Muons	0.2
τ-lepton	0.4
Other	1.6
MC statistical uncertainty	1.7
Total uncertainty	7.6

8 % uncertainty

$$\mu = 1.11^{+0.09}_{-0.08} = 1.11 \pm 0.05\,(\text{stat.})\,^{+0.05}_{-0.04}\,(\text{exp.})\,^{+0.05}_{-0.04}\,(\text{sig. th.}) \pm 0.03\,(\text{bkg. th.})$$

CMS Higgs combination

arXiv 1809.10733

- CMS exploits 2015 and 2016 dataset for the combination (~36 fb^{-1})
- The following decay channels are included in the combination: H→γγ, H→ZZ, H→WW, H→ττ, H→bb, and H → μμ

$$\mu = 1.17 \pm 0.10 = 1.17 \pm 0.06\,(\mathrm{stat})\,^{+0.06}_{-0.05}\,(\mathrm{sig\,theo})\,\pm 0.06\,(\mathrm{other\,syst})$$

9 % uncertainty

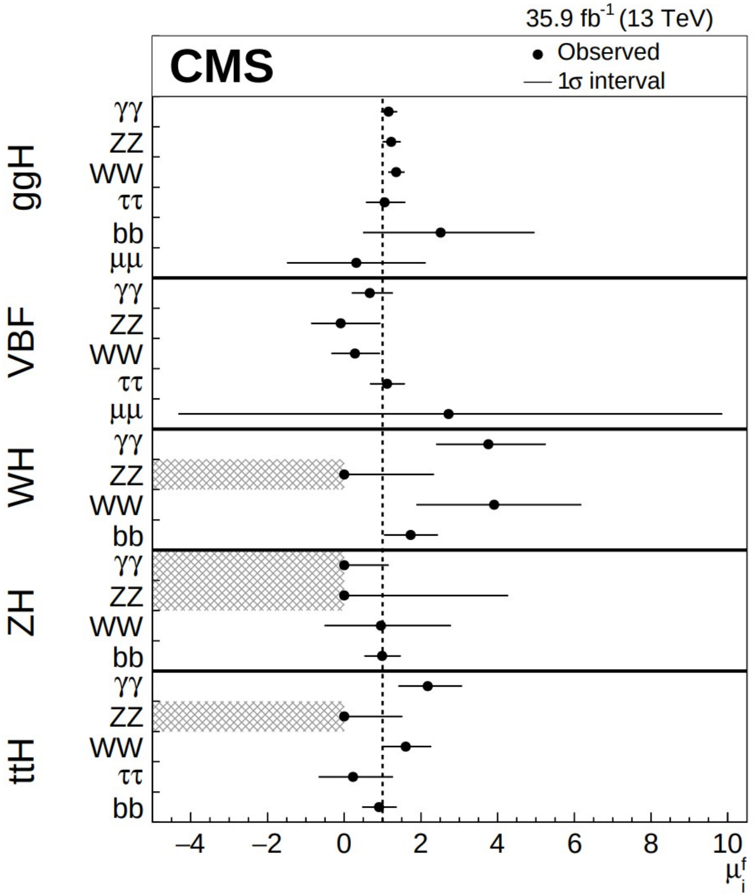

- Dominant uncertainties: Signal theory (5%), luminosity (2.5%)
- 50% level improvement compared to Run-1 due to increased cross-section, improved theory uncertainty, additional event categories

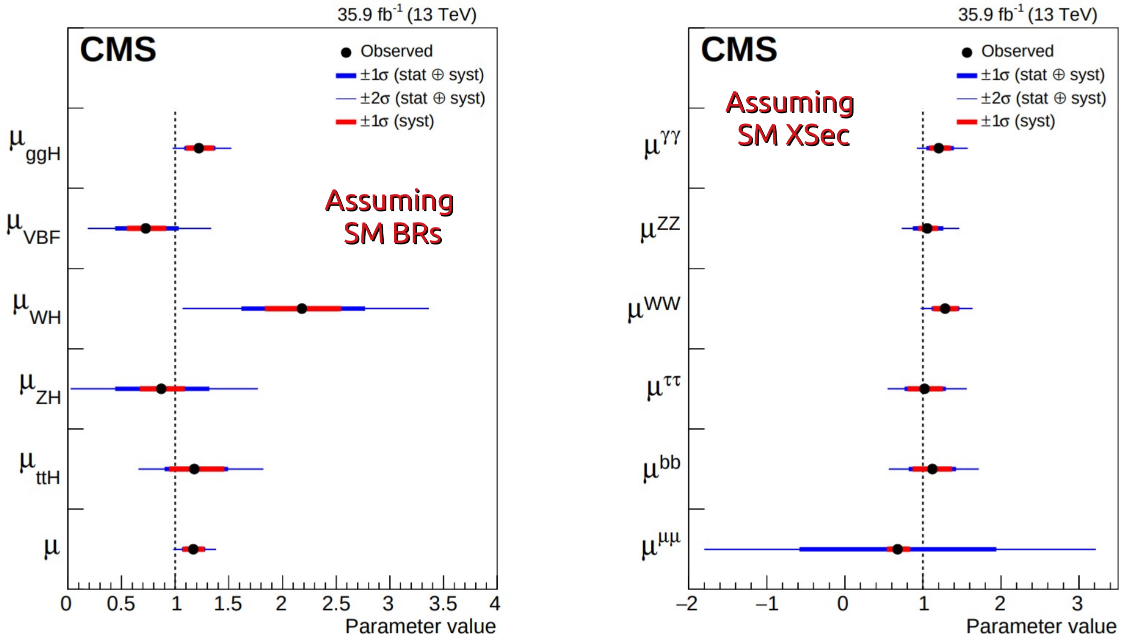

Signal strength modifiers per-production mode (left) and per-decay mode (right)

Simplified Template Cross-Section method

- Simplified template cross-section (STXS) define a common categorization framework for Higgs analyses
- Allows to measure the Higgs boson production cross-section in exclusive kinematic bins
- Reduce model dependence, maximize sensitivity to new physics, minimize the theoretical uncertainties, constrain coupling modifiers (kappa), EFT coefficients, BSM tests

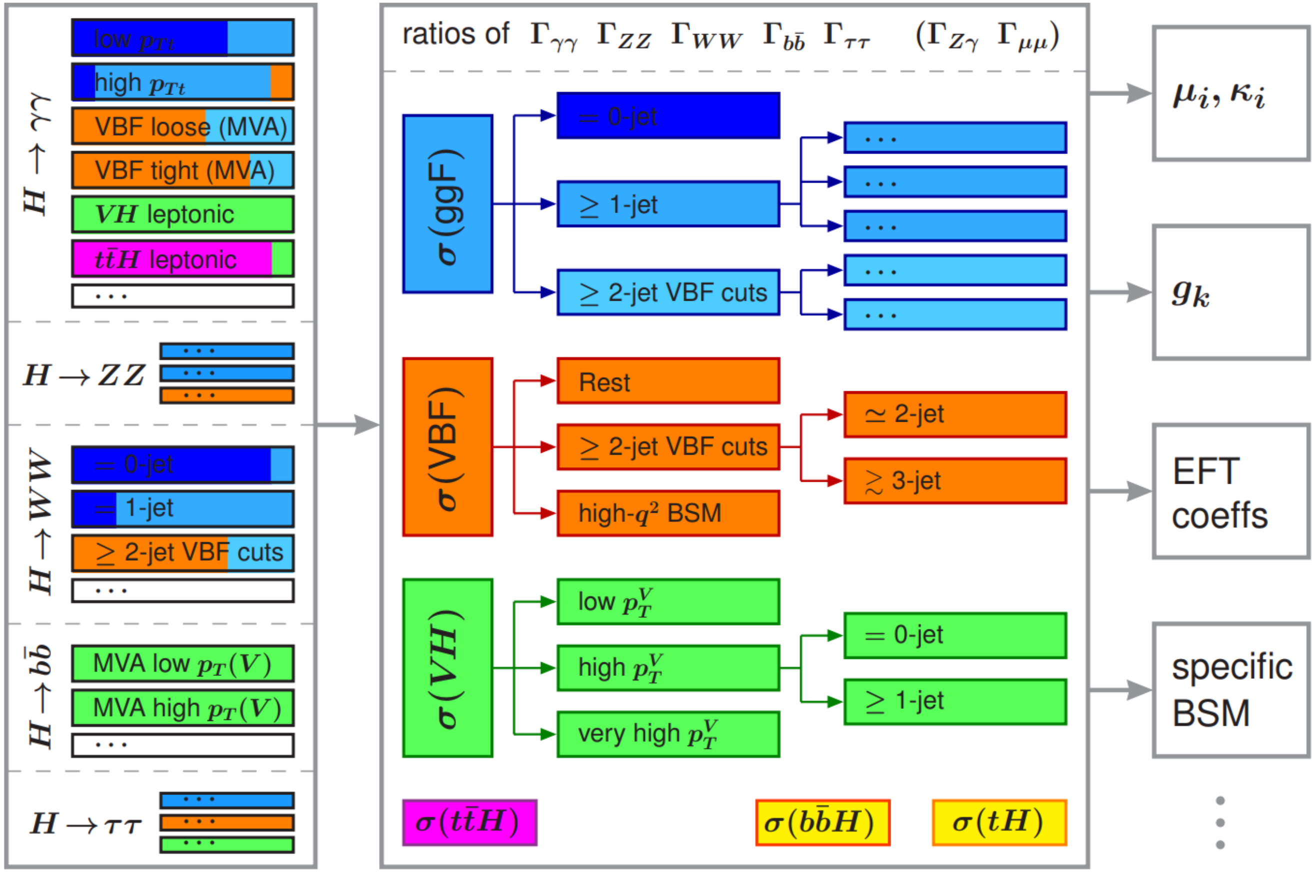

arXiv 1610.07922

Simplified Template Cross-Section method

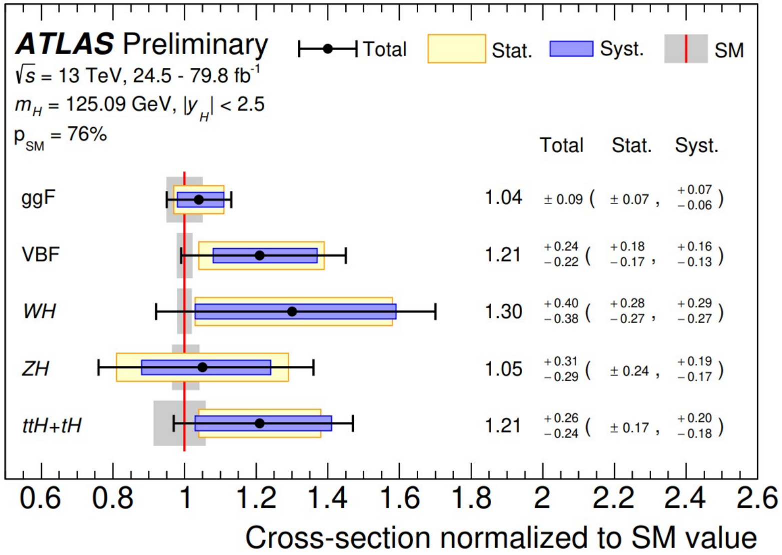

Cross sections for ggF, VBF, WH, ZH and tt̄H+tH normalized to their SM predictions, measured with the assumption of SM branching fractions

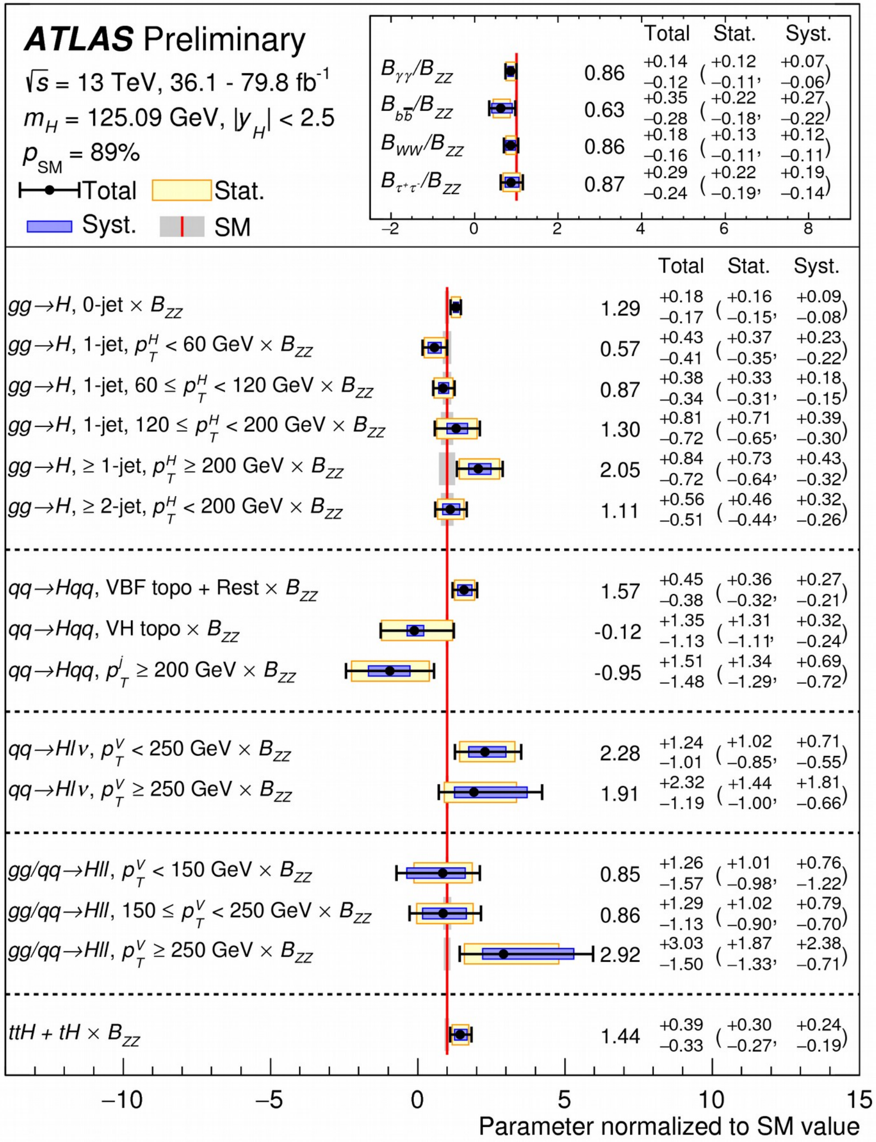

Stage 1 STXS

Fermion and gauge boson couplings

- Extended Higgs sector models allow for non-SM couplings to fermions and bosons
- Assumption 1: universal coupling modifiers for all vector boson and fermion couplings

$$\kappa_V = \kappa_W = \kappa_Z$$
$$\kappa_F = \kappa_t = \kappa_b = \kappa_\tau = \kappa_\mu$$

- Assumption 2: no new particles in the loops → $\mathrm{BR}_{\mathrm{BSM}} = 0$

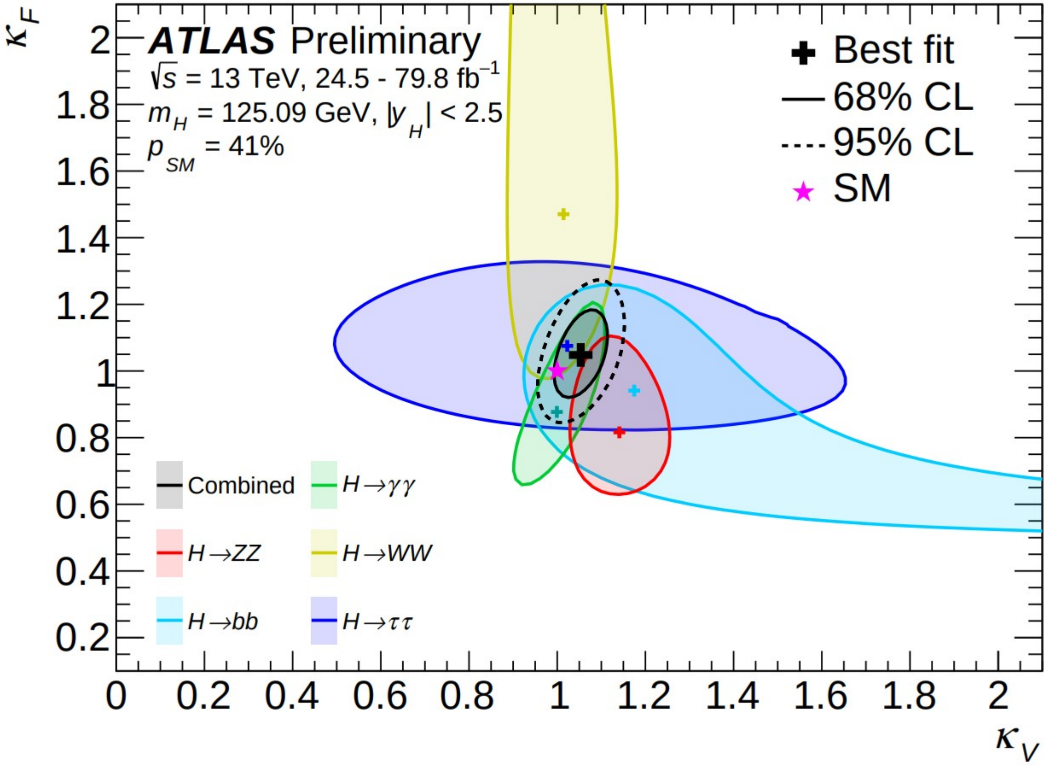

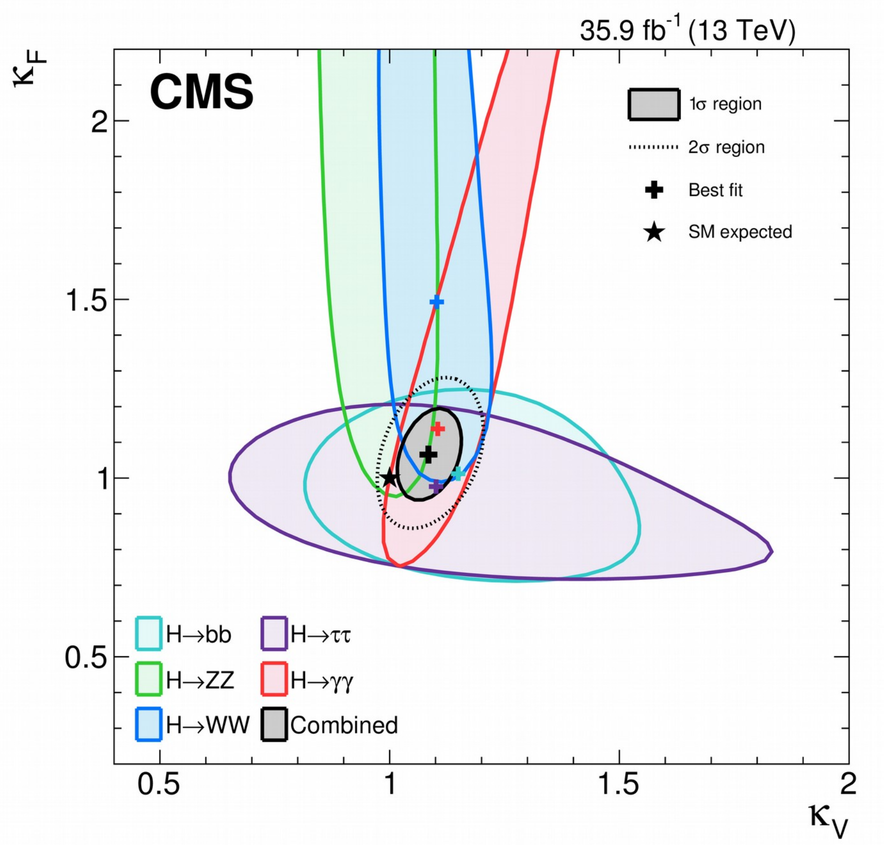

Tree Level Higgs couplings

- In SM coupling of Higgs to fermions ∝ m_F and for massive weak bosons ∝ m_V^2
- Within current precision, Higgs couplings scale with particle masses
- Good agreement with expectation from SM across wide particle mass range

$$\boxed{g_V \sim \frac{\kappa_V \cdot m_V^2}{\nu^2}}$$

$$\boxed{\lambda_f \sim \frac{\kappa_f m_f}{\nu}}$$

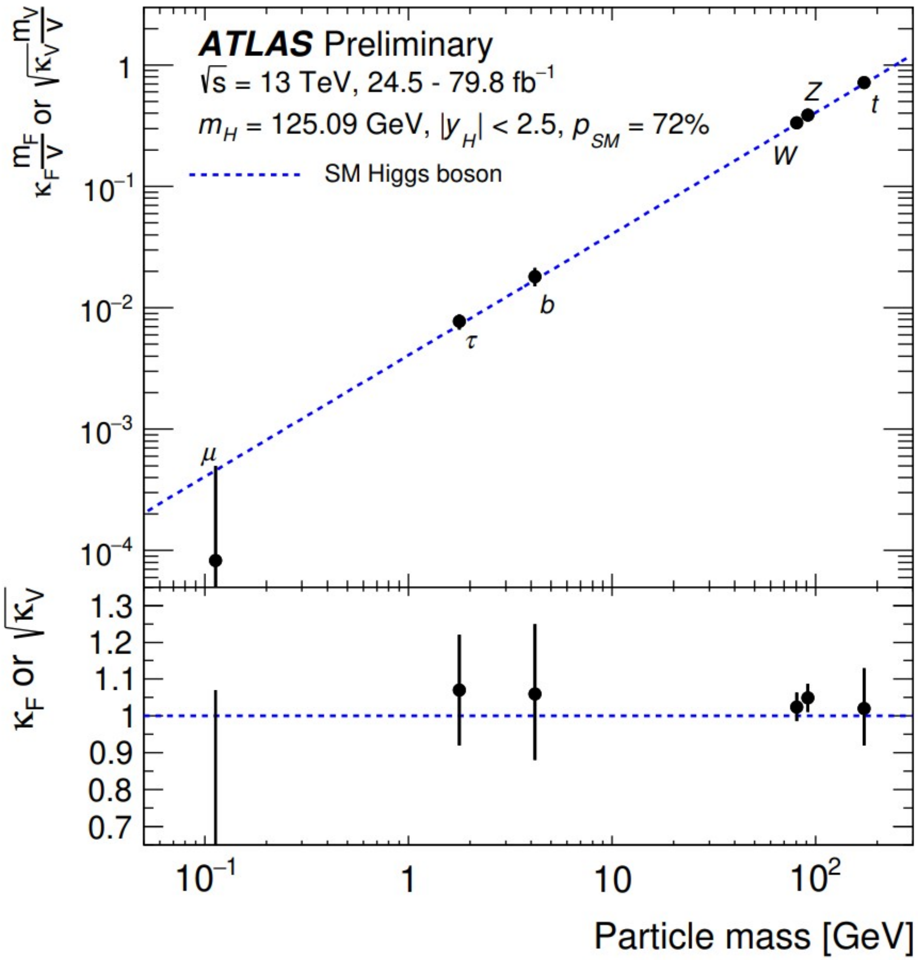

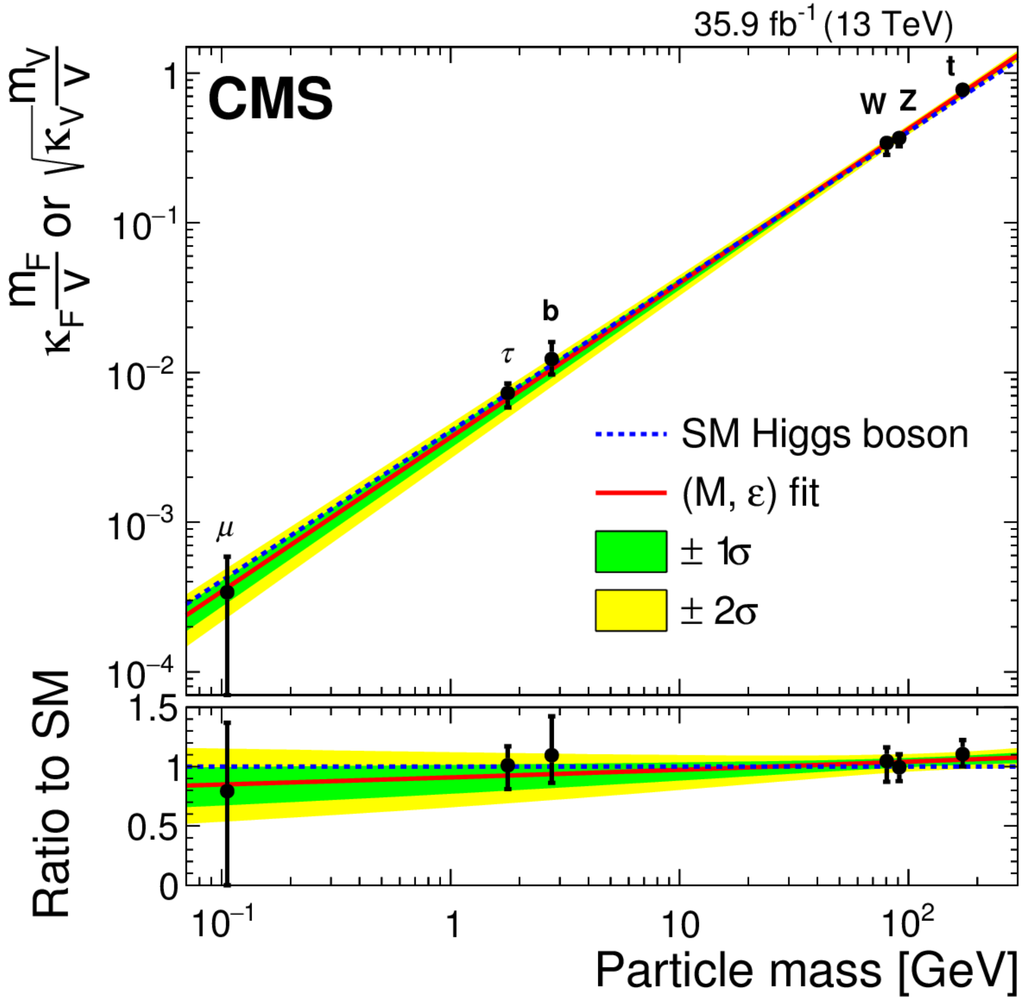

Higgs properties

Higgs mass (ATLAS)

Phys. Lett. B 784 (2018) 345

- Higgs mass measured using the γγ and ZZ*→4lep Higgs decays @ 13 TeV

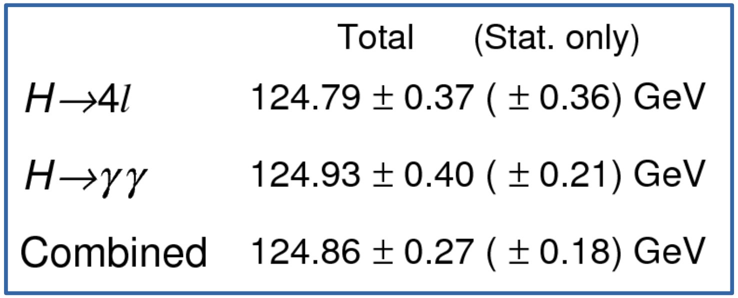

	Total	(Stat. only)
$H\rightarrow 4l$	124.79 ± 0.37	(± 0.36) GeV
$H\rightarrow\gamma\gamma$	124.93 ± 0.40	(± 0.21) GeV
Combined	124.86 ± 0.27	(± 0.18) GeV

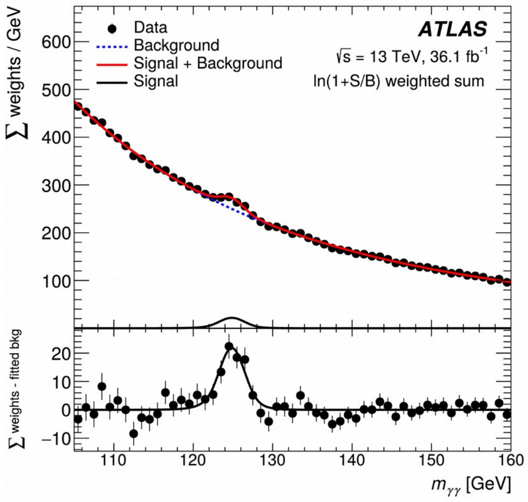

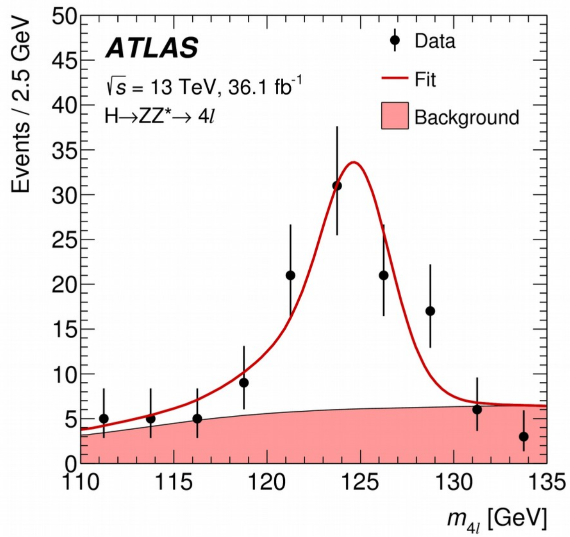

- Still room for improvements for the 4lep channel, dominated by statistics

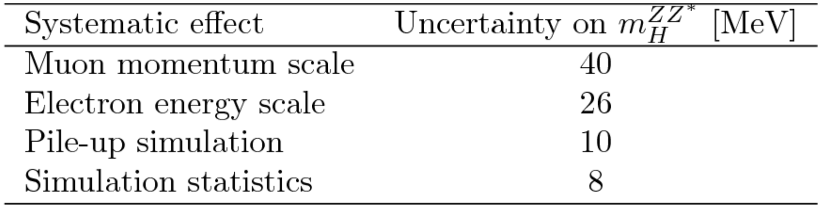

Systematic effect	Uncertainty on $m_H^{ZZ^*}$ [MeV]
Muon momentum scale	40
Electron energy scale	26
Pile-up simulation	10
Simulation statistics	8

- Syst. uncertainty comparable with the stat. uncertainty in the γγ channel

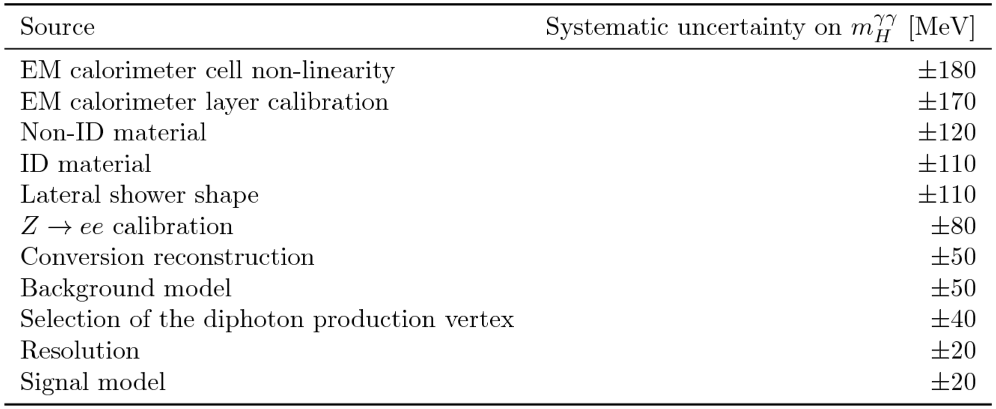

Source	Systematic uncertainty on $m_H^{\gamma\gamma}$ [MeV]
EM calorimeter cell non-linearity	±180
EM calorimeter layer calibration	±170
Non-ID material	±120
ID material	±110
Lateral shower shape	±110
$Z\rightarrow ee$ calibration	±80
Conversion reconstruction	±50
Background model	±50
Selection of the diphoton production vertex	±40
Resolution	±20
Signal model	±20

- In both channels, syst. uncertainties dominated by experimental ones: energy / momentum scale and resolution

Higgs mass

ATLAS: Phys. Lett. B 784 (2018) 345
CMS: JHEP11(2017)047

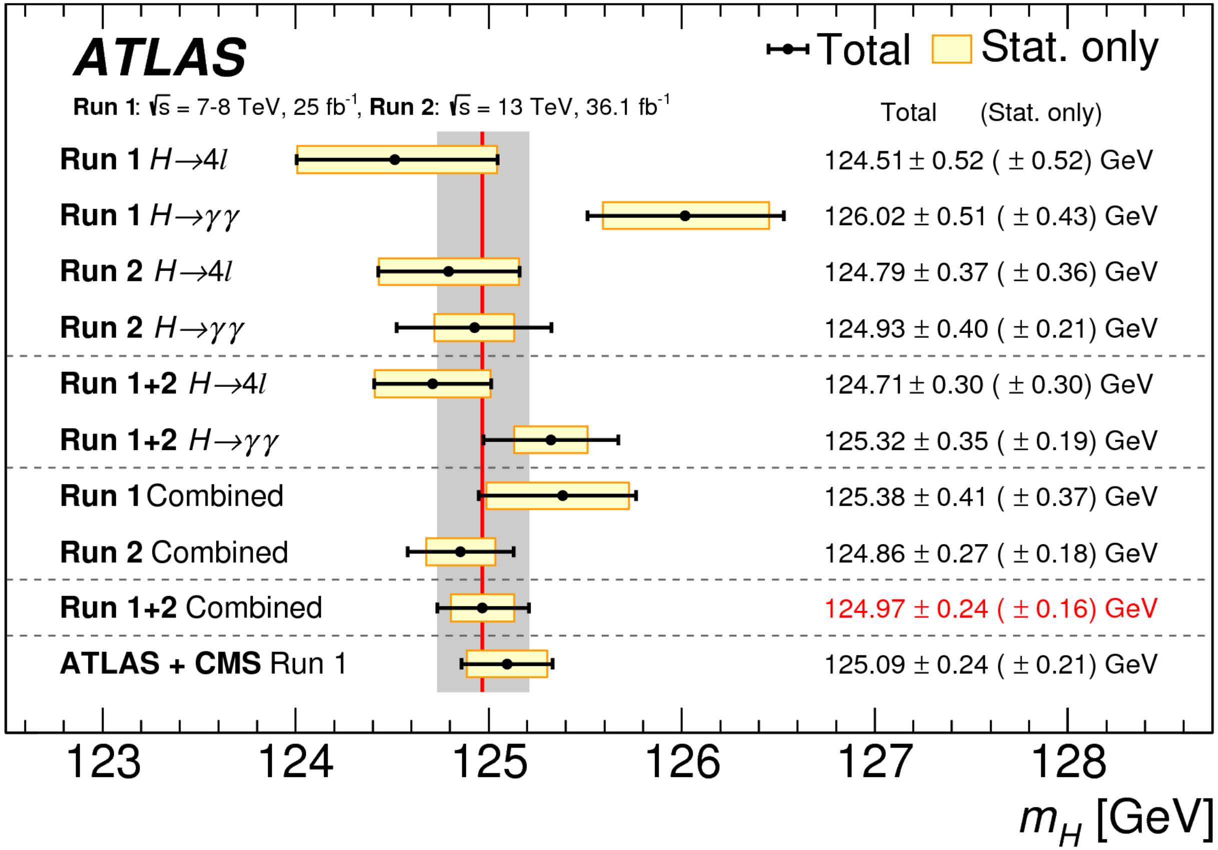

- ATLAS (γγ+4ℓ, Run 1 + Run 2): m_H = 124.97 ± 0.16 (stat.) ± 0.18 (syst.) GeV **0.19 % uncertainty**
- CMS (4ℓ only, Run 2 with 36 fb^{-1}): m_H = 125.26 ± 0.20 (stat.) ± 0.08 (syst.) GeV **0.17 % uncertainty**

Higgs width

- SM prediction for a Higgs boson with m_H = 125 GeV → 4 MeV
  - Γ_h too small to be measured directly at the LHC → experiment mass resolution ~ 1-2 GeV in the best measured channels

- Any deviation would imply a decay to non-SM particles

- Best direct limit from CMS H→4ℓ channel (36 fb^{-1}) : **Γ_h< 1.10 GeV (95% C.L.)** JHEP11(2017)047

- **Indirect limit** from ATLAS: in the Higgs off-shell regime, $\sigma_{off\text{-}shell}$ does not depend on the total width Γ_H , while $\sigma_{on\text{-}shell}$ does Phys. Lett. B 786 (2018) 223

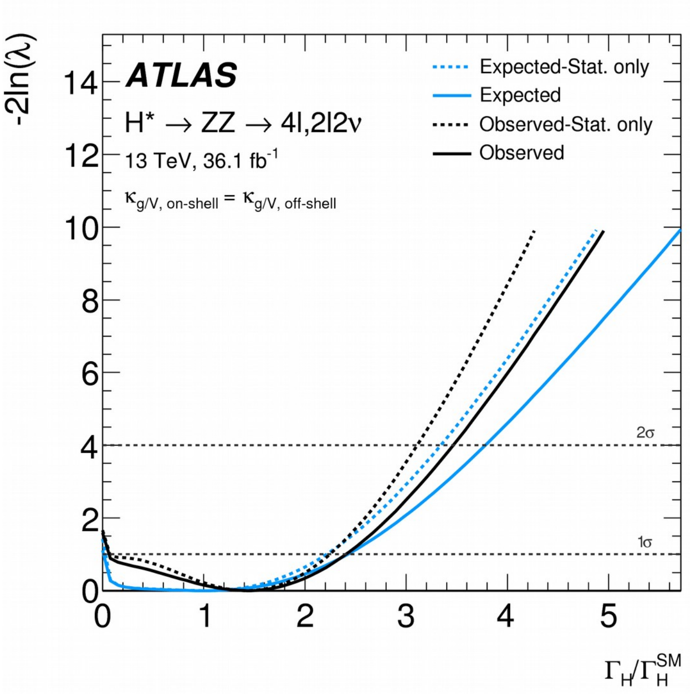

$$\frac{\left(\sigma_H^{off}/\sigma_H^{on}\right)_{exp}}{\left(\sigma_H^{off}/\sigma_H^{on}\right)_{SM}} \sim \frac{\Gamma_H}{\Gamma_H^{SM}}$$

experimentally: $\mu_{on/off} \equiv \dfrac{\sigma_{exp}^{on/off}}{\sigma_{SM}^{on/off}} \Longrightarrow \mu_{off} = \mu_{on} \cdot \dfrac{\Gamma_H}{\Gamma_H^{SM}}$

- Assuming the ratio of the Higgs boson couplings to the SM predictions are constant with energy from on-shell production to the high-mass range and $\mu_{\text{off-shell}}^{\text{ggF}}/\mu_{\text{off-shell}}^{\text{VBF}} = 1$
- combining H→ZZ*→4ℓ and H→ZZ*→2ℓ2ν channels (36 fb-1)

Observed (expected) 95% C.L. limit on **Γ_H< 14.4 (15.2) MeV**

Update from CMS on Higgs width

- CMS H→4ℓ analysis with ~80 fb^{-1} (2016 + 2017)
- Results combined with ones at 7 and 8 TeV
- Studying both the on-shell and off-shell Higgs production, CMS put the most precise measurement on Higgs width:

Parameter	Observed	Expected
Γ_H (MeV)	$3.2^{+2.8}_{-2.2}$ [0.08, 9.16]*	$4.1^{+5.0}_{-4.0}$ [0.0, 13.7]*

*** 95% C.L. interval**

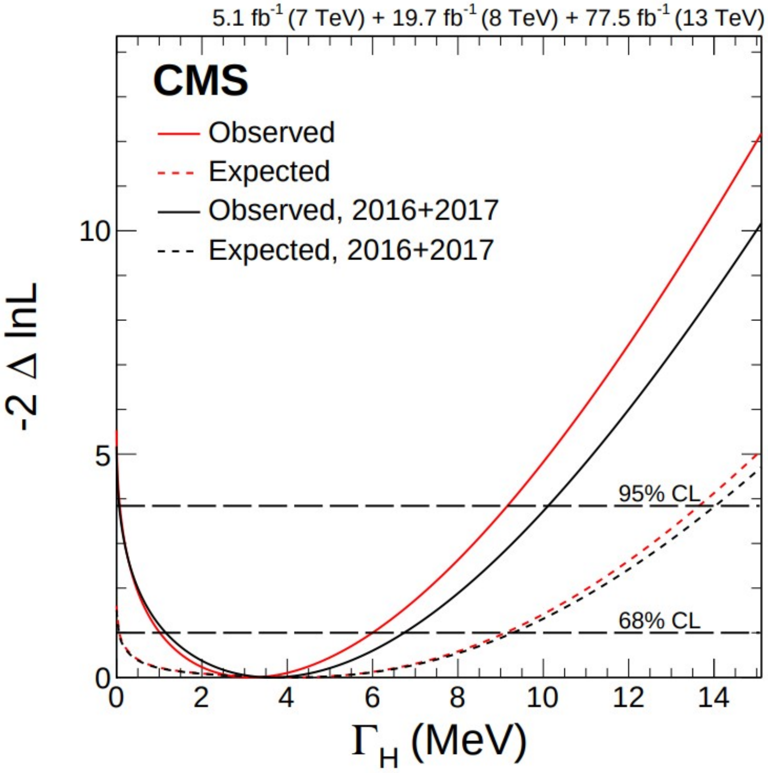

arXiv 1901.00174

Di-Higgs searches

ATLAS di-Higgs searches

- Measuring Higgs self coupling (λ_{HHH}) provides direct probe of Higgs potential
- Measuring $\kappa_\lambda = \lambda_{HHH}/\lambda_{HHH}^{SM}$ helps verify SM electroweak symmetry breaking
- Measurement of κ_λ possible by studying HH production
- HH production cross-section at 13TeV is ~ 30 fb
  - 1000 times smaller than single Higgs cross-section
- Two Higgs decays → many final states available
  - bbγγ has low branching ratio
  - bbττ , bbbb have higher background
  - new channels added recently: WWWW, WWγγ and WWbb
- Results of searches for non-resonant and resonant production presented here
  - Both ATLAS and CMS results use 2015 and 2016 dataset @ 13 TeV

HDBS-2018-58

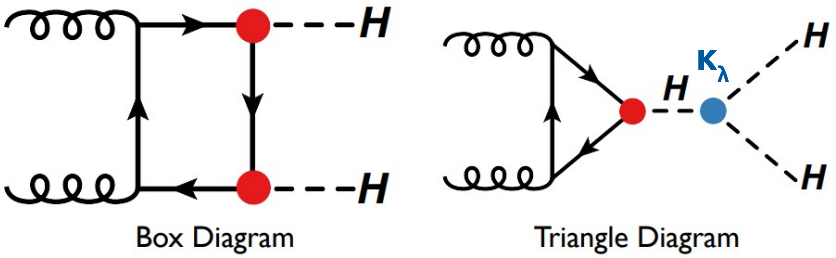

ATLAS di-Higgs searches

HDBS-2018-58

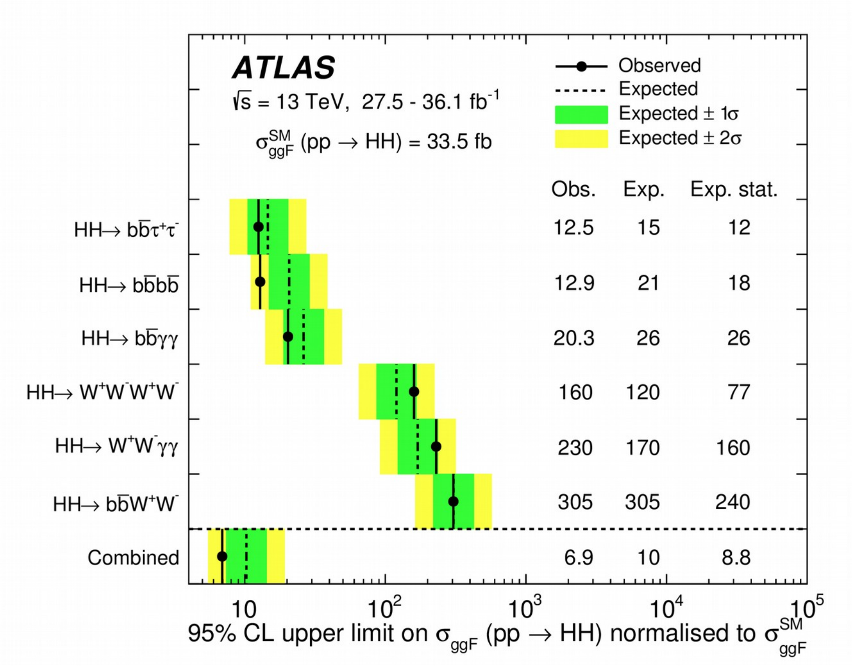

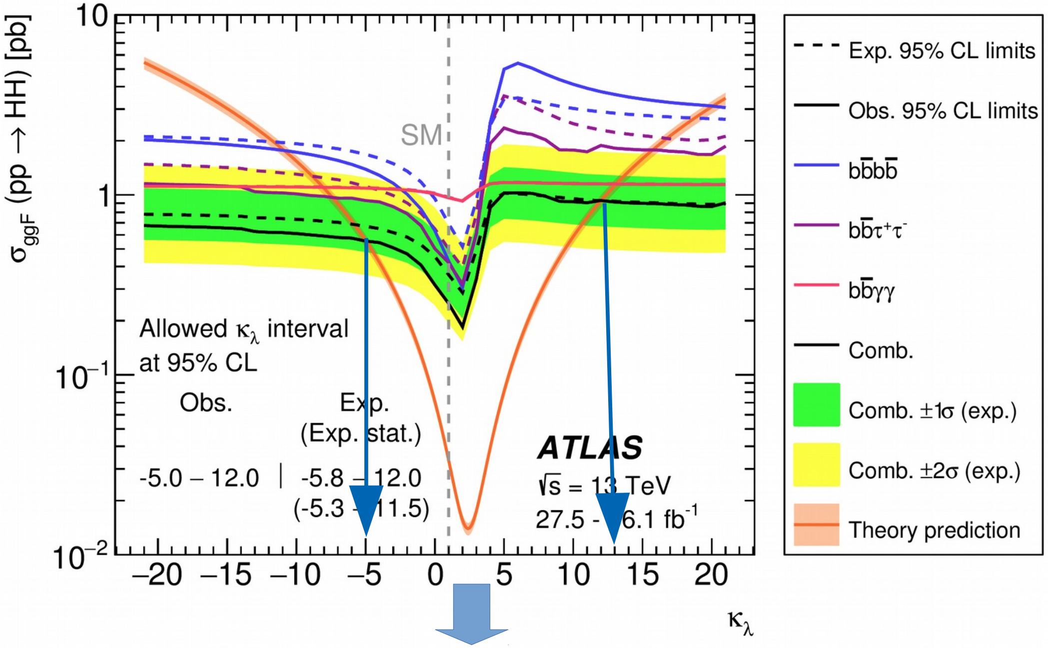

Allowed κ_λ interval at 95% CL

-5.0 — 12.0

- Di-higgs production studied in 6 channels
- Limit on renormalized ggF(HH) cross-section is found to be 6.9 times SM expectation
- No statistically significant excess of events above the Standard Model predictions is found
- Limits on resonant production mechanism (both spin-0 and spin-2 hypothesis explored)
- Results statistically limited, will benefit from full Run 2 dataset!

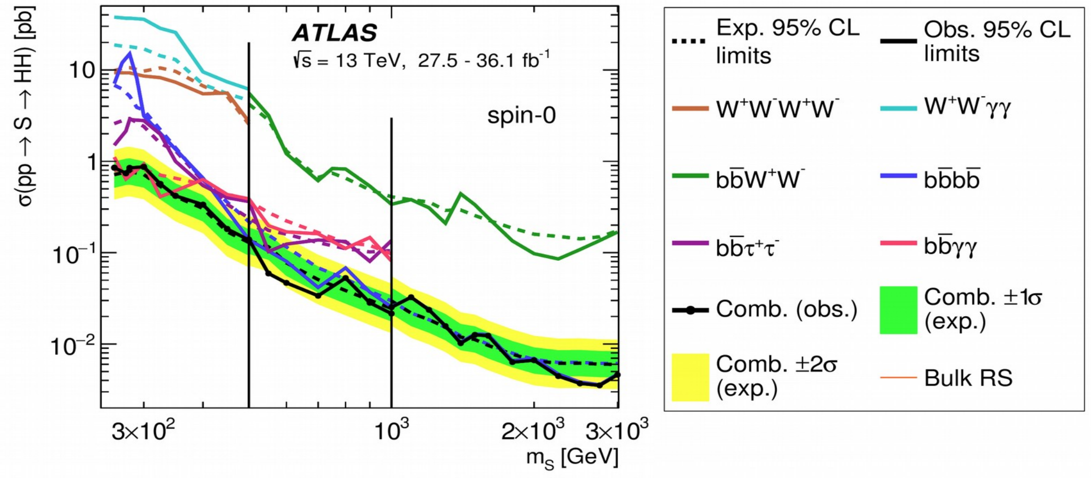

CMS di-Higgs searches

Phys. Rev. Lett. 122 (2019) 121803

- CMS result on HH search includes the bbγγ, bbττ, bbbb, and bbVV channels, where V represents a W or Z boson
- For the non-resonant production mechanism, the observed (expected) 95% C.L. corresponds to 22.2 (12.8) times the theoretical prediction for the standard model cross section
  - Expected limits similar between ATLAS and CMS: 10 vs 12.8 times SM prediction respectively
- Values of k_λ in the range $-11.8 < k_\lambda < 18.8$ are still allowed (95% C.L.) by the observed data
- For the resonant production mechanism, upper exclusion limits at 95% C.L. are obtained for the production of a narrow resonance with mass ranging from 250 to 3000 GeV (for either spin-0 and spin-2 resonances)

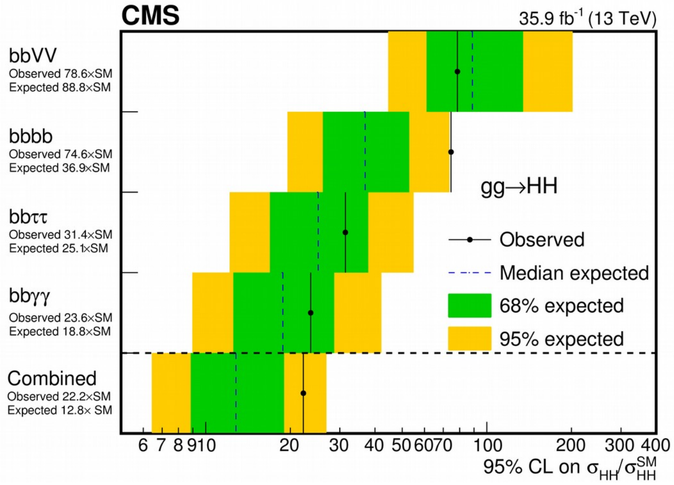

Non-resonant analysis
Observed limit 22.2

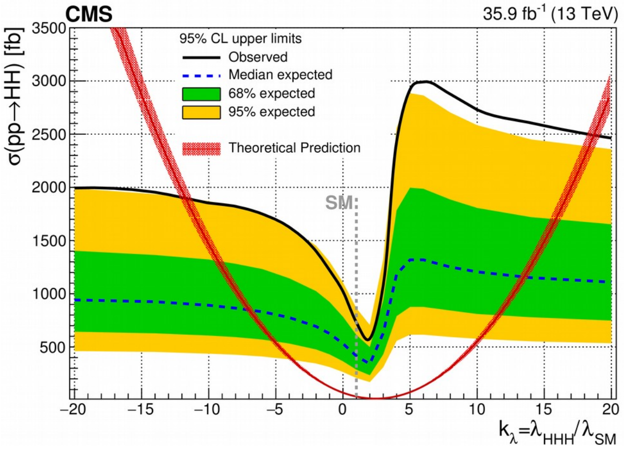

Non-resonant analysis
$-11.8 < k_\lambda < 18.8$

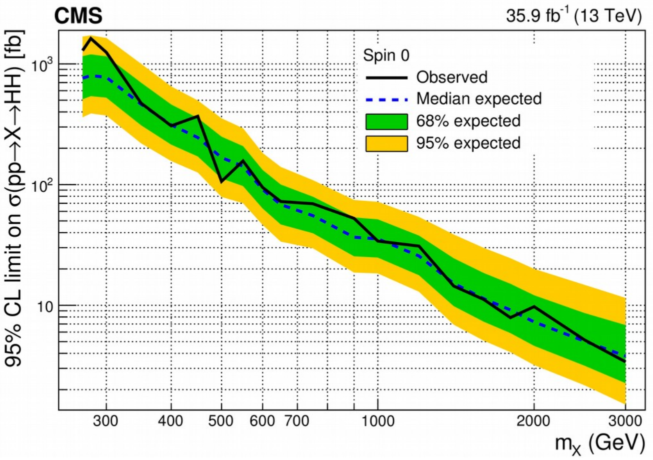

Resonant analysis
Spin 0 hypothesis

Constraint of κ_λ from single Higgs measurements

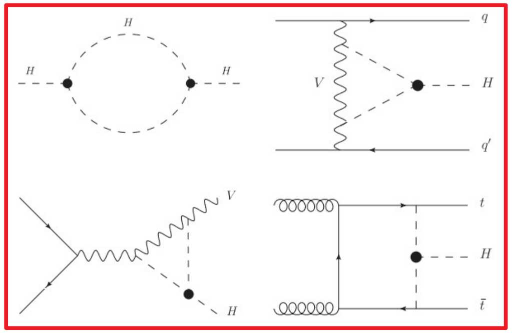

- The most recent constraints on the Higgs boson trilinear self-coupling, λ_{HHH}, have been set in the context of a direct search of double Higgs boson production
- Single Higgs processes do not depend on λ_{HHH} at leading order (LO), but the Higgs trilinear self-coupling contributions need to be taken into account for the calculation of the complete next-to-leading (NLO) electro-weak (EW) corrections
- Global fit to constrain the Higgs trilinear coupling, where all the Higgs boson production and decay channels are modified by parameters:

$$\mu_{if}(\kappa_\lambda) = \mu_i(\kappa_\lambda) \times \mu_f(\kappa_\lambda) \equiv \frac{\sigma_i(\kappa_\lambda)}{\sigma_{\mathrm{SM},i}} \times \frac{\mathrm{BR}_f(\kappa_\lambda)}{\mathrm{BR}_{\mathrm{SM},f}}$$

- The differential distributions of the VBF, WH and ZH production modes are exploited to constrain κ_λ by using the cross-section measurements in regions defined within the STXS framework

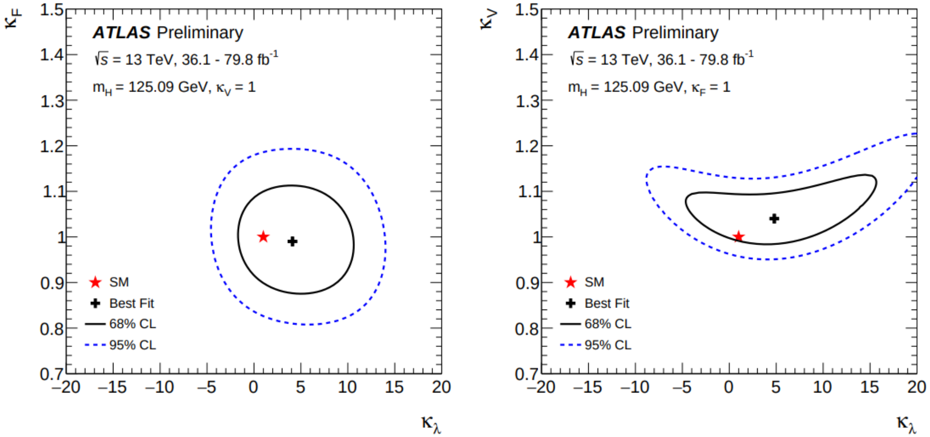

ATL-PHYS-PUB-2019-009

Analysis	Integrated luminosity (fb^{-1})
$H \to \gamma\gamma$ (including $t\bar{t}H$, $H \to \gamma\gamma$)	79.8
$H \to ZZ^* \to 4\ell$ (including $t\bar{t}H$, $H \to ZZ^* \to 4\ell$)	79.8
$H \to WW^* \to e\nu\mu\nu$	36.1
$H \to \tau\tau$	36.1
VH, $H \to b\bar{b}$	79.8
$t\bar{t}H$, $H \to b\bar{b}$ and $t\bar{t}H$ multilepton	36.1

$$\kappa_\lambda = 4.0^{+4.3}_{-4.1} = 4.0^{+3.7}_{-3.6}\,(\mathrm{stat.})\,^{+1.6}_{-1.5}\,(\mathrm{exp.})\,^{+1.3}_{-0.9}\,(\mathrm{sig.\ th.})\,^{+0.8}_{-0.9}\,(\mathrm{bkg.\ th.})$$

excluding at the 95% C.L. values outside the interval $-3.2 < \kappa_\lambda < 11.9$

Prospects for Physics at HL-LHC

High Luminosity LHC (HL-LHC)

Where we are now!

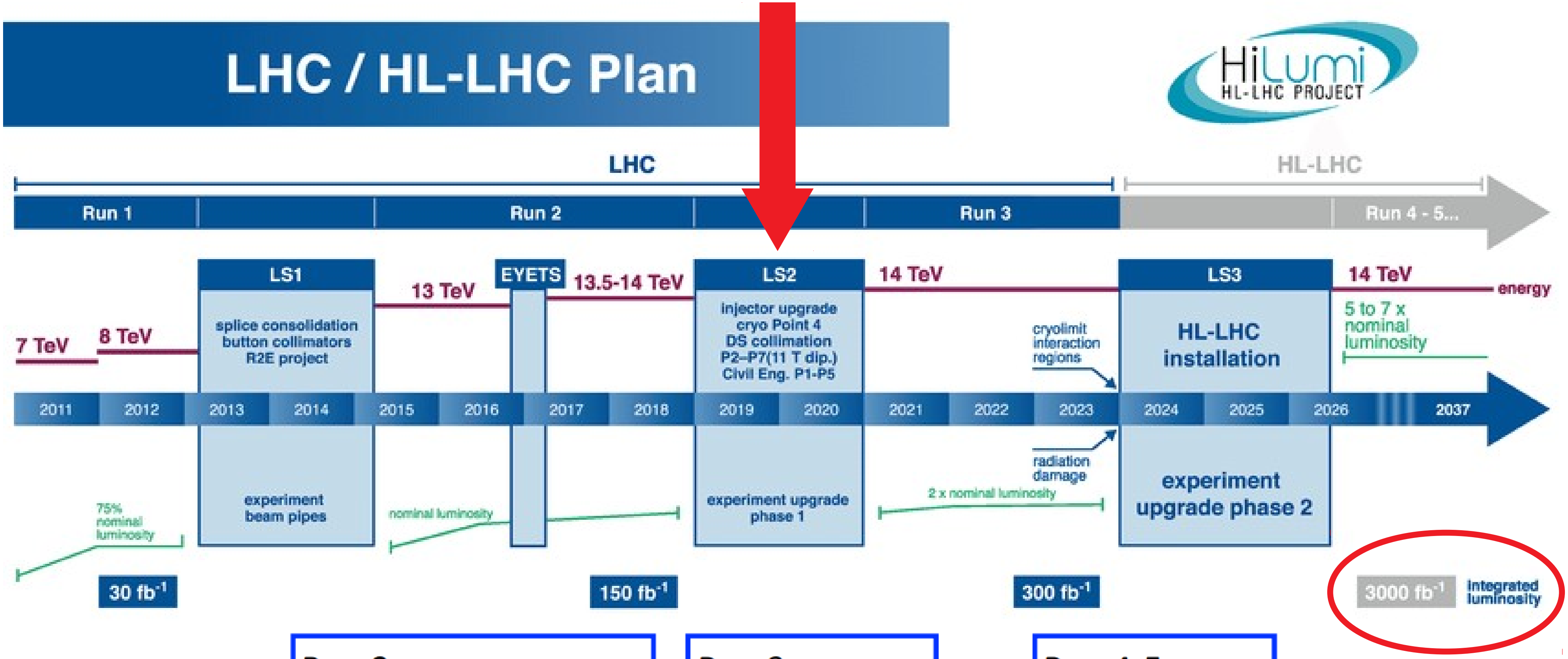

Run 2
<μ>~37
L up to 2.0E34 Hz/cm²

Run 3
<μ>~55
L up to 2.0E34

Run 4-5
<μ>~140-200
L up to 7.5E34

- So far we have collected only ~5% of the total potential dataset!
- Many upgrades to the LHC and the detectors are needed to achieve the final goal

ATLAS Phase-2 upgrades

ATLAS Phase-2 TDRs

New trigger system
organized in 3 levels
Expected trigger rate ~10 kHz

Front-End electronics
in the calorimeter system

Muon System:
Innermost RPC layer for trigger redundancy
Small MDT to sustain higher particle rate
MDT included in trigger

Total replacement of the
Inner Tracker
(silicon pixel and strips)
with better radiation hardness
and up to |η|<4.0

High Granularity
Timing Detector
(forward calorimeter)

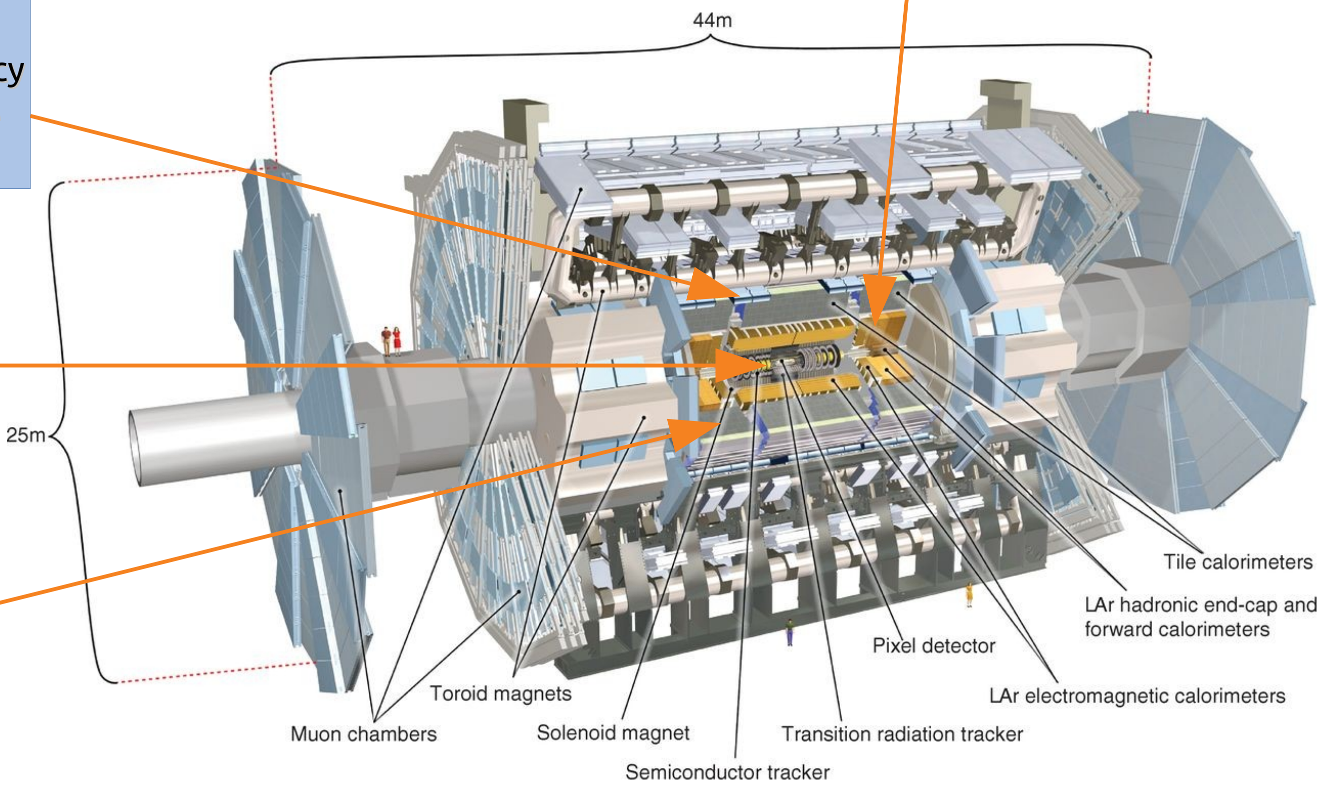

arXiv 1902.00134

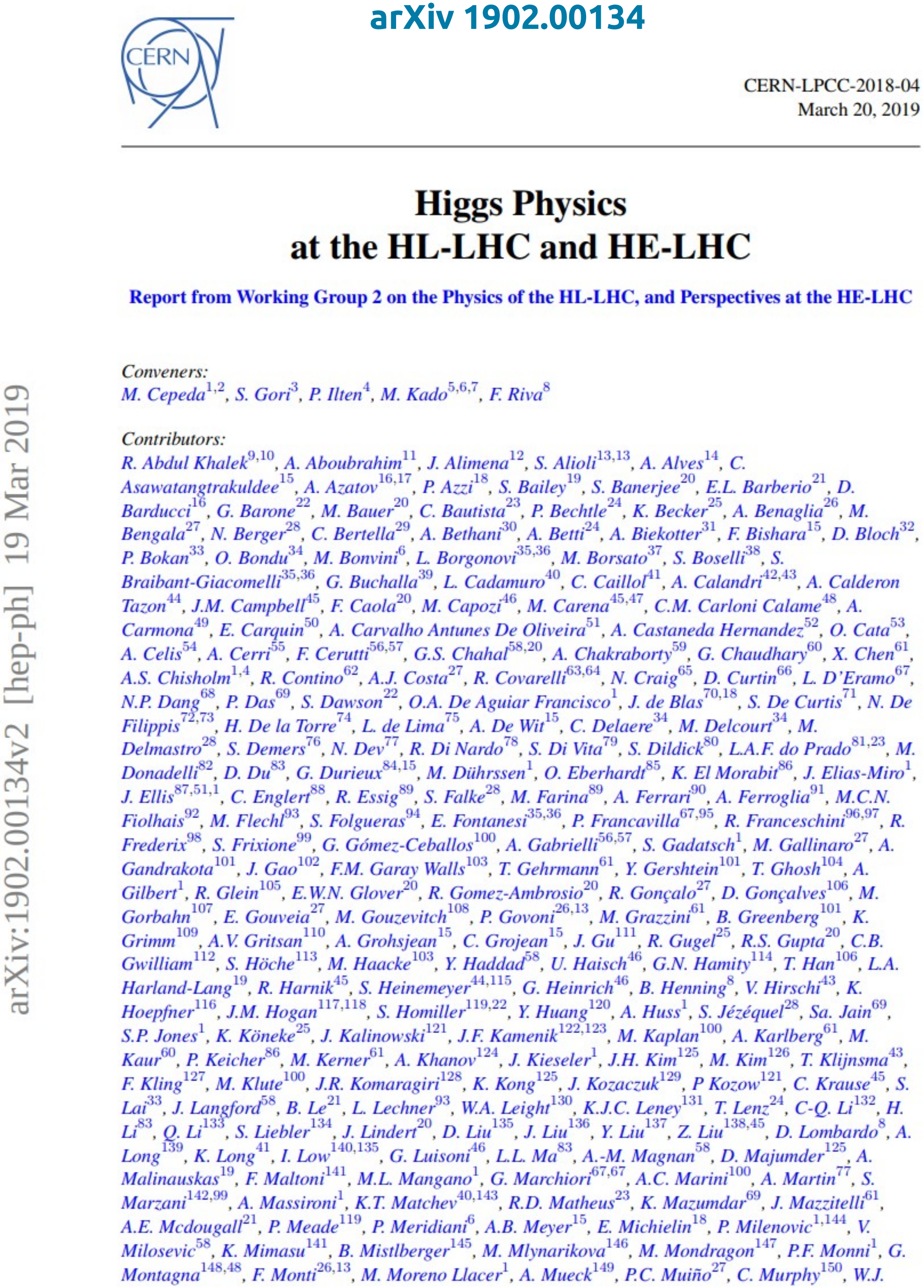

CERN-LPCC-2018-04
March 20, 2019

Higgs Physics
at the HL-LHC and HE-LHC

Report from Working Group 2 on the Physics of the HL-LHC, and Perspectives at the HE-LHC

Conveners:
M. Cepeda[1,2], S. Gori[3], P. Ilten[4], M. Kado[5,6,7], F. Riva[8]

Contributors:
R. Abdul Khalek[9,10], A. Aboubrahim[11], J. Alimena[12], S. Alioli[13,13], A. Alves[14], C. Asawatangtrakuldee[15], A. Azatov[16,17], P. Azzi[18], S. Bailey[19], S. Banerjee[20], E.L. Barberio[21], D. Barducci[16], G. Barone[22], M. Bauer[20], C. Bautista[23], P. Bechtle[24], K. Becker[25], A. Benaglia[26], M. Bengala[27], N. Berger[28], C. Bertella[29], A. Bethani[30], A. Betti[24], A. Biekotter[31], F. Bishara[15], D. Bloch[32], P. Bokan[33], O. Bondu[34], M. Bonvini[6], L. Borgonovi[35,36], M. Borsato[37], S. Boselli[38], S. Braibant-Giacomelli[35,36], G. Buchalla[39], L. Cadamuro[40], C. Caillol[41], A. Calandri[42,43], A. Calderon Tazon[44], J.M. Campbell[45], F. Caola[20], M. Capozi[46], M. Carena[45,47], C.M. Carloni Calame[48], A. Carmona[49], E. Carquin[50], A. Carvalho Antunes De Oliveira[51], A. Castaneda Hernandez[52], O. Cata[53], A. Celis[54], A. Cerri[55], F. Cerutti[56,57], G.S. Chahal[58,20], A. Chakraborty[59], G. Chaudhary[60], X. Chen[61], A.S. Chisholm[1,4], R. Contino[62], A.J. Costa[27], R. Covarelli[63,64], N. Craig[65], D. Curtin[66], L. D'Eramo[67], N.P. Dang[68], P. Das[69], S. Dawson[22], O.A. De Aguiar Francisco[1], J. de Blas[70,18], S. De Curtis[71], N. De Filippis[72,73], H. De la Torre[74], L. de Lima[75], A. De Wit[15], C. Delaere[34], M. Delcourt[34], M. Delmastro[28], S. Demers[76], N. Dev[77], R. Di Nardo[78], S. Di Vita[79], S. Dildick[80], L.A.F. do Prado[81,23], M. Donadelli[82], D. Du[83], G. Durieux[84,15], M. Dührssen[1], O. Eberhardt[85], K. El Morabit[86], J. Elias-Miro[1], J. Ellis[87,51,1], C. Englert[88], R. Essig[89], S. Falke[28], M. Farina[89], A. Ferrari[90], A. Ferroglia[91], M.C.N. Fiolhais[92], M. Flechl[93], S. Folgueras[94], E. Fontanesi[35,36], P. Francavilla[67,95], R. Franceschini[96,97], R. Frederix[98], S. Frixione[99], G. Gómez-Ceballos[100], A. Gabrielli[56,57], S. Gadatsch[1], M. Gallinaro[27], A. Gandrakota[101], J. Gao[102], F.M. Garay Walls[103], T. Gehrmann[61], Y. Gershtein[101], T. Ghosh[104], A. Gilbert[1], R. Glein[105], E.W.N. Glover[20], R. Gomez-Ambrosio[20], R. Gonçalo[27], D. Gonçalves[106], M. Gorbahn[107], E. Gouveia[27], M. Gouzevitch[108], P. Govoni[26,13], M. Grazzini[61], B. Greenberg[101], K. Grimm[109], A.V. Gritsan[110], A. Grohsjean[15], C. Grojean[15], J. Gu[111], R. Gugel[25], R.S. Gupta[20], C.B. Gwilliam[112], S. Höche[113], M. Haacke[103], Y. Haddad[58], U. Haisch[46], G.N. Hamity[114], T. Han[106], L.A. Harland-Lang[19], R. Harnik[45], S. Heinemeyer[44,115], G. Heinrich[46], B. Henning[8], V. Hirschi[43], K. Hoepfner[116], J.M. Hogan[117,118], S. Homiller[119,22], Y. Huang[120], A. Huss[1], S. Jézéquel[28], Sa. Jain[69], S.P. Jones[1], K. Köneke[25], J. Kalinowski[121], J.F. Kamenik[122,123], M. Kaplan[100], A. Karlberg[61], M. Kaur[60], P. Keicher[86], M. Kerner[61], A. Khanov[124], J. Kieseler[1], J.H. Kim[125], M. Kim[126], T. Klijnsma[43], F. Kling[127], M. Klute[100], J.R. Komaragiri[128], K. Kong[125], J. Kozaczuk[129], P Kozow[121], C. Krause[45], S. Lai[33], J. Langford[58], B. Le[21], L. Lechner[93], W.A. Leight[130], K.J.C. Leney[131], T. Lenz[24], C-Q. Li[132], H. Li[83], Q. Li[133], S. Liebler[134], J. Lindert[20], D. Liu[135], J. Liu[136], Y. Liu[137], Z. Liu[138,45], D. Lombardo[8], A. Long[139], K. Long[41], I. Low[140,135], G. Luisoni[46], L.L. Ma[83], A.-M. Magnan[58], D. Majumder[125], A. Malinauskas[19], F. Maltoni[141], M.L. Mangano[1], G. Marchiori[67,67], A.C. Marini[100], A. Martin[77], S. Marzani[142,99], A. Massironi[1], K.T. Matchev[40,143], R.D. Matheus[23], K. Mazumdar[69], J. Mazzitelli[61], A.E. Mcdougall[21], P. Meade[119], P. Meridiani[6], A.B. Meyer[15], E. Michielin[18], P. Milenovic[1,144], V. Milosevic[58], K. Mimasu[141], B. Mistlberger[145], M. Mlynarikova[146], M. Mondragon[147], P.F. Monni[1], G. Montagna[148,48], F. Monti[26,13], M. Moreno Llacer[1], A. Mueck[149], P.C. Muiño[27], C. Murphy[150], W.J.

Systematic uncertainty assumptions

- Two scenarios have been explored with different predictions of the systematic impact at HL-LHC
- Scenario 1 (S1): conservative scenario using the uncertainties of the current Run 2 measurements (not realistic, just for reference)
- Scenario 2 (S2): this scenario implements a reduction of the systematic uncertainties according to the improvements expected to be reached at the end of HL-LHC program in twenty years from now
  - Theoretical uncertainties for signal and background are generally reduced by a factor of 2 (joint study with LHC Higgs Cross-Section Working Group and theory community)
  - Luminosity uncertainty (~1%) w.r.t. the current 2-3%
  - Uncertainty due to the size of MC simulations negligible
  - For certain analyses, some systematic uncertainties are treated in a specific way → details be found here: arXiv 1902.00134v2

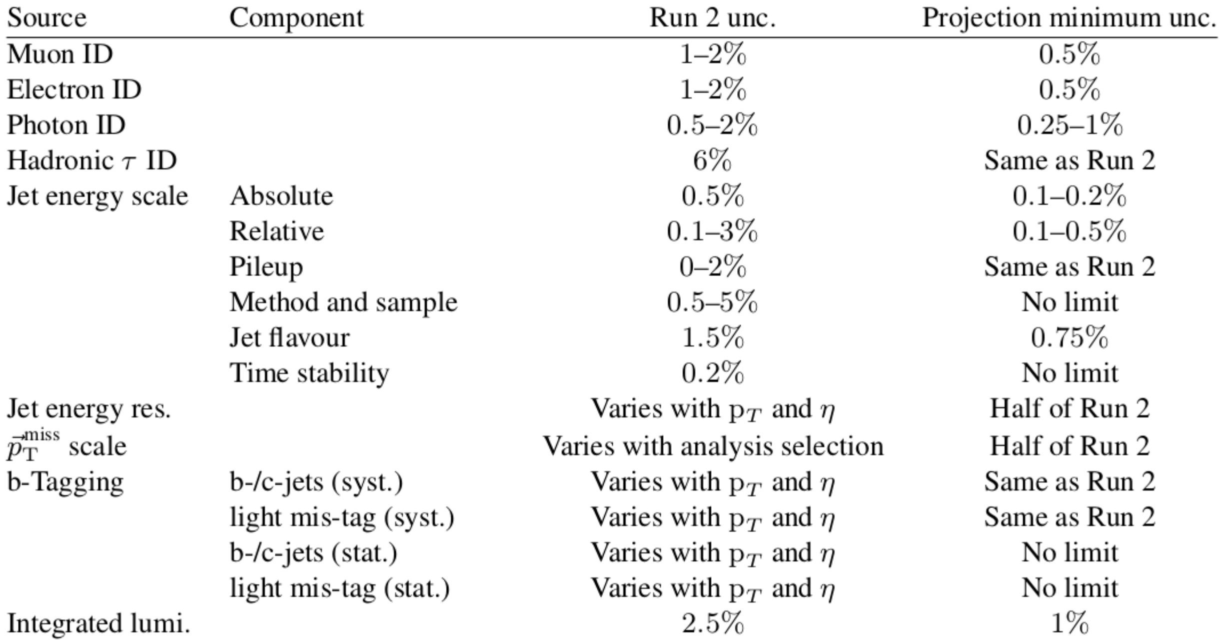

Source	Component	Run 2 unc.	Projection minimum unc.
Muon ID		1–2%	0.5%
Electron ID		1–2%	0.5%
Photon ID		0.5–2%	0.25–1%
Hadronic τ ID		6%	Same as Run 2
Jet energy scale	Absolute	0.5%	0.1–0.2%
	Relative	0.1–3%	0.1–0.5%
	Pileup	0–2%	Same as Run 2
	Method and sample	0.5–5%	No limit
	Jet flavour	1.5%	0.75%
	Time stability	0.2%	No limit
Jet energy res.		Varies with p_T and η	Half of Run 2
$\vec{p}_{\mathrm{T}}^{\mathrm{miss}}$ scale		Varies with analysis selection	Half of Run 2
b-Tagging	b-/c-jets (syst.)	Varies with p_T and η	Same as Run 2
	light mis-tag (syst.)	Varies with p_T and η	Same as Run 2
	b-/c-jets (stat.)	Varies with p_T and η	No limit
	light mis-tag (stat.)	Varies with p_T and η	No limit
Integrated lumi.		2.5%	1%

Systematic uncertainty assumptions

- Two scenarios have been explored with different predictions of the systematic impact at HL-LHC
- Scenario 1 (S1): conservative scenario using the uncertainties of the current Run 2 measurements (not realistic, just for reference)
- Scenario 2 (S2): this scenario implements a reduction of the systematic uncertainties according to the improvements expected to be reached at the end of HL-LHC program in twenty years from now
  - Theoretical uncertainties for signal and background are generally reduced by a factor of 2 (joint study with LHC Higgs Cross-Section Working Group and theory community)
  - Luminosity uncertainty (~1%) w.r.t. the current 2-3%
  - Uncertainty due to the size of MC simulations negligible
  - For certain analyses, some systematic uncertainties are treated in a specific way → details be found here: arXiv 1902.00134v2

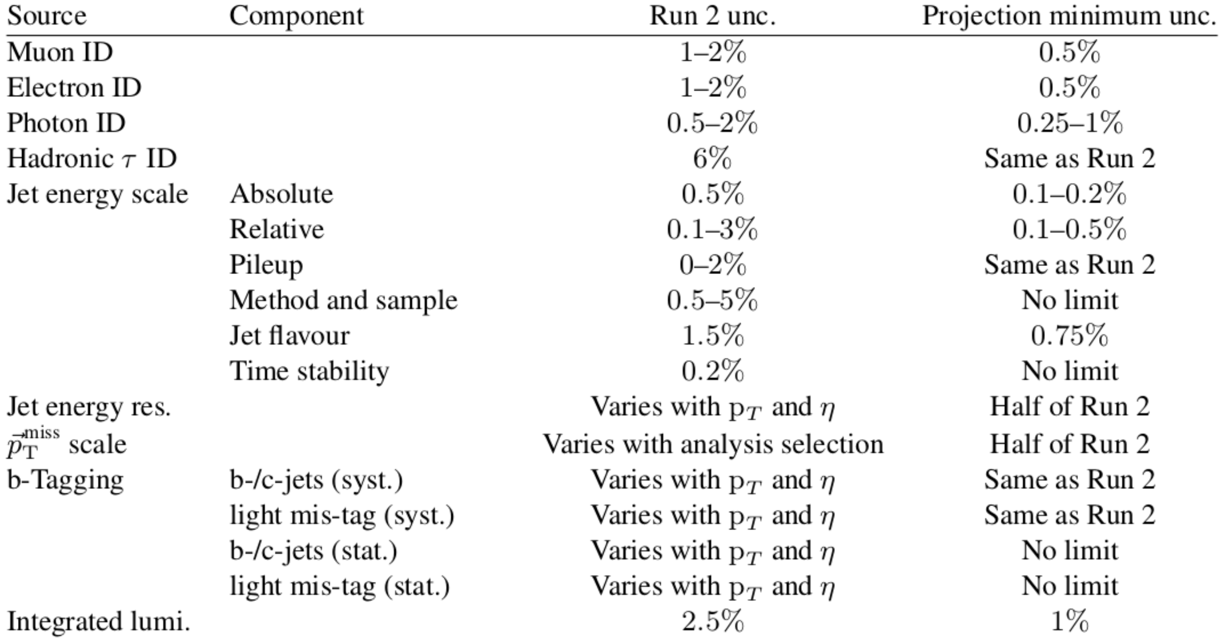

Source	Component	Run 2 unc.	Projection minimum unc.
Muon ID		1–2%	0.5%
Electron ID		1–2%	0.5%
Photon ID		0.5–2%	0.25–1%
Hadronic τ ID		6%	Same as Run 2
Jet energy scale	Absolute	0.5%	0.1–0.2%
	Relative	0.1–3%	0.1–0.5%
	Pileup	0–2%	Same as Run 2
	Method and sample	0.5–5%	No limit
	Jet flavour	1.5%	0.75%
	Time stability	0.2%	No limit
Jet energy res.		Varies with p_T and η	Half of Run 2
$\vec{p}_{\mathrm{T}}^{\mathrm{miss}}$ scale		Varies with analysis selection	Half of Run 2
b-Tagging	b-/c-jets (syst.)	Varies with p_T and η	Same as Run 2
	light mis-tag (syst.)	Varies with p_T and η	Same as Run 2
	b-/c-jets (stat.)	Varies with p_T and η	No limit
	light mis-tag (stat.)	Varies with p_T and η	No limit
Integrated lumi.		2.5%	1%

Projected precision per production (S2)

- ggF will be measured at ~2% level precision, even less combining ATLAS+CMS results
- ttH will be measured at ~4% level precision

Uncertainties on XSec/SM_XSec

Single experiment measurement

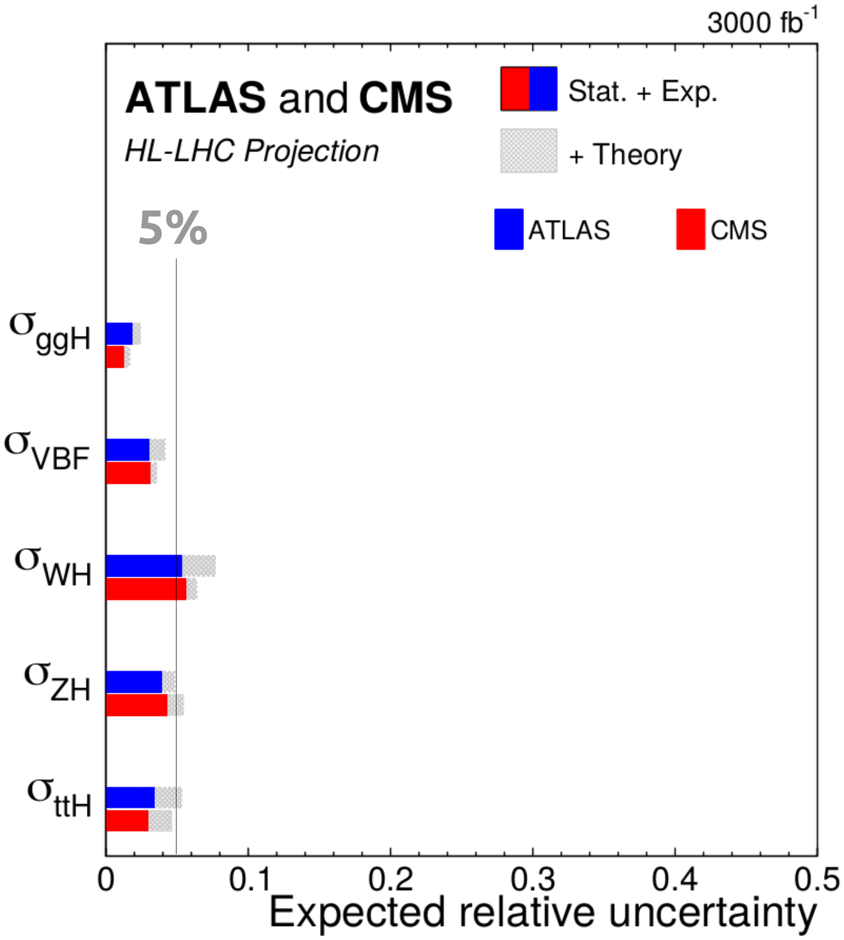

ATLAS+CMS combination

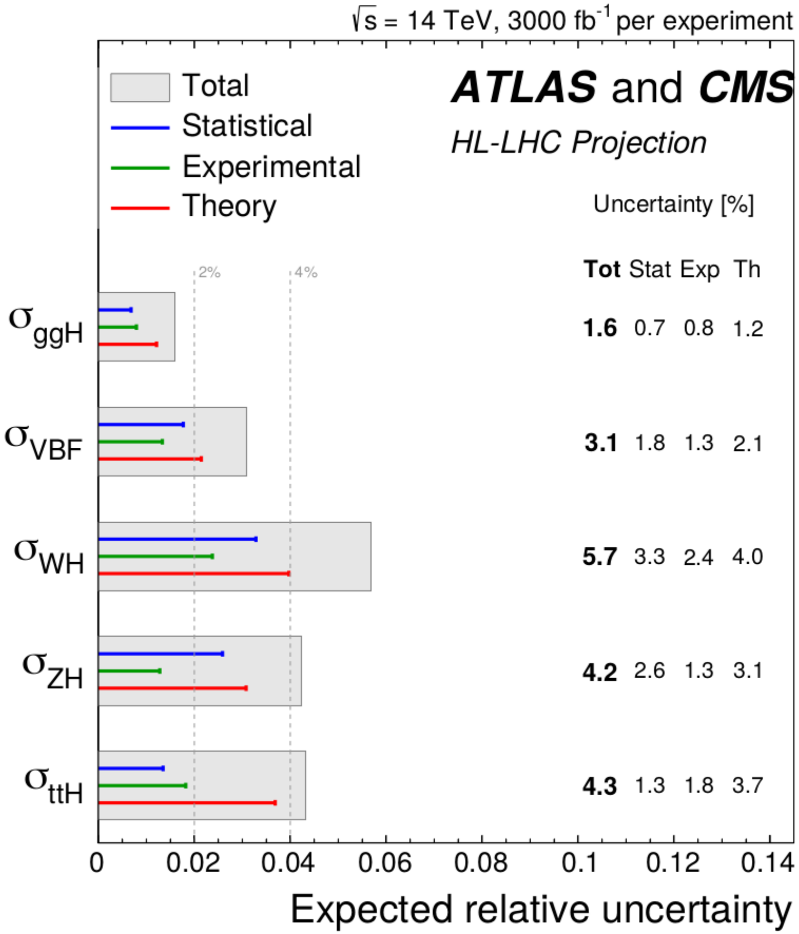

Projected precision per decay (S2)

- Branching fraction with vector bosons will be measured at ~2.5% level precision
- Slightly higher for fermions

Uncertainties on BR/SM_BR

Single experiment measurement

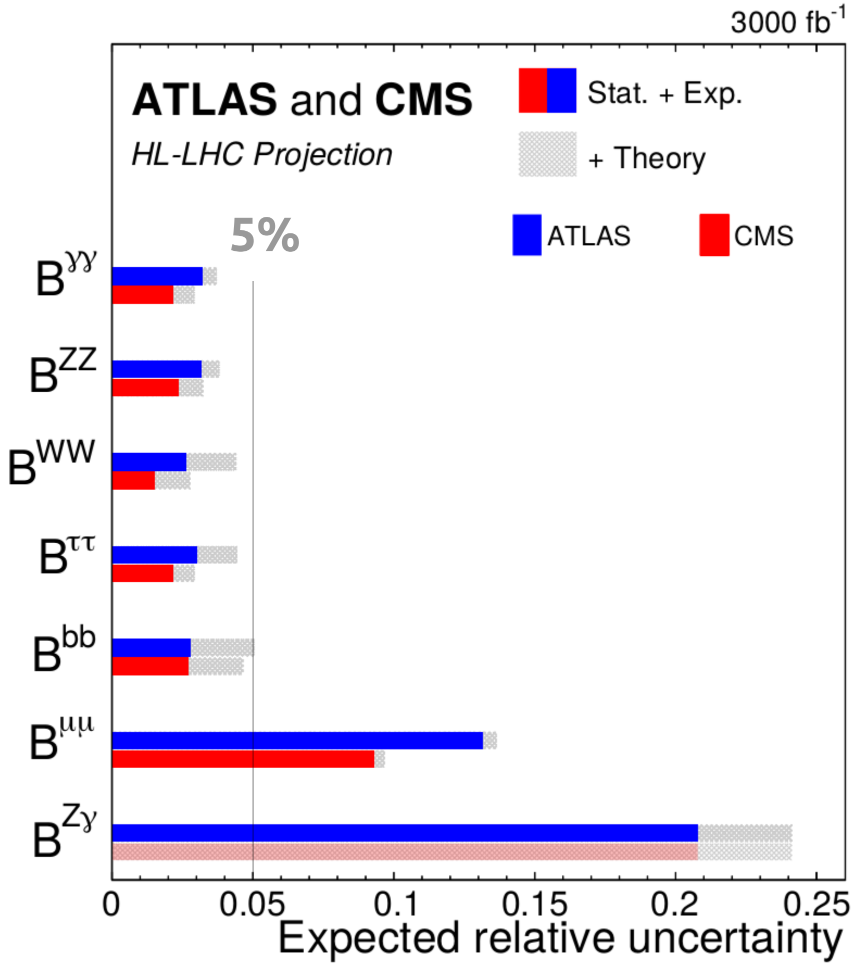

ATLAS+CMS combination

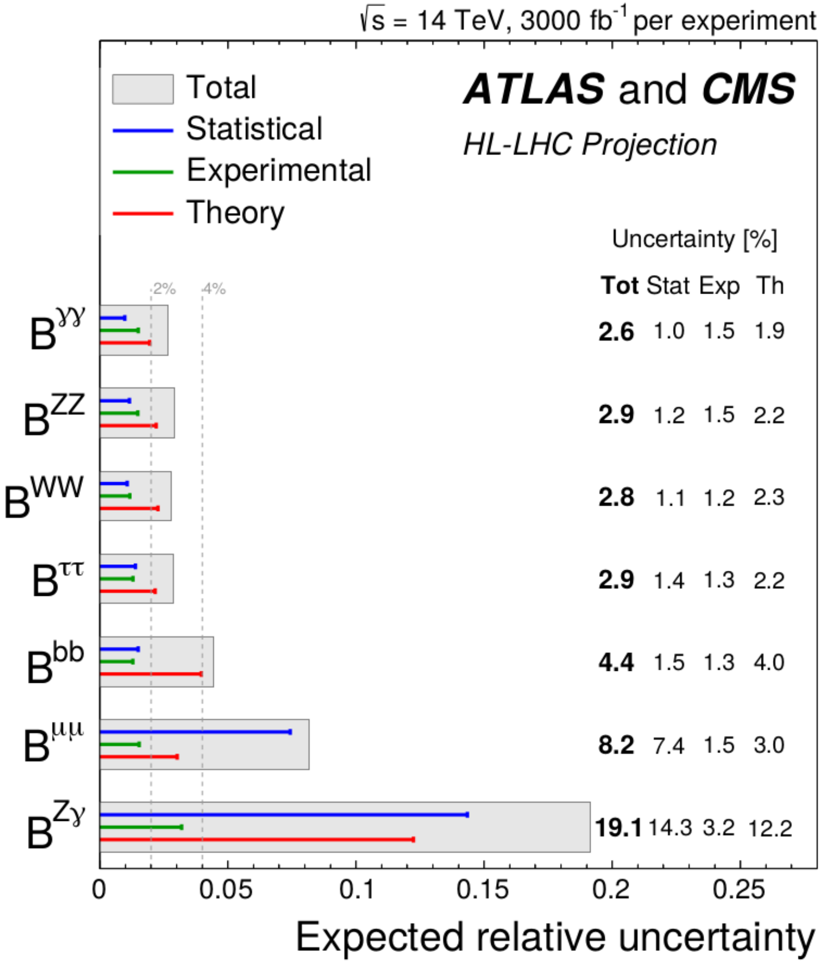

Uncertainty [%]

	Tot	Stat	Exp	Th
$B^{\gamma\gamma}$	**2.6**	1.0	1.5	1.9
B^{ZZ}	**2.9**	1.2	1.5	2.2
B^{WW}	**2.8**	1.1	1.2	2.3
$B^{\tau\tau}$	**2.9**	1.4	1.3	2.2
B^{bb}	**4.4**	1.5	1.3	4.0
$B^{\mu\mu}$	**8.2**	7.4	1.5	3.0
$B^{Z\gamma}$	**19.1**	14.3	3.2	12.2

Projected precision on couplings (S2)

- Most of the couplings will be measured with a precision of ~2%
- Only k_{μ} and $k_{Z\gamma}$ will remain statistically dominated

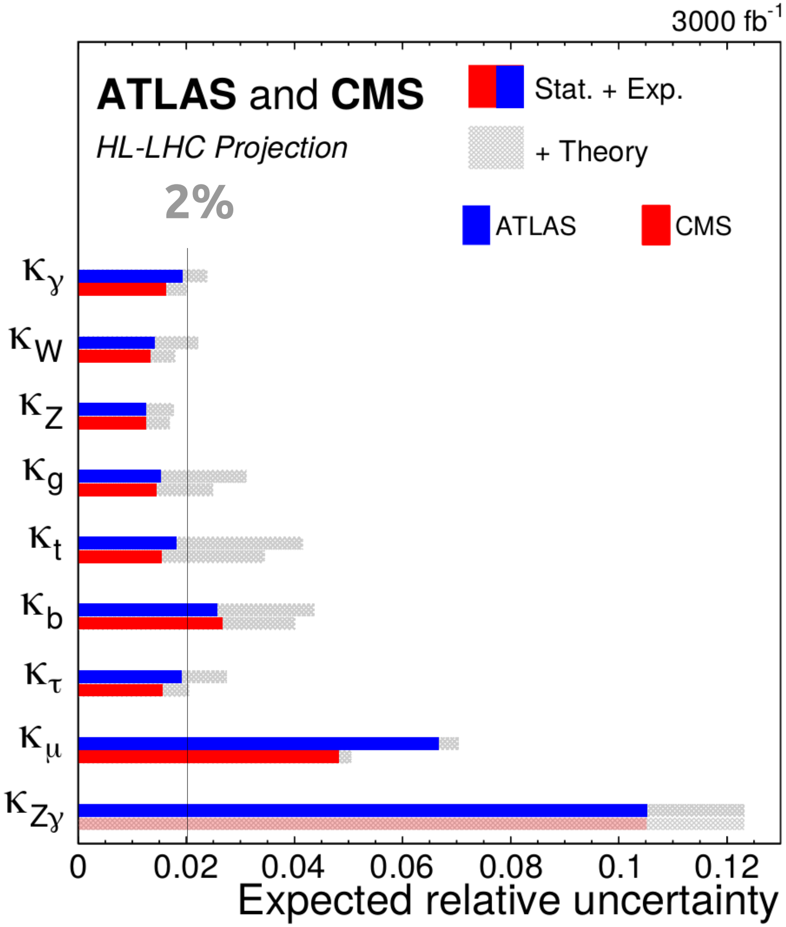

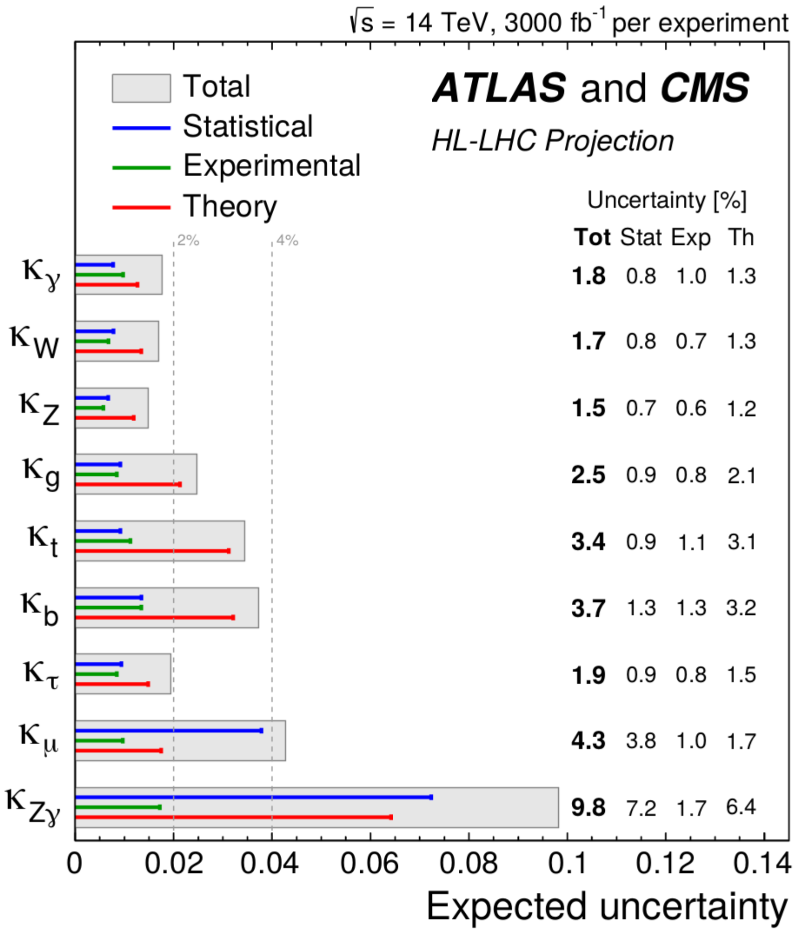

Differential distributions

- We expect to probe Higgs p_T up to 1 TeV with about 10% precision
- Left: ATLAS H→4ℓ + H→γγ combination for 3 different scenarios
- Right: CMS H→4ℓ + H→γγ + H→bb for Scenario 2

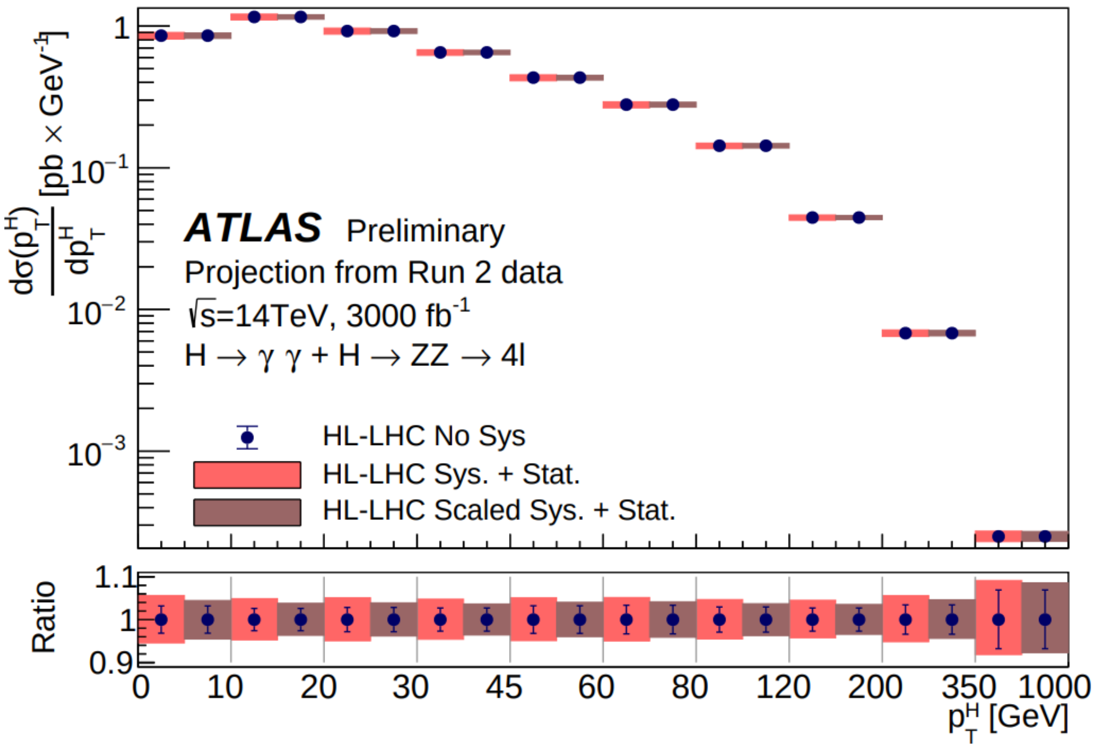

ATL-PHYS-PUB-2018-040

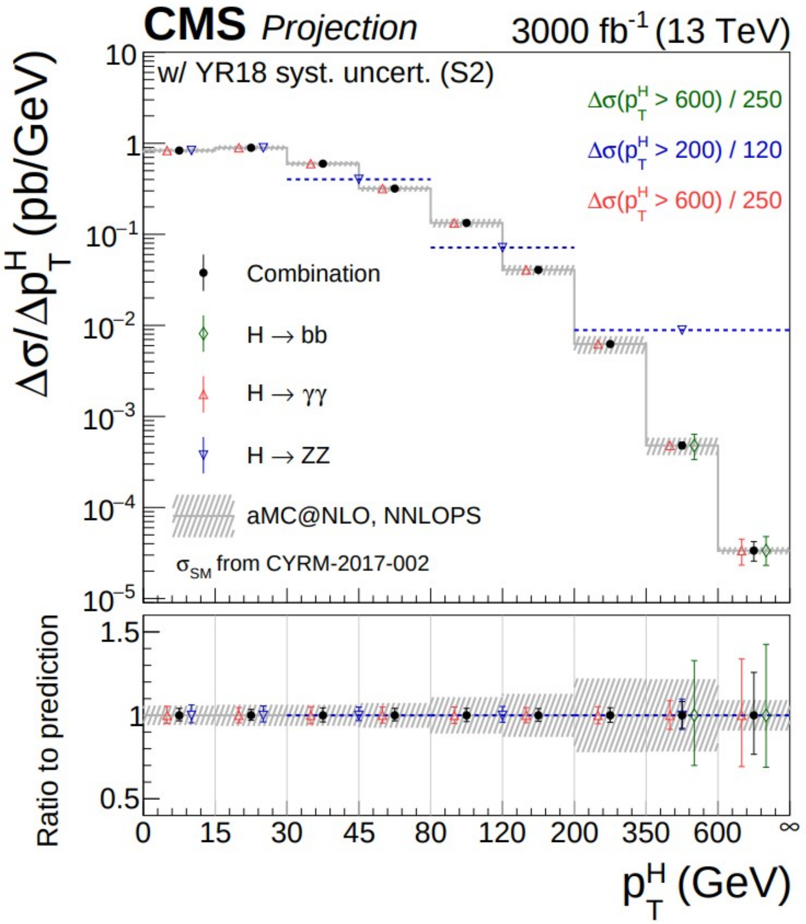

CMS-PAS-FTR-18-011

Prospects on Higgs mass and width

- H→ZZ*→4ℓ channel has the best precision on the Higgs mass and width
- The precision on the mass value will be driven by the muon channel. The table shows the expected precision by ATLAS with 3000 fb^{-1} for different scenarios (improvements due to upgrades in the Inner Tracker)

ATL-PHYS-PUB-2018-054

	Δ_{tot} (MeV)	Δ_{stat} (MeV)	Δ_{syst} (MeV)
Current Detector	52	39	35
μ momentum resolution improvement by 30% or similar	47	30	37
μ momentum resolution/scale improvement of 30% / 50%	38	30	24
μ momentum resolution/scale improvement 30% / 80%	33	30	14

Combining ATLAS and CMS results from 4ℓ and γγ channels a precision on Higgs mass of 10-20 MeV is expected

arXiv 1902.00134

Today: ~220 MeV of uncertainty

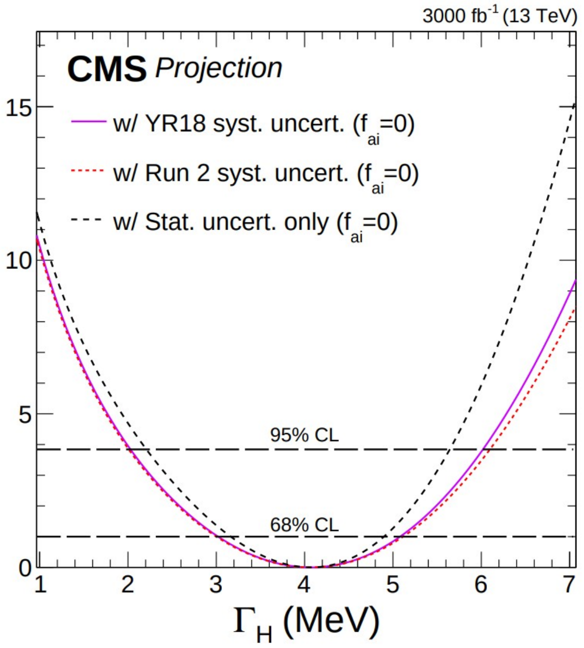

- CMS gives these predictions on Higgs width 95% C.L. interval for both S1 and S2 scenarios:

Parameter	Scenario	Projected 95% CL interval
Γ_{H} (MeV)	S1	$[2.0, 6.1]$
Γ_{H} (MeV)	S2	$[2.0, 6.0]$

to be compared with the current value: $[0.0, 13.7]$

CMS-PAS-FTR-18-011

Prospects on di-Higgs production

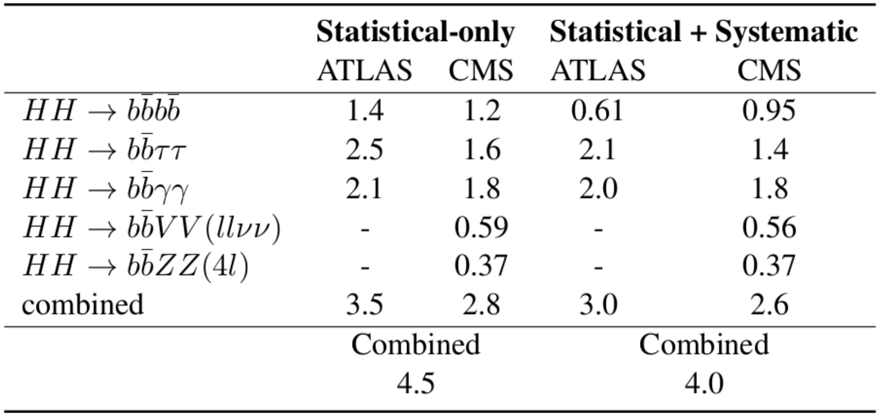

	Statistical-only		Statistical + Systematic	
	ATLAS	CMS	ATLAS	CMS
$HH \to b\bar{b}b\bar{b}$	1.4	1.2	0.61	0.95
$HH \to b\bar{b}\tau\tau$	2.5	1.6	2.1	1.4
$HH \to b\bar{b}\gamma\gamma$	2.1	1.8	2.0	1.8
$HH \to b\bar{b}VV(ll\nu\nu)$	-	0.59	-	0.56
$HH \to b\bar{b}ZZ(4l)$	-	0.37	-	0.37
combined	3.5	2.8	3.0	2.6
	Combined 4.5		Combined 4.0	

- Expected significance of the di-Higgs search for each individual channels as well as their combination with 3000 fb^{-1}

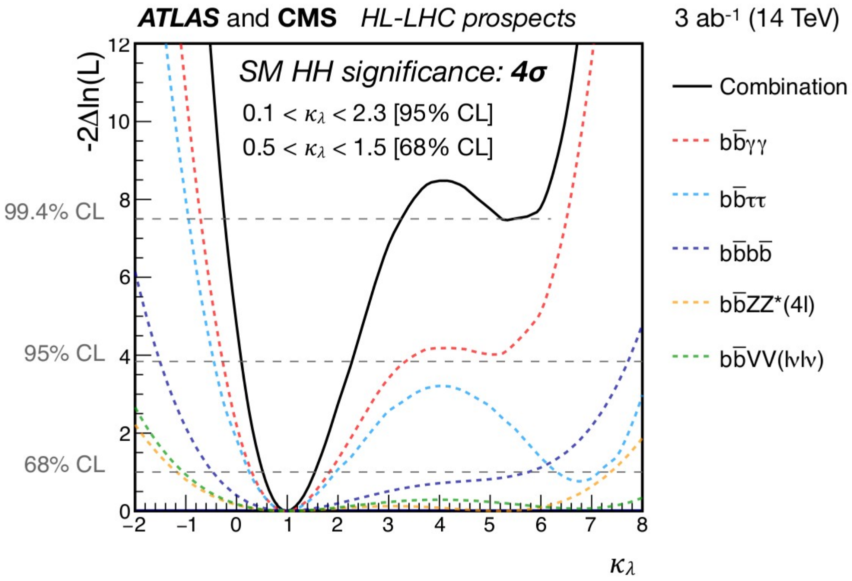

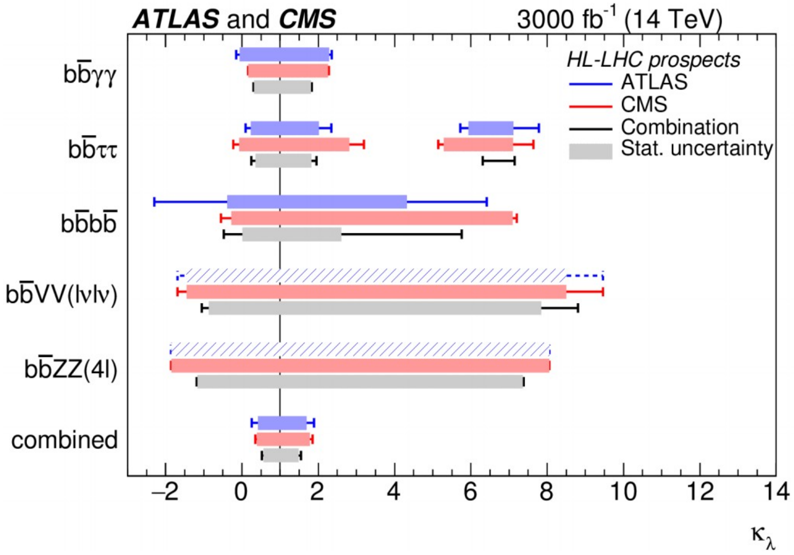

- 95% CL expected limit on λ/λ_{SM}:
  [-0.18,3.6] for CMS
  [-0.40,7.3] for ATLAS
  [0.1,2.3] for the combination

- Second minimum of the likelihood is excluded at 99.4% CL
- Expected a measurement of κ_λ at 50%, if HH is observed with a significance of 4σ

Conclusions

- Overview of the Higgs boson measurements updated with Run 2 data
- Results shown in terms of total and differential cross-sections, couplings and Higgs boson properties (width, mass)
- Bosonic decay channels continue leading Run 2 measurements of ggF (reaching 10% precision) and VBF (reaching 30% level precision) cross-sections
- All the results are consistent with the SM predictions
- Theoretical uncertainties are coming to play an important role
- Many analyses to be updated with the full Run 2 dataset → ATLAS and CMS combinations expected
- The Higgs boson is yet to be fully explored. Currently <5% of the LHC potential has been used. The HL-LHC promises to deliver a much larger dataset where precision measurements will be possible → entering a new era of Higgs precision measurements

Back-up slides

Exotics searches - Summary

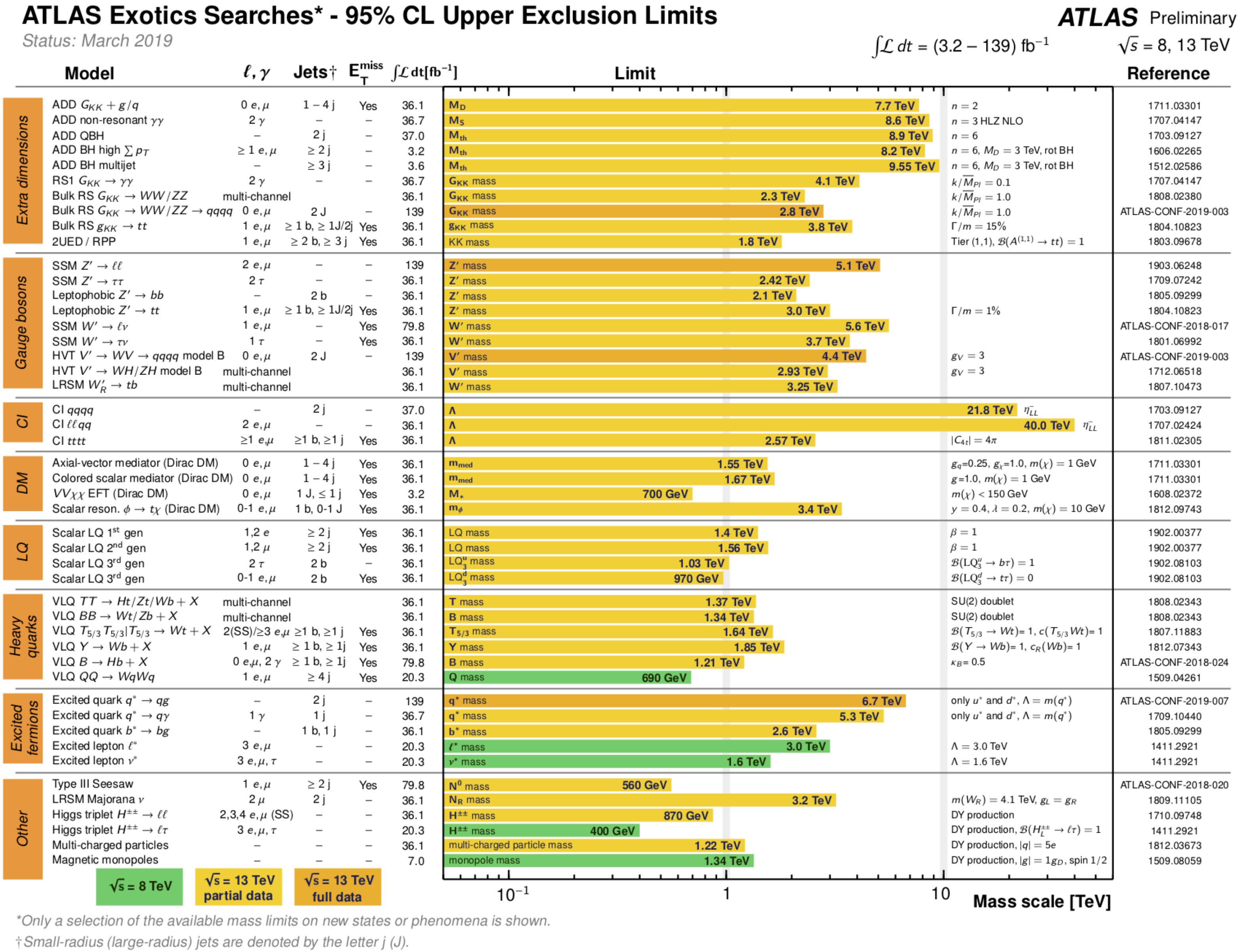

ATLAS Exotics Searches* - 95% CL Upper Exclusion Limits

Status: March 2019

ATLAS Preliminary

$\int \mathcal{L}\, dt = (3.2 - 139)\ \text{fb}^{-1}$

$\sqrt{s} = 8, 13$ TeV

	Model	ℓ, γ	Jets†	E_T^{miss}	$\int \mathcal{L}\, dt[\text{fb}^{-1}]$	Limit		Reference
Extra dimensions	ADD $G_{KK} + g/q$	0 e, μ	1 – 4 j	Yes	36.1	M_D 7.7 TeV	$n = 2$	1711.03301
	ADD non-resonant $\gamma\gamma$	2 γ	–	–	36.7	M_S 8.6 TeV	$n = 3$ HLZ NLO	1707.04147
	ADD QBH	–	2 j	–	37.0	M_{th} 8.9 TeV	$n = 6$	1703.09127
	ADD BH high $\sum p_T$	≥ 1 e, μ	≥ 2 j	–	3.2	M_{th} 8.2 TeV	$n = 6$, $M_D = 3$ TeV, rot BH	1606.02265
	ADD BH multijet	–	≥ 3 j	–	3.6	M_{th} 9.55 TeV	$n = 6$, $M_D = 3$ TeV, rot BH	1512.02586
	RS1 $G_{KK} \to \gamma\gamma$	2 γ	–	–	36.7	G_{KK} mass 4.1 TeV	$k/\overline{M}_{Pl} = 0.1$	1707.04147
	Bulk RS $G_{KK} \to WW/ZZ$	multi-channel			36.1	G_{KK} mass 2.3 TeV	$k/\overline{M}_{Pl} = 1.0$	1808.02380
	Bulk RS $G_{KK} \to WW/ZZ \to qqqq$	0 e, μ	2 J	–	139	G_{KK} mass 2.8 TeV	$k/\overline{M}_{Pl} = 1.0$	ATLAS-CONF-2019-003
	Bulk RS $g_{KK} \to tt$	1 e, μ	≥ 1 b, ≥ 1J/2j	Yes	36.1	g_{KK} mass 3.8 TeV	$\Gamma/m = 15\%$	1804.10823
	2UED / RPP	1 e, μ	≥ 2 b, ≥ 3 j	Yes	36.1	KK mass 1.8 TeV	Tier (1,1), $\mathcal{B}(A^{(1,1)} \to tt) = 1$	1803.09678
Gauge bosons	SSM $Z' \to \ell\ell$	2 e, μ	–	–	139	Z' mass 5.1 TeV		1903.06248
	SSM $Z' \to \tau\tau$	2 τ	–	–	36.1	Z' mass 2.42 TeV		1709.07242
	Leptophobic $Z' \to bb$	–	2 b	–	36.1	Z' mass 2.1 TeV		1805.09299
	Leptophobic $Z' \to tt$	1 e, μ	≥ 1 b, ≥ 1J/2j	Yes	36.1	Z' mass 3.0 TeV	$\Gamma/m = 1\%$	1804.10823
	SSM $W' \to \ell\nu$	1 e, μ	–	Yes	79.8	W' mass 5.6 TeV		ATLAS-CONF-2018-017
	SSM $W' \to \tau\nu$	1 τ	–	Yes	36.1	W' mass 3.7 TeV		1801.06992
	HVT $V' \to WV \to qqqq$ model B	0 e, μ	2 J	–	139	V' mass 4.4 TeV	$g_V = 3$	ATLAS-CONF-2019-003
	HVT $V' \to WH/ZH$ model B	multi-channel			36.1	V' mass 2.93 TeV	$g_V = 3$	1712.06518
	LRSM $W'_R \to tb$	multi-channel			36.1	W' mass 3.25 TeV		1807.10473
CI	CI $qqqq$	–	2 j	–	37.0	Λ 21.8 TeV	η^-_{LL}	1703.09127
	CI $\ell\ell qq$	2 e, μ	–	–	36.1	Λ 40.0 TeV	η^-_{LL}	1707.02424
	CI $tttt$	≥1 e,μ	≥1 b, ≥1 j	Yes	36.1	Λ 2.57 TeV	$\lvert C_{4t}\rvert = 4\pi$	1811.02305
DM	Axial-vector mediator (Dirac DM)	0 e, μ	1 – 4 j	Yes	36.1	m_{med} 1.55 TeV	g_q=0.25, g_χ=1.0, $m(\chi) = 1$ GeV	1711.03301
	Colored scalar mediator (Dirac DM)	0 e, μ	1 – 4 j	Yes	36.1	m_{med} 1.67 TeV	g=1.0, $m(\chi) = 1$ GeV	1711.03301
	$VV\chi\chi$ EFT (Dirac DM)	0 e, μ	1 J, ≤ 1 j	Yes	3.2	M_* 700 GeV	$m(\chi) < 150$ GeV	1608.02372
	Scalar reson. $\phi \to t\chi$ (Dirac DM)	0-1 e, μ	1 b, 0-1 J	Yes	36.1	m_ϕ 3.4 TeV	$y = 0.4$, $\lambda = 0.2$, $m(\chi) = 10$ GeV	1812.09743
LQ	Scalar LQ 1st gen	1,2 e	≥ 2 j	Yes	36.1	LQ mass 1.4 TeV	$\beta = 1$	1902.00377
	Scalar LQ 2nd gen	1,2 μ	≥ 2 j	Yes	36.1	LQ mass 1.56 TeV	$\beta = 1$	1902.00377
	Scalar LQ 3rd gen	2 τ	2 b	–	36.1	LQ_3^u mass 1.03 TeV	$\mathcal{B}(\text{LQ}_3^u \to b\tau) = 1$	1902.08103
	Scalar LQ 3rd gen	0-1 e, μ	2 b	Yes	36.1	LQ_3^d mass 970 GeV	$\mathcal{B}(\text{LQ}_3^d \to t\tau) = 0$	1902.08103
Heavy quarks	VLQ $TT \to Ht/Zt/Wb + X$	multi-channel			36.1	T mass 1.37 TeV	SU(2) doublet	1808.02343
	VLQ $BB \to Wt/Zb + X$	multi-channel			36.1	B mass 1.34 TeV	SU(2) doublet	1808.02343
	VLQ $T_{5/3}T_{5/3} \vert T_{5/3} \to Wt + X$	2(SS)/≥3 e,μ	≥1 b, ≥1 j	Yes	36.1	$T_{5/3}$ mass 1.64 TeV	$\mathcal{B}(T_{5/3} \to Wt)$= 1, $c(T_{5/3}Wt)$= 1	1807.11883
	VLQ $Y \to Wb + X$	1 e, μ	≥ 1 b, ≥ 1j	Yes	36.1	Y mass 1.85 TeV	$\mathcal{B}(Y \to Wb)$= 1, $c_R(Wb)$= 1	1812.07343
	VLQ $B \to Hb + X$	0 e,μ, 2 γ	≥ 1 b, ≥ 1j	Yes	79.8	B mass 1.21 TeV	κ_B= 0.5	ATLAS-CONF-2018-024
	VLQ $QQ \to WqWq$	1 e, μ	≥ 4 j	Yes	20.3	Q mass 690 GeV		1509.04261
Excited fermions	Excited quark $q^* \to qg$	–	2 j	–	139	q^* mass 6.7 TeV	only u^* and d^*, $\Lambda = m(q^*)$	ATLAS-CONF-2019-007
	Excited quark $q^* \to q\gamma$	1 γ	1 j	–	36.7	q^* mass 5.3 TeV	only u^* and d^*, $\Lambda = m(q^*)$	1709.10440
	Excited quark $b^* \to bg$	–	1 b, 1 j	–	36.1	b^* mass 2.6 TeV		1805.09299
	Excited lepton ℓ^*	3 e, μ	–	–	20.3	ℓ^* mass 3.0 TeV	$\Lambda = 3.0$ TeV	1411.2921
	Excited lepton ν^*	3 e, μ, τ	–	–	20.3	ν^* mass 1.6 TeV	$\Lambda = 1.6$ TeV	1411.2921
Other	Type III Seesaw	1 e, μ	≥ 2 j	Yes	79.8	N^0 mass 560 GeV		ATLAS-CONF-2018-020
	LRSM Majorana ν	2 μ	2 j	–	36.1	N_R mass 3.2 TeV	$m(W_R) = 4.1$ TeV, $g_L = g_R$	1809.11105
	Higgs triplet $H^{\pm\pm} \to \ell\ell$	2,3,4 e, μ (SS)	–	–	36.1	$H^{\pm\pm}$ mass 870 GeV	DY production	1710.09748
	Higgs triplet $H^{\pm\pm} \to \ell\tau$	3 e, μ, τ	–	–	20.3	$H^{\pm\pm}$ mass 400 GeV	DY production, $\mathcal{B}(H_L^{\pm\pm} \to \ell\tau) = 1$	1411.2921
	Multi-charged particles	–	–	–	36.1	multi-charged particle mass 1.22 TeV	DY production, $\lvert q\rvert = 5e$	1812.03673
	Magnetic monopoles	–	–	–	7.0	monopole mass 1.34 TeV	DY production, $\lvert g\rvert = 1g_D$, spin 1/2	1509.08059

🟩 $\sqrt{s}$ = 8 TeV

🟨 $\sqrt{s}$ = 13 TeV partial data

🟧 $\sqrt{s}$ = 13 TeV full data

*Only a selection of the available mass limits on new states or phenomena is shown.

†Small-radius (large-radius) jets are denoted by the letter j (J).

Summary of Long Lived particle searches

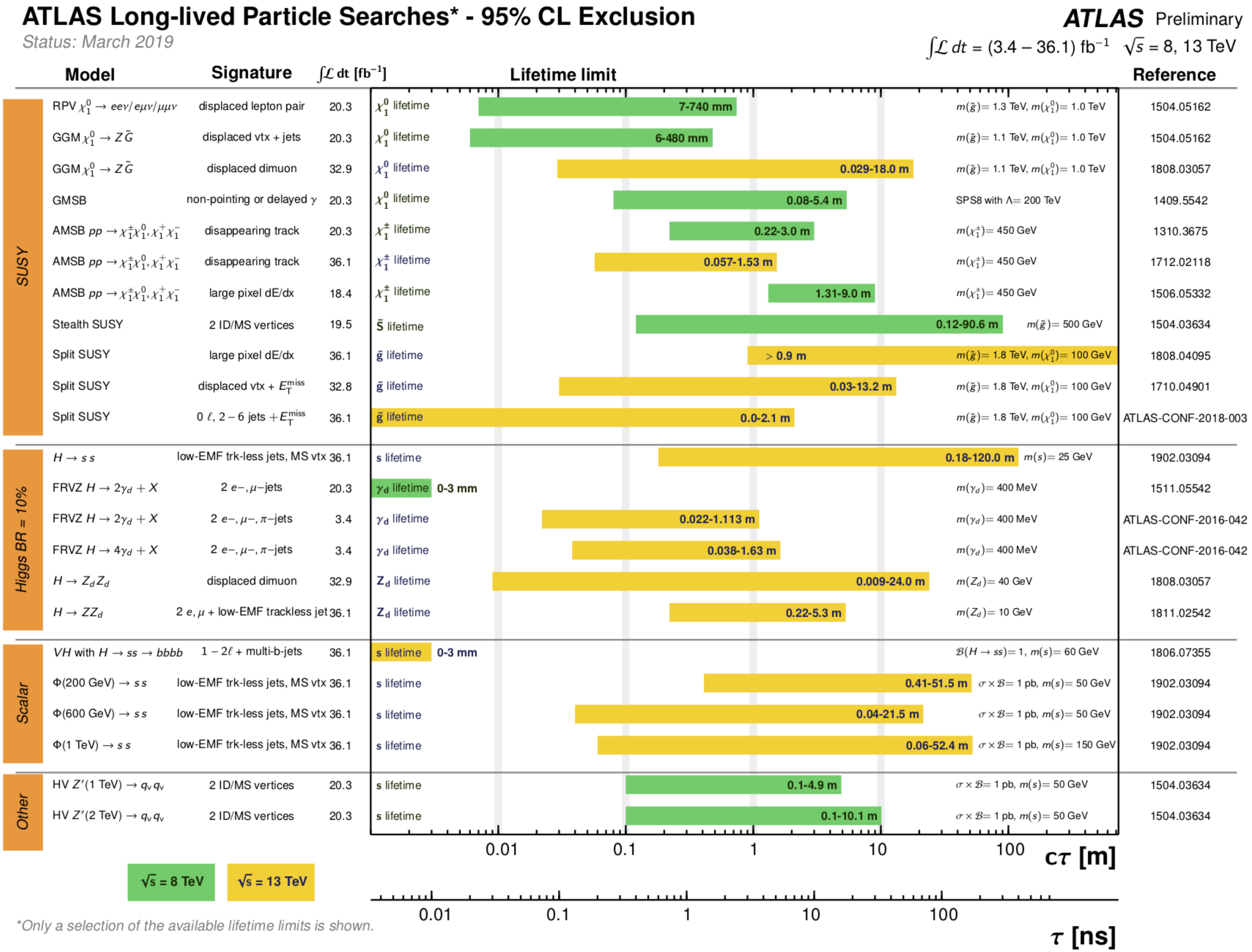

Top mass and ttbar cross-section

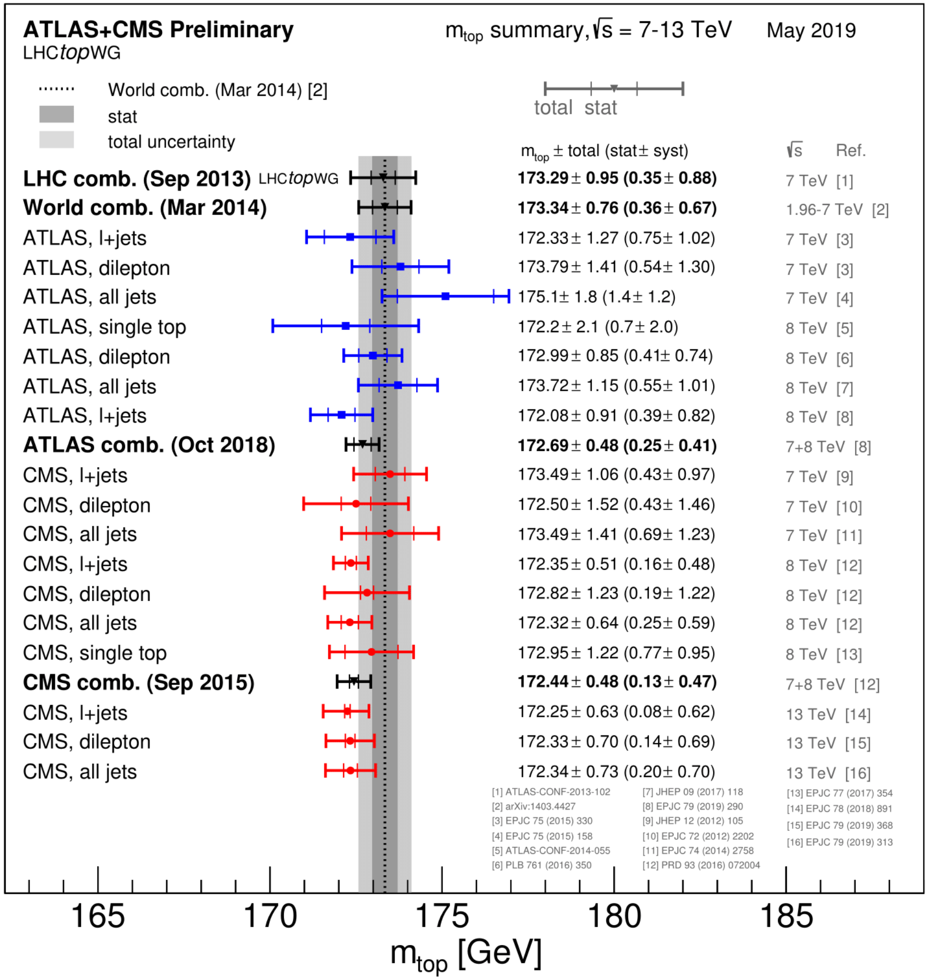

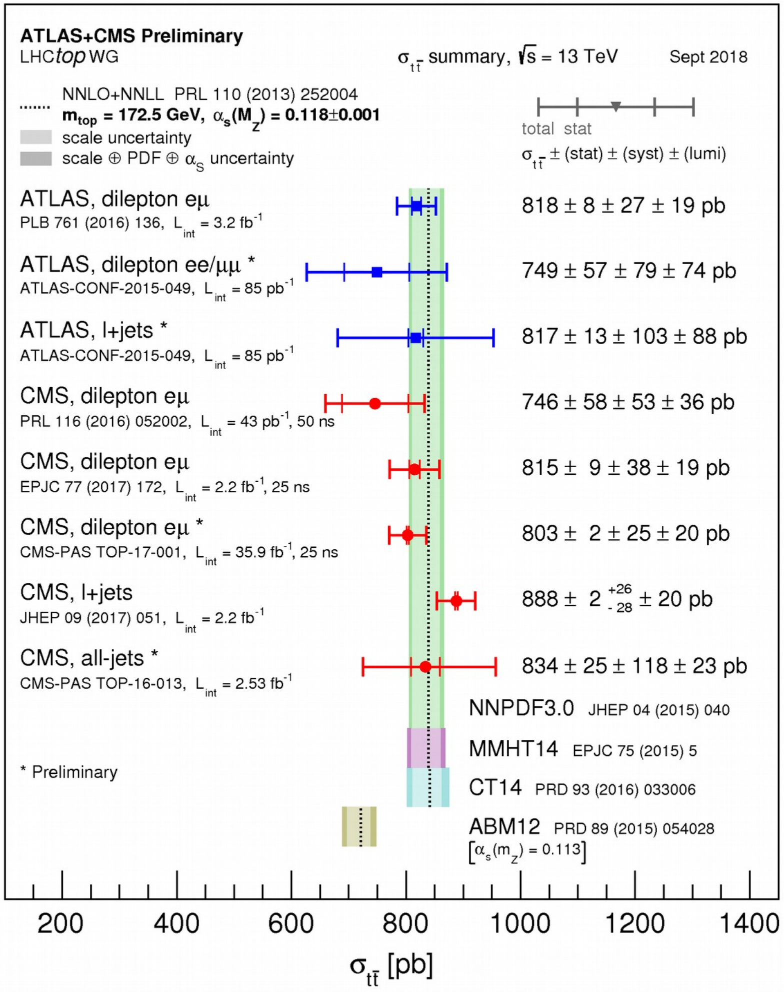

- Precision reached by ATLAS on Top mass: 0.3%
- Waiting for updates at 13 TeV

Searches for high-mass resonances

Di-jet analysis

ATLAS-CONF-2019-007

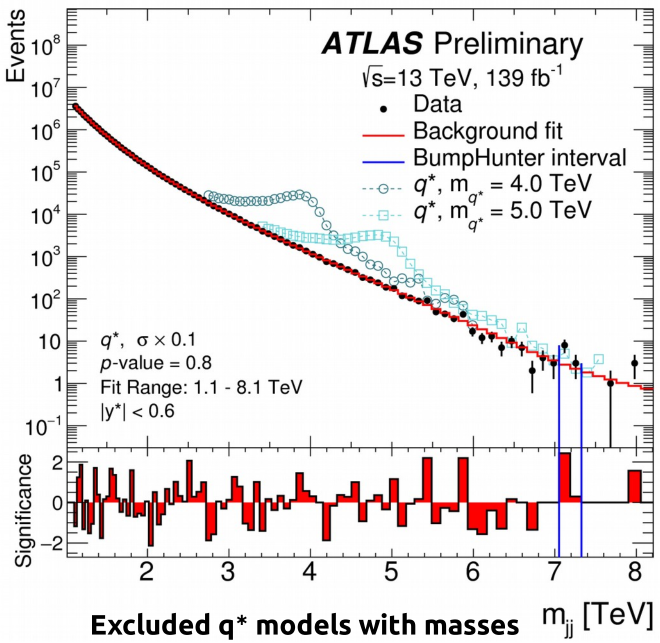

Excluded q* models with masses below 6.7 TeV at 95% CL

Di-lepton analysis (ee and μμ)

arXiv 1903.06248

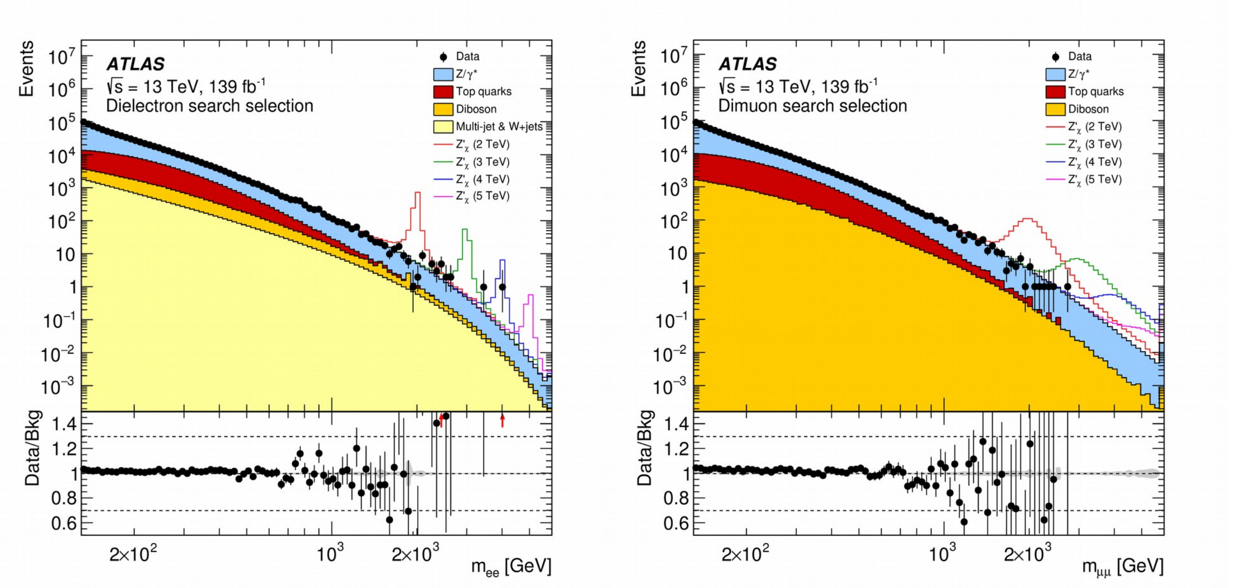

Z' excluded below 4.5 TeV at 95% CL
(W' excluded below 5.1 TeV at 95% CL)

Di-boson analysis (WZ, WW and ZZ)

arXiv 1906.08589

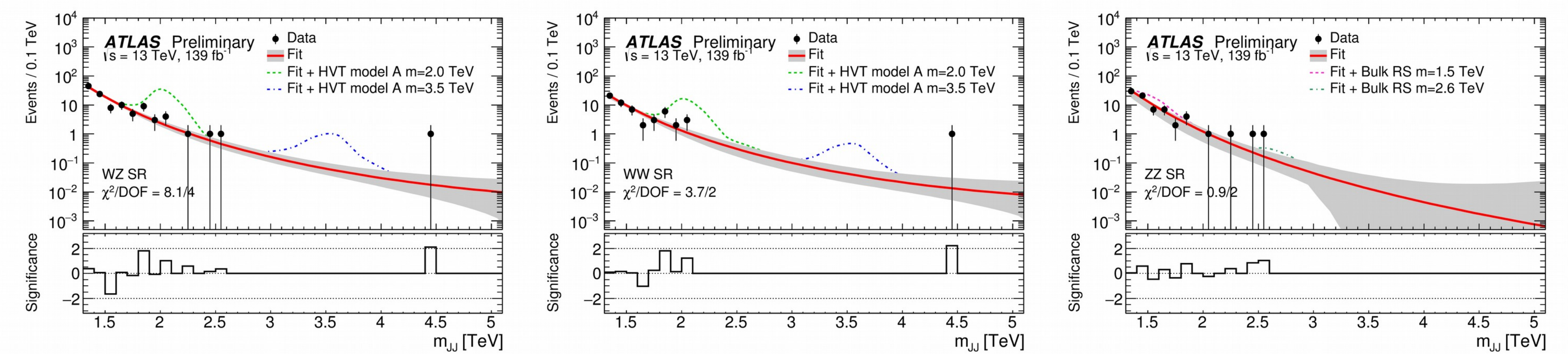

Searches for high-mass resonances

Di-boson analysis (WZ, WW and ZZ)

arXiv 1906.08589

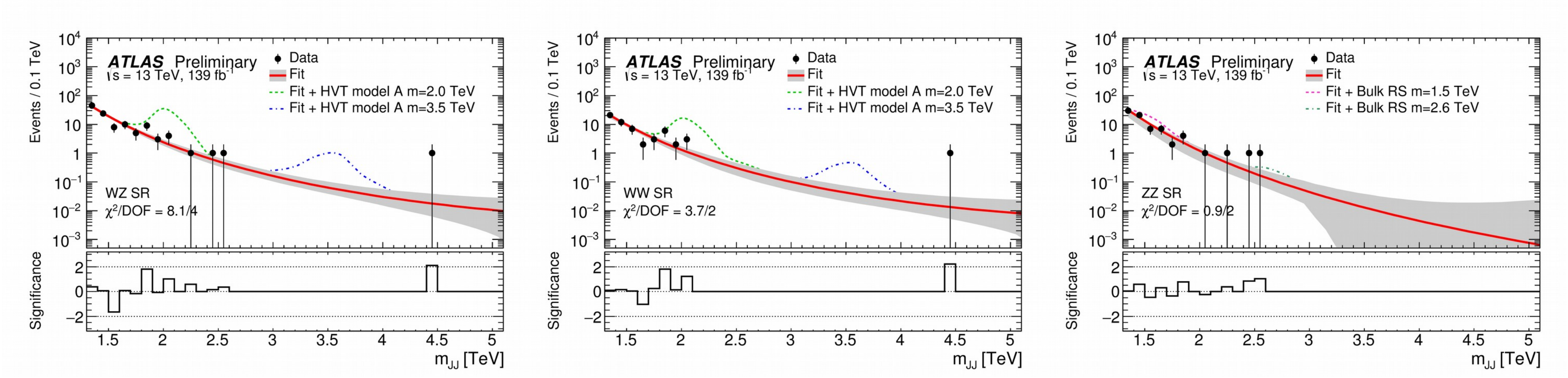

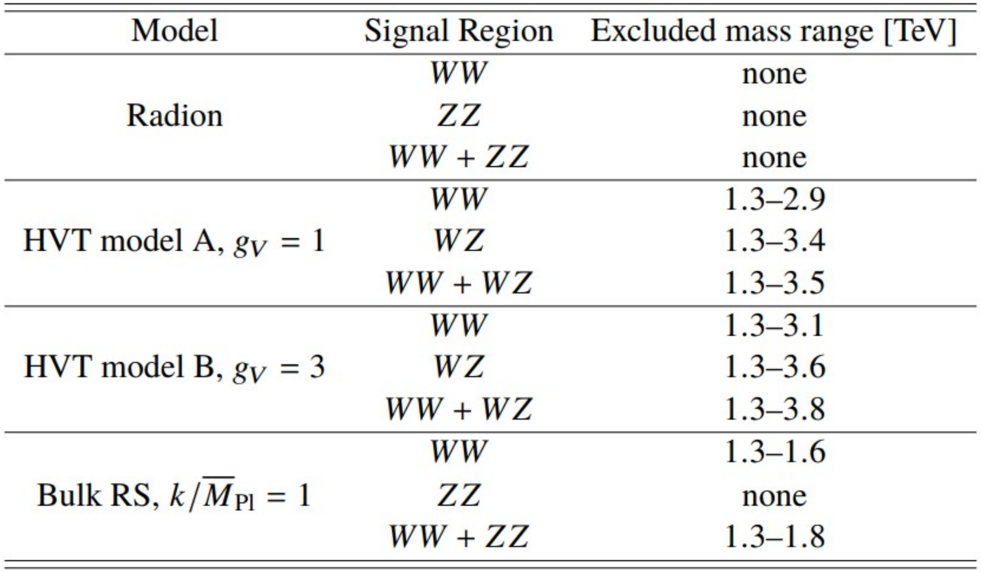

Model	Signal Region	Excluded mass range [TeV]
Radion	WW	none
	ZZ	none
	$WW + ZZ$	none
HVT model A, $g_V = 1$	WW	1.3–2.9
	WZ	1.3–3.4
	$WW + WZ$	1.3–3.5
HVT model B, $g_V = 3$	WW	1.3–3.1
	WZ	1.3–3.6
	$WW + WZ$	1.3–3.8
Bulk RS, $k/\overline{M}_{\rm Pl} = 1$	WW	1.3–1.6
	ZZ	none
	$WW + ZZ$	1.3–1.8

Constraints on Supersymmetry

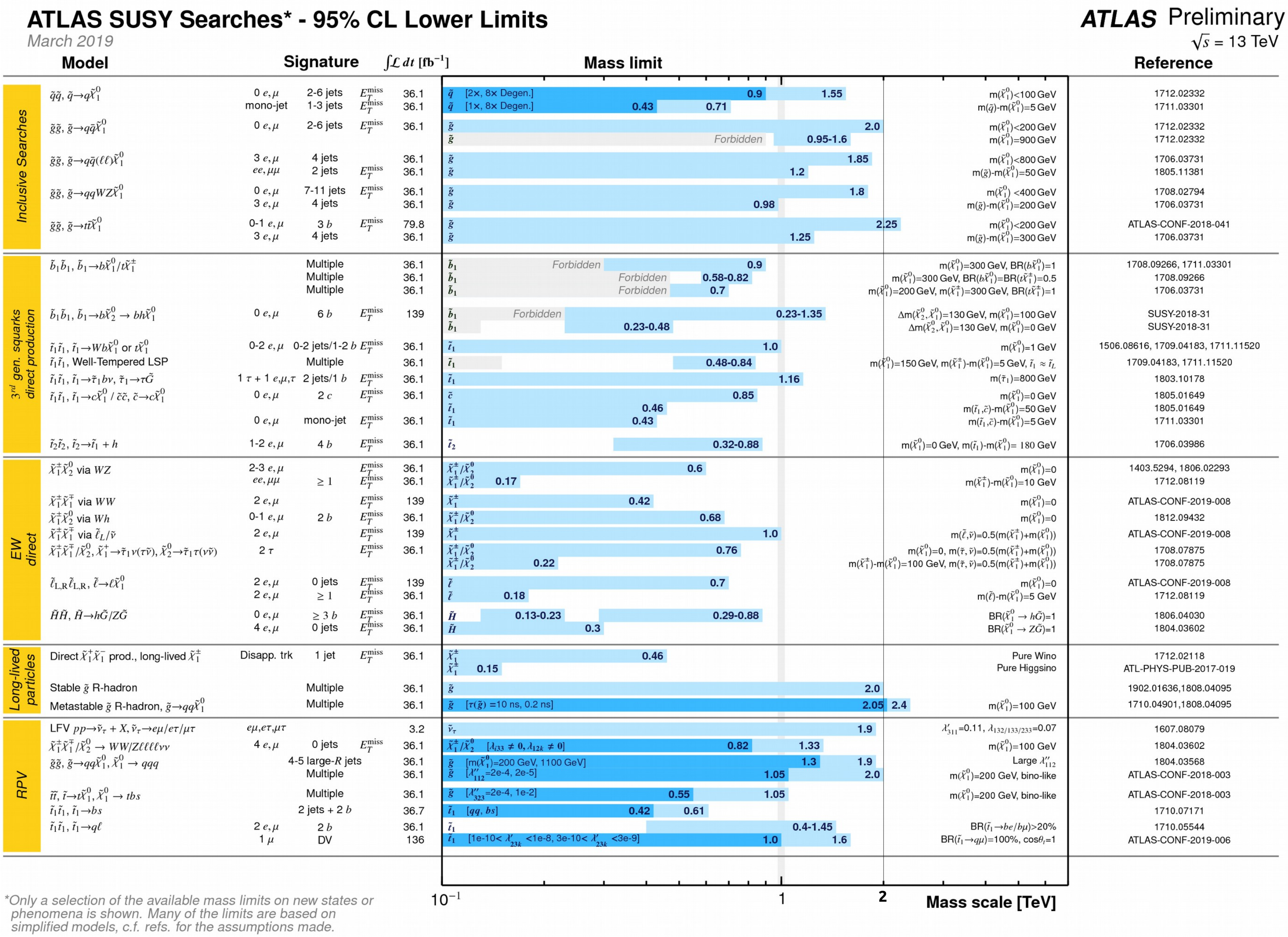

ATLAS SUSY Searches* - 95% CL Lower Limits

March 2019

ATLAS Preliminary
$\sqrt{s}$ = 13 TeV

	Model	Signature			$\int\mathcal{L}\,dt$ [fb^{-1}]	Mass limit			Reference
Inclusive Searches	$\tilde{q}\tilde{q}$, $\tilde{q}\rightarrow q\tilde{\chi}^0_1$	0 e,μ	2-6 jets	E_T^{miss}	36.1	$\tilde{q}$ [2×, 8× Degen.]	0.9 1.55	m($\tilde{\chi}^0_1$)<100 GeV	1712.02332
		mono-jet	1-3 jets	E_T^{miss}	36.1	$\tilde{q}$ [1×, 8× Degen.]	0.43 0.71	m($\tilde{q}$)-m($\tilde{\chi}^0_1$)=5 GeV	1711.03301
	$\tilde{g}\tilde{g}$, $\tilde{g}\rightarrow q\bar{q}\tilde{\chi}^0_1$	0 e,μ	2-6 jets	E_T^{miss}	36.1	$\tilde{g}$	2.0	m($\tilde{\chi}^0_1$)<200 GeV	1712.02332
						$\tilde{g}$ Forbidden	0.95-1.6	m($\tilde{\chi}^0_1$)=900 GeV	1712.02332
	$\tilde{g}\tilde{g}$, $\tilde{g}\rightarrow q\bar{q}(\ell\ell)\tilde{\chi}^0_1$	3 e,μ	4 jets		36.1	$\tilde{g}$	1.85	m($\tilde{\chi}^0_1$)<800 GeV	1706.03731
		$ee,\mu\mu$	2 jets	E_T^{miss}	36.1	$\tilde{g}$	1.2	m($\tilde{g}$)-m($\tilde{\chi}^0_1$)=50 GeV	1805.11381
	$\tilde{g}\tilde{g}$, $\tilde{g}\rightarrow qqWZ\tilde{\chi}^0_1$	0 e,μ	7-11 jets	E_T^{miss}	36.1	$\tilde{g}$	1.8	m($\tilde{\chi}^0_1$) <400 GeV	1708.02794
		3 e,μ	4 jets		36.1	$\tilde{g}$	0.98	m($\tilde{g}$)-m($\tilde{\chi}^0_1$)=200 GeV	1706.03731
	$\tilde{g}\tilde{g}$, $\tilde{g}\rightarrow t\bar{t}\tilde{\chi}^0_1$	0-1 e,μ	3 b	E_T^{miss}	79.8	$\tilde{g}$	2.25	m($\tilde{\chi}^0_1$)<200 GeV	ATLAS-CONF-2018-041
		3 e,μ	4 jets		36.1	$\tilde{g}$	1.25	m($\tilde{g}$)-m($\tilde{\chi}^0_1$)=300 GeV	1706.03731
3^{rd} gen. squarks direct production	$\tilde{b}_1\tilde{b}_1$, $\tilde{b}_1\rightarrow b\tilde{\chi}^0_1/t\tilde{\chi}^\pm_1$		Multiple		36.1	$\tilde{b}_1$ Forbidden	0.9	m($\tilde{\chi}^0_1$)=300 GeV, BR($b\tilde{\chi}^0_1$)=1	1708.09266, 1711.03301
			Multiple		36.1	$\tilde{b}_1$ Forbidden	0.58-0.82	m($\tilde{\chi}^0_1$)=300 GeV, BR($b\tilde{\chi}^0_1$)=BR($t\tilde{\chi}^\pm_1$)=0.5	1708.09266
			Multiple		36.1	$\tilde{b}_1$ Forbidden	0.7	m($\tilde{\chi}^0_1$)=200 GeV, m($\tilde{\chi}^\pm_1$)=300 GeV, BR($t\tilde{\chi}^\pm_1$)=1	1706.03731
	$\tilde{b}_1\tilde{b}_1$, $\tilde{b}_1\rightarrow b\tilde{\chi}^0_2\rightarrow bh\tilde{\chi}^0_1$	0 e,μ	6 b	E_T^{miss}	139	$\tilde{b}_1$ Forbidden	0.23-1.35	Δm($\tilde{\chi}^0_2,\tilde{\chi}^0_1$)=130 GeV, m($\tilde{\chi}^0_1$)=100 GeV	SUSY-2018-31
						$\tilde{b}_1$	0.23-0.48	Δm($\tilde{\chi}^0_2,\tilde{\chi}^0_1$)=130 GeV, m($\tilde{\chi}^0_1$)=0 GeV	SUSY-2018-31
	$\tilde{t}_1\tilde{t}_1$, $\tilde{t}_1\rightarrow Wb\tilde{\chi}^0_1$ or $t\tilde{\chi}^0_1$	0-2 e,μ	0-2 jets/1-2 b	E_T^{miss}	36.1	$\tilde{t}_1$	1.0	m($\tilde{\chi}^0_1$)=1 GeV	1506.08616, 1709.04183, 1711.11520
	$\tilde{t}_1\tilde{t}_1$, Well-Tempered LSP		Multiple		36.1	$\tilde{t}_1$	0.48-0.84	m($\tilde{\chi}^0_1$)=150 GeV, m($\tilde{\chi}^\pm_1$)-m($\tilde{\chi}^0_1$)=5 GeV, $\tilde{t}_1\approx\tilde{t}_L$	1709.04183, 1711.11520
	$\tilde{t}_1\tilde{t}_1$, $\tilde{t}_1\rightarrow\tilde{\tau}_1b\nu$, $\tilde{\tau}_1\rightarrow\tau\tilde{G}$	1 τ + 1 e,μ,τ	2 jets/1 b	E_T^{miss}	36.1	$\tilde{t}_1$	1.16	m($\tilde{\tau}_1$)=800 GeV	1803.10178
	$\tilde{t}_1\tilde{t}_1$, $\tilde{t}_1\rightarrow c\tilde{\chi}^0_1$ / $\tilde{c}\tilde{c}$, $\tilde{c}\rightarrow c\tilde{\chi}^0_1$	0 e,μ	2 c	E_T^{miss}	36.1	$\tilde{c}$	0.85	m($\tilde{\chi}^0_1$)=0 GeV	1805.01649
						$\tilde{t}_1$	0.46	m($\tilde{t}_1$,$\tilde{c}$)-m($\tilde{\chi}^0_1$)=50 GeV	1805.01649
		0 e,μ	mono-jet	E_T^{miss}	36.1	$\tilde{t}_1$	0.43	m($\tilde{t}_1$,$\tilde{c}$)-m($\tilde{\chi}^0_1$)=5 GeV	1711.03301
	$\tilde{t}_2\tilde{t}_2$, $\tilde{t}_2\rightarrow\tilde{t}_1+h$	1-2 e,μ	4 b	E_T^{miss}	36.1	$\tilde{t}_2$	0.32-0.88	m($\tilde{\chi}^0_1$)=0 GeV, m($\tilde{t}_1$)-m($\tilde{\chi}^0_1$)= 180 GeV	1706.03986
EW direct	$\tilde{\chi}^\pm_1\tilde{\chi}^0_2$ via WZ	2-3 e,μ		E_T^{miss}	36.1	$\tilde{\chi}^\pm_1/\tilde{\chi}^0_2$	0.6	m($\tilde{\chi}^0_1$)=0	1403.5294, 1806.02293
		$ee,\mu\mu$	≥ 1	E_T^{miss}	36.1	$\tilde{\chi}^\pm_1/\tilde{\chi}^0_2$	0.17	m($\tilde{\chi}^\pm_1$)-m($\tilde{\chi}^0_1$)=10 GeV	1712.08119
	$\tilde{\chi}^\pm_1\tilde{\chi}^\mp_1$ via WW	2 e,μ		E_T^{miss}	139	$\tilde{\chi}^\pm_1$	0.42	m($\tilde{\chi}^0_1$)=0	ATLAS-CONF-2019-008
	$\tilde{\chi}^\pm_1\tilde{\chi}^0_2$ via Wh	0-1 e,μ	2 b	E_T^{miss}	36.1	$\tilde{\chi}^\pm_1/\tilde{\chi}^0_2$	0.68	m($\tilde{\chi}^0_1$)=0	1812.09432
	$\tilde{\chi}^\pm_1\tilde{\chi}^\mp_1$ via $\tilde{\ell}_L/\tilde{\nu}$	2 e,μ		E_T^{miss}	139	$\tilde{\chi}^\pm_1$	1.0	m($\tilde{\ell},\tilde{\nu}$)=0.5(m($\tilde{\chi}^\pm_1$)+m($\tilde{\chi}^0_1$))	ATLAS-CONF-2019-008
	$\tilde{\chi}^\pm_1\tilde{\chi}^\mp_1/\tilde{\chi}^0_2$, $\tilde{\chi}^+_1\rightarrow\tilde{\tau}_1\nu(\tau\tilde{\nu})$, $\tilde{\chi}^0_2\rightarrow\tilde{\tau}_1\tau(\nu\tilde{\nu})$	2 τ		E_T^{miss}	36.1	$\tilde{\chi}^\pm_1/\tilde{\chi}^0_2$	0.76	m($\tilde{\chi}^0_1$)=0, m($\tilde{\tau},\tilde{\nu}$)=0.5(m($\tilde{\chi}^\pm_1$)+m($\tilde{\chi}^0_1$))	1708.07875
						$\tilde{\chi}^\pm_1/\tilde{\chi}^0_2$	0.22	m($\tilde{\chi}^\pm_1$)-m($\tilde{\chi}^0_1$)=100 GeV, m($\tilde{\tau},\tilde{\nu}$)=0.5(m($\tilde{\chi}^\pm_1$)+m($\tilde{\chi}^0_1$))	1708.07875
	$\tilde{\ell}_{\text{L,R}}\tilde{\ell}_{\text{L,R}}$, $\tilde{\ell}\rightarrow\ell\tilde{\chi}^0_1$	2 e,μ	0 jets	E_T^{miss}	139	$\tilde{\ell}$	0.7	m($\tilde{\chi}^0_1$)=0	ATLAS-CONF-2019-008
		2 e,μ	≥ 1	E_T^{miss}	36.1	$\tilde{\ell}$	0.18	m($\tilde{\ell}$)-m($\tilde{\chi}^0_1$)=5 GeV	1712.08119
	$\tilde{H}\tilde{H}$, $\tilde{H}\rightarrow h\tilde{G}/Z\tilde{G}$	0 e,μ	≥ 3 b	E_T^{miss}	36.1	$\tilde{H}$	0.13-0.23 0.29-0.88	BR($\tilde{\chi}^0_1\rightarrow h\tilde{G}$)=1	1806.04030
		4 e,μ	0 jets	E_T^{miss}	36.1	$\tilde{H}$	0.3	BR($\tilde{\chi}^0_1\rightarrow Z\tilde{G}$)=1	1804.03602
Long-lived particles	Direct $\tilde{\chi}^+_1\tilde{\chi}^-_1$ prod., long-lived $\tilde{\chi}^\pm_1$	Disapp. trk	1 jet	E_T^{miss}	36.1	$\tilde{\chi}^\pm_1$	0.46	Pure Wino	1712.02118
						$\tilde{\chi}^\pm_1$	0.15	Pure Higgsino	ATL-PHYS-PUB-2017-019
	Stable $\tilde{g}$ R-hadron		Multiple		36.1	$\tilde{g}$	2.0		1902.01636,1808.04095
	Metastable $\tilde{g}$ R-hadron, $\tilde{g}\rightarrow qq\tilde{\chi}^0_1$		Multiple		36.1	$\tilde{g}$ [$\tau(\tilde{g})$ =10 ns, 0.2 ns]	2.05 2.4	m($\tilde{\chi}^0_1$)=100 GeV	1710.04901,1808.04095
RPV	LFV $pp\rightarrow\tilde{\nu}_\tau+X$, $\tilde{\nu}_\tau\rightarrow e\mu/e\tau/\mu\tau$	$e\mu$,$e\tau$,$\mu\tau$			3.2	$\tilde{\nu}_\tau$	1.9	λ'_{311}=0.11, $\lambda_{132/133/233}$=0.07	1607.08079
	$\tilde{\chi}^\pm_1\tilde{\chi}^\mp_1/\tilde{\chi}^0_2\rightarrow WW/Z\ell\ell\ell\ell\nu\nu$	4 e,μ	0 jets	E_T^{miss}	36.1	$\tilde{\chi}^\pm_1/\tilde{\chi}^0_2$ [$\lambda_{i33}\neq 0, \lambda_{12k}\neq 0$]	0.82 1.33	m($\tilde{\chi}^0_1$)=100 GeV	1804.03602
	$\tilde{g}\tilde{g}$, $\tilde{g}\rightarrow qq\tilde{\chi}^0_1$, $\tilde{\chi}^0_1\rightarrow qqq$		4-5 large-R jets		36.1	$\tilde{g}$ [m($\tilde{\chi}^0_1$)=200 GeV, 1100 GeV]	1.3 1.9	Large λ''_{112}	1804.03568
			Multiple		36.1	$\tilde{g}$ [λ''_{112}=2e-4, 2e-5]	1.05 2.0	m($\tilde{\chi}^0_1$)=200 GeV, bino-like	ATLAS-CONF-2018-003
	$\tilde{t}\tilde{t}$, $\tilde{t}\rightarrow t\tilde{\chi}^0_1$, $\tilde{\chi}^0_1\rightarrow tbs$		Multiple		36.1	$\tilde{g}$ [λ''_{323}=2e-4, 1e-2]	0.55 1.05	m($\tilde{\chi}^0_1$)=200 GeV, bino-like	ATLAS-CONF-2018-003
	$\tilde{t}_1\tilde{t}_1$, $\tilde{t}_1\rightarrow bs$		2 jets + 2 b		36.7	$\tilde{t}_1$ [qq, bs]	0.42 0.61		1710.07171
	$\tilde{t}_1\tilde{t}_1$, $\tilde{t}_1\rightarrow q\ell$	2 e,μ	2 b		36.1	$\tilde{t}_1$	0.4-1.45	BR($\tilde{t}_1\rightarrow be/b\mu$)>20%	1710.05544
		1 μ	DV		136	$\tilde{t}_1$ [1e-10< λ'_{23k} <1e-8, 3e-10< λ'_{23k} <3e-9]	1.0 1.6	BR($\tilde{t}_1\rightarrow q\mu$)=100%, cos$\theta_t$=1	ATLAS-CONF-2019-006

*Only a selection of the available mass limits on new states or phenomena is shown. Many of the limits are based on simplified models, c.f. refs. for the assumptions made.

R-parity violating

Constraints on Supersymmetry

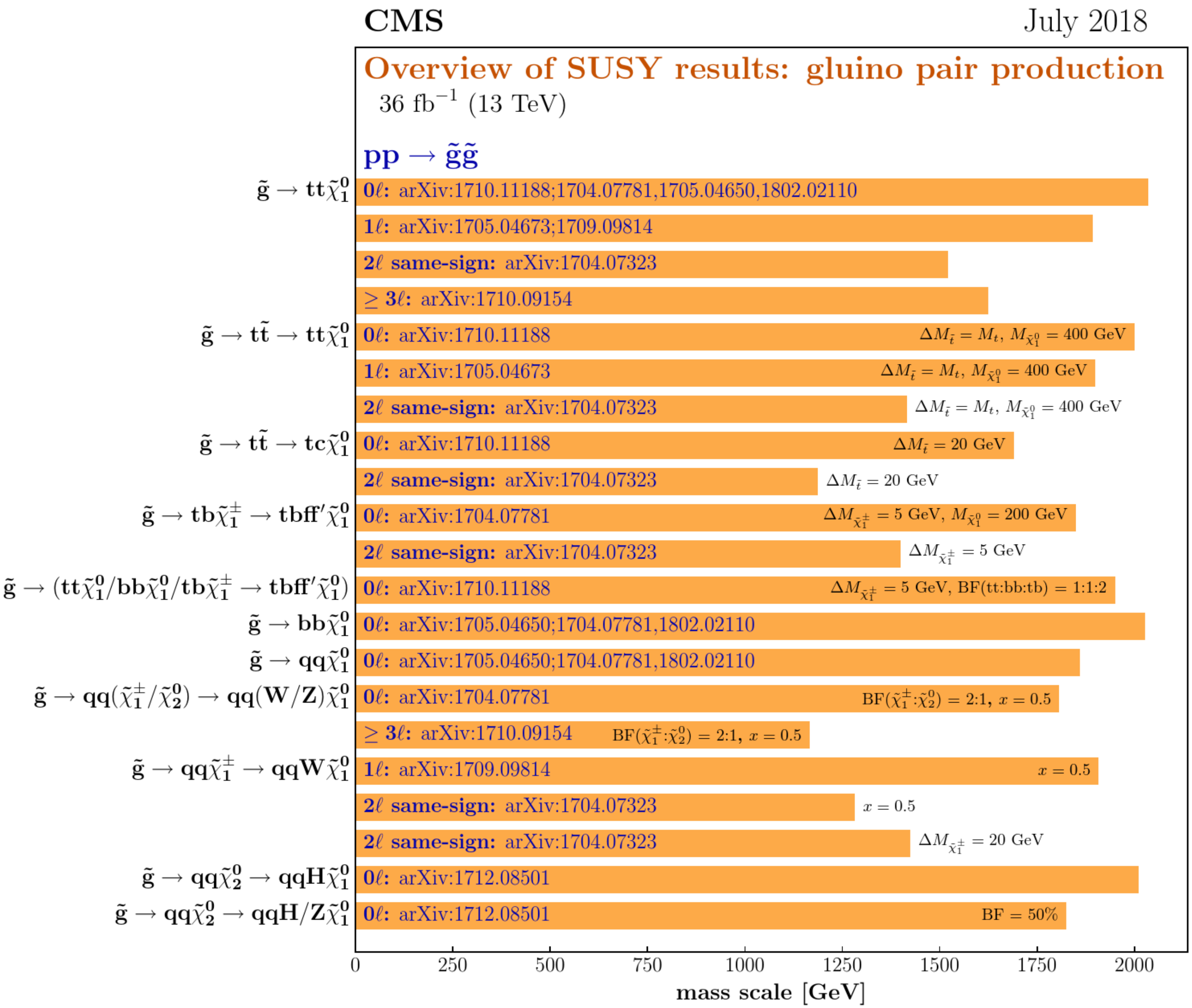

Selection of observed limits at 95% C.L. (theory uncertainties are not included). Probe **up to** the quoted mass limit for light LSPs unless stated otherwise. The quantities ΔM and x represent the absolute mass difference between the primary sparticle and the LSP, and the difference between the intermediate sparticle and the LSP relative to ΔM, respectively, unless indicated otherwise.

Constraints on Supersymmetry

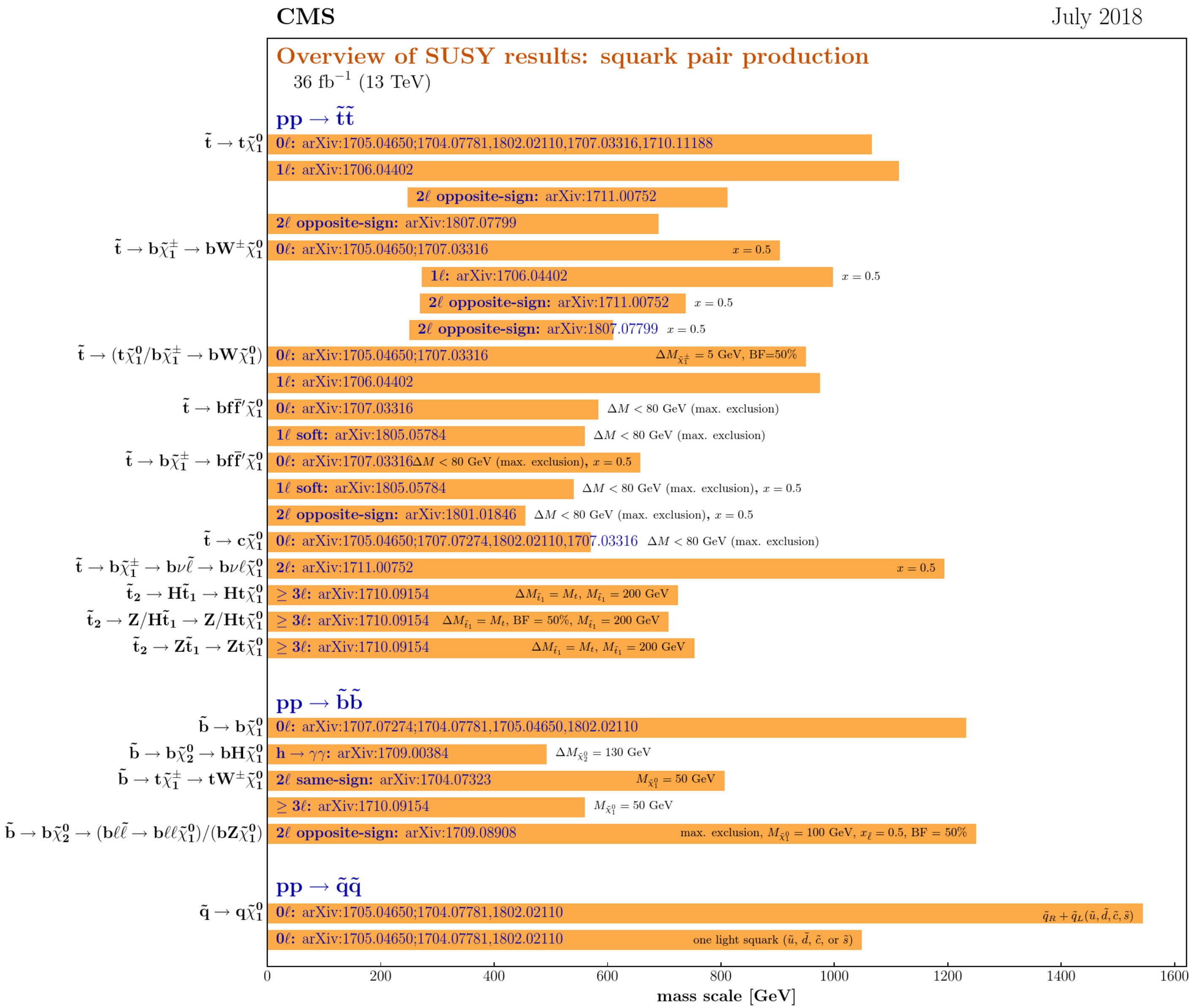

Selection of observed limits at 95% C.L. (theory uncertainties are not included). Probe **up to** the quoted mass limit for light LSPs unless stated otherwise. The quantities ΔM and x represent the absolute mass difference between the primary sparticle and the LSP, and the difference between the intermediate sparticle and the LSP relative to ΔM, respectively, unless indicated otherwise.

Constraints on Supersymmetry

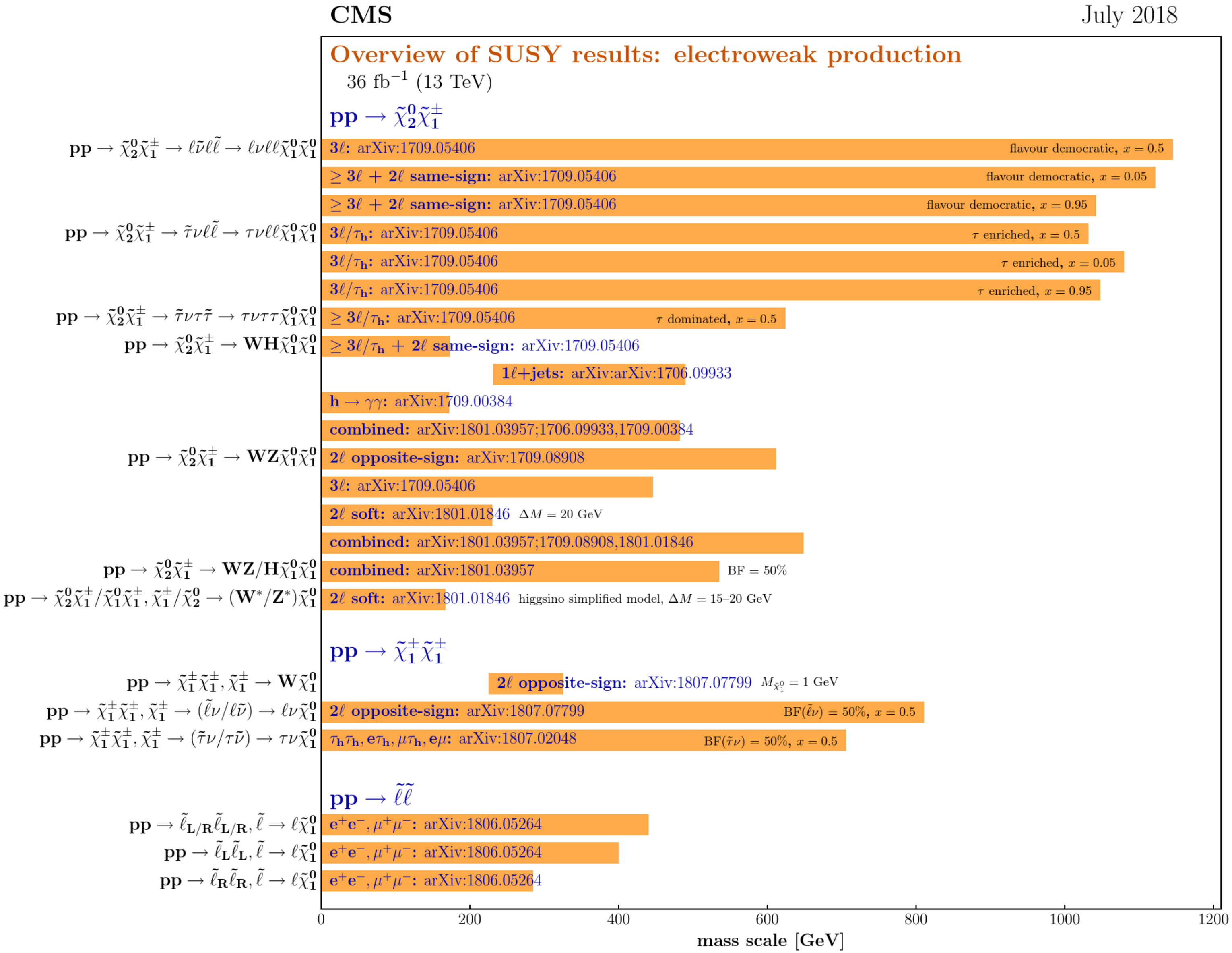

Selection of observed limits at 95% C.L. (theory uncertainties are not included). Probe **up to** the quoted mass limit for light LSPs unless stated otherwise. The quantities ΔM and x represent the absolute mass difference between the primary sparticle and the LSP, and the difference between the intermediate sparticle and the LSP relative to ΔM, respectively, unless indicated otherwise.

Higgs in invisible (ATLAS)

ATLAS-CONF-2018-054

- ★ Search for dark matter in Higgs decays
  - ➡ Signatures: E_T^{miss} plus leptons and/or jets
  - ➡ Several channels used in the combination
    - VBF H(inv)
    - Z(ℓℓ)H(inv)
    - V(had)H(inv)

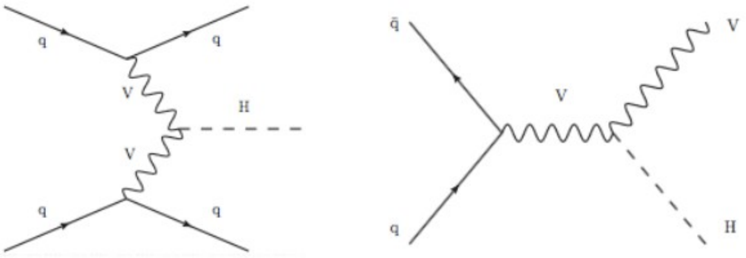

- ★ Run 1+ Run 2 observed (expected) limit: $\mathcal{B}_{H\to\text{inv}} < 0.26\ (0.17^{+0.07}_{-0.05})$ at 95% CL

Patricia Conde Muíño

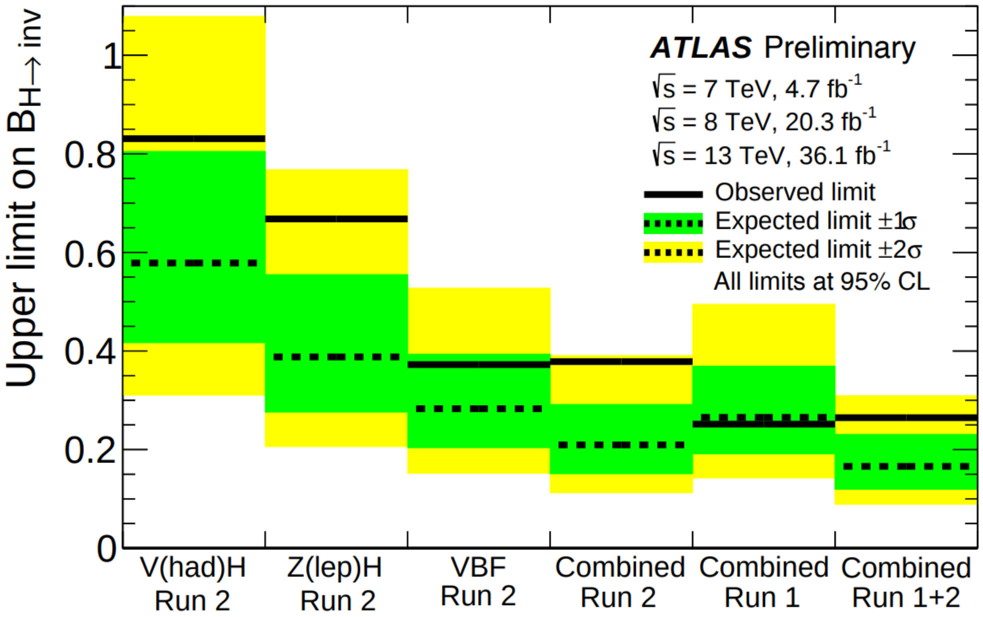

Two Higgs doublet model

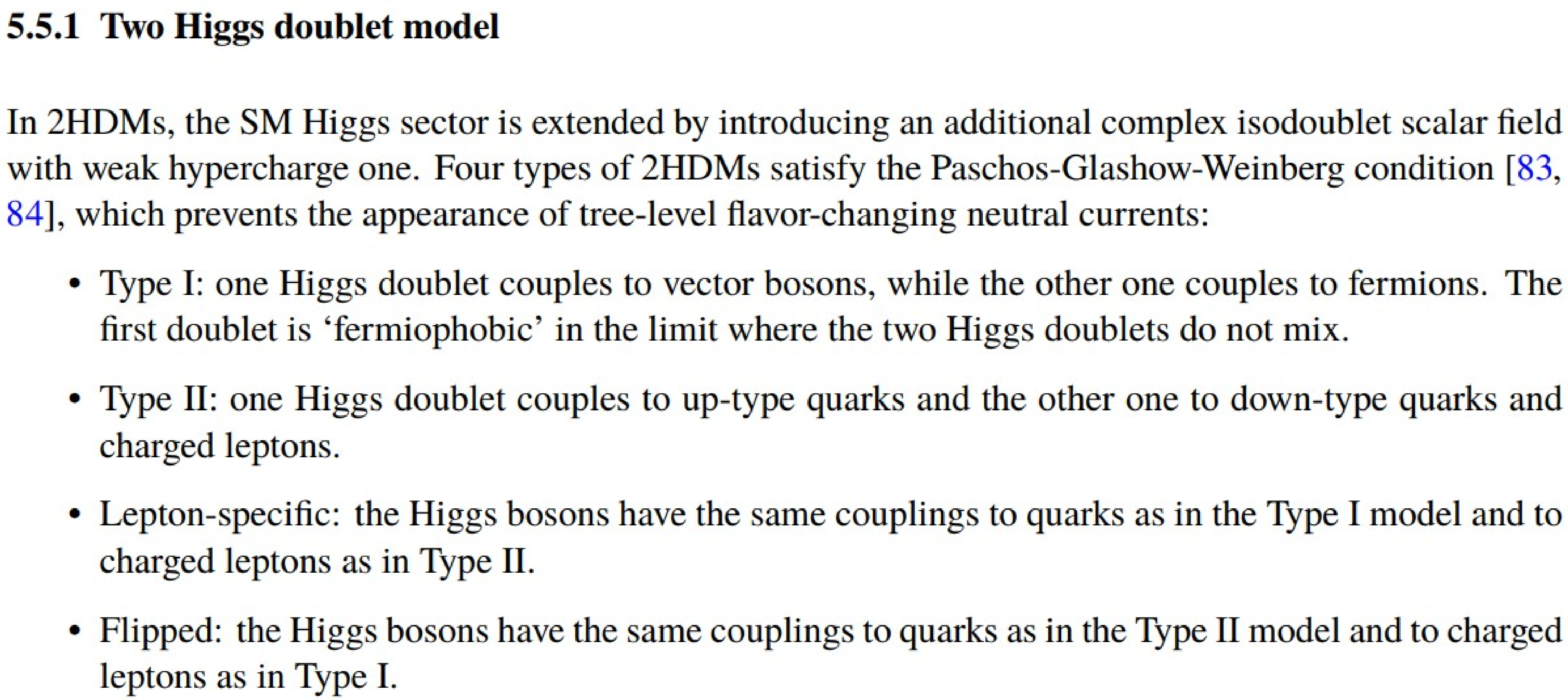

5.5.1 Two Higgs doublet model

In 2HDMs, the SM Higgs sector is extended by introducing an additional complex isodoublet scalar field with weak hypercharge one. Four types of 2HDMs satisfy the Paschos-Glashow-Weinberg condition [83, 84], which prevents the appearance of tree-level flavor-changing neutral currents:

- Type I: one Higgs doublet couples to vector bosons, while the other one couples to fermions. The first doublet is 'fermiophobic' in the limit where the two Higgs doublets do not mix.
- Type II: one Higgs doublet couples to up-type quarks and the other one to down-type quarks and charged leptons.
- Lepton-specific: the Higgs bosons have the same couplings to quarks as in the Type I model and to charged leptons as in Type II.
- Flipped: the Higgs bosons have the same couplings to quarks as in the Type II model and to charged leptons as in Type I.

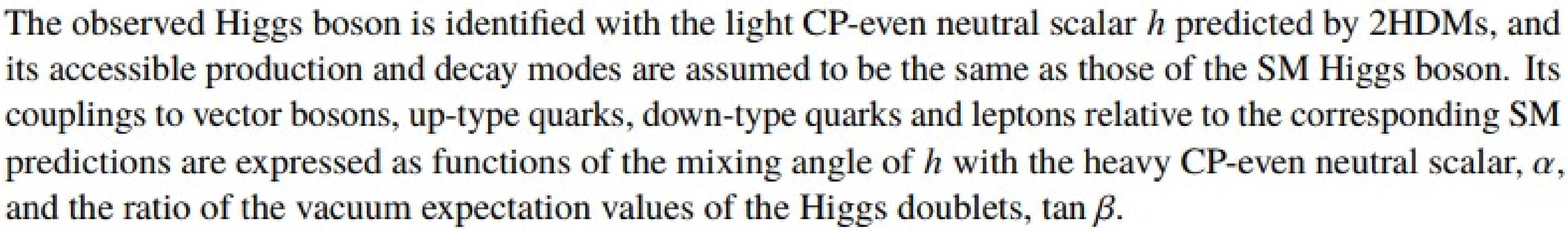

The observed Higgs boson is identified with the light CP-even neutral scalar h predicted by 2HDMs, and its accessible production and decay modes are assumed to be the same as those of the SM Higgs boson. Its couplings to vector bosons, up-type quarks, down-type quarks and leptons relative to the corresponding SM predictions are expressed as functions of the mixing angle of h with the heavy CP-even neutral scalar, α, and the ratio of the vacuum expectation values of the Higgs doublets, $\tan\beta$.

Constraints on new phenomena

- The combined results are interpreted in the context of two-Higgs doublet models and the hMSSM
- No significant deviations from the Standard Model predictions are observed
- Constraints are set in the (cos(β – α), tan β) plane in 2HDM Type-I, Type-II, Lepton-specific and Flipped models

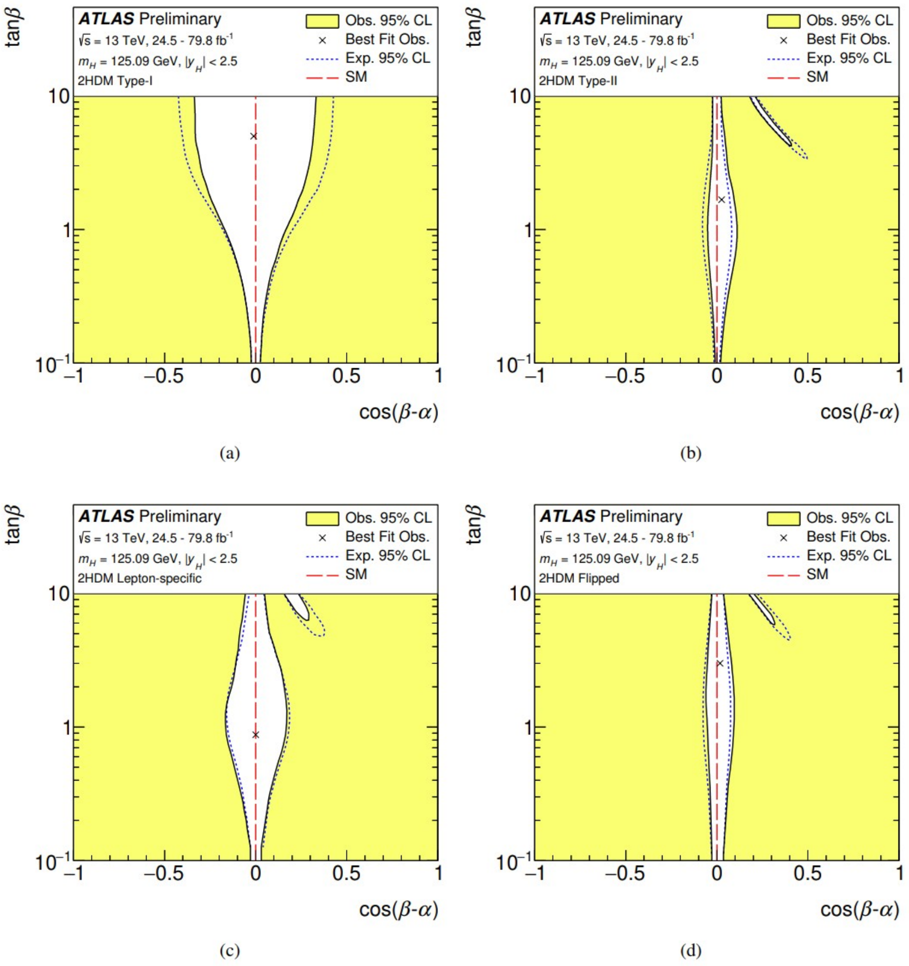

(a) (b)

(c) (d)

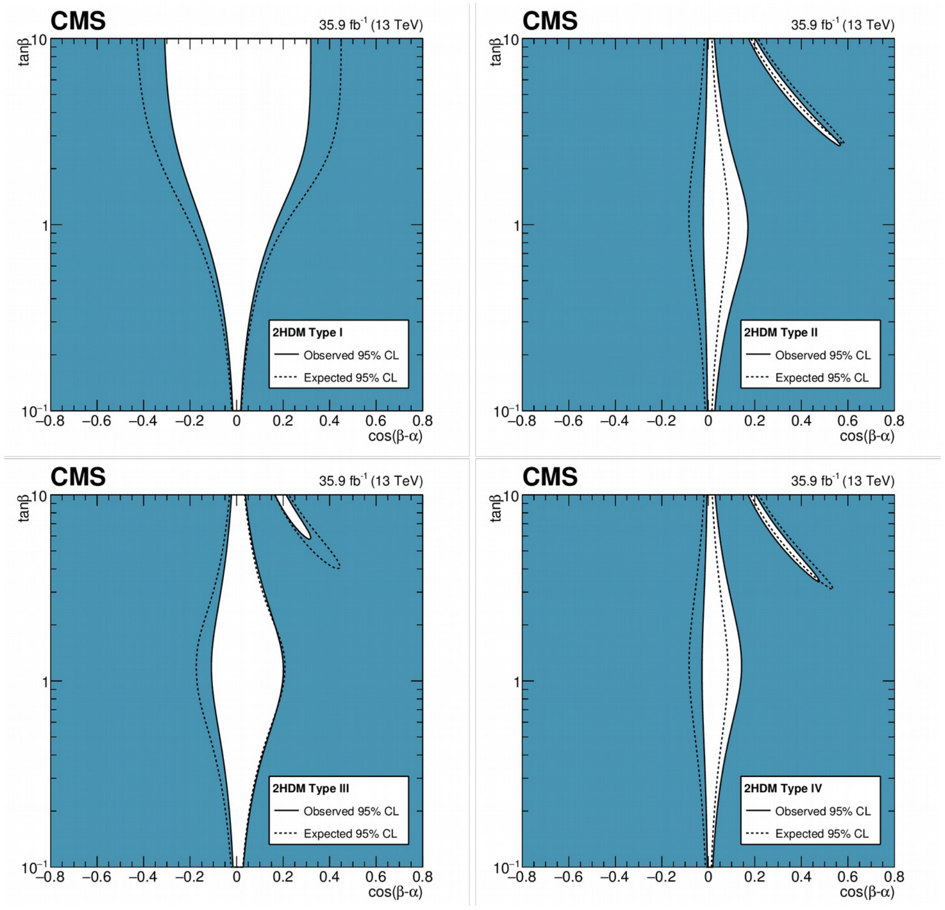

Constraints on new phenomena

- The combined results are interpreted in the context of two-Higgs doublet models and the hMSSM
- No significant deviations from the Standard Model predictions are observed
- Constraints are set in the (mA,tan β) plane of the hMSSM

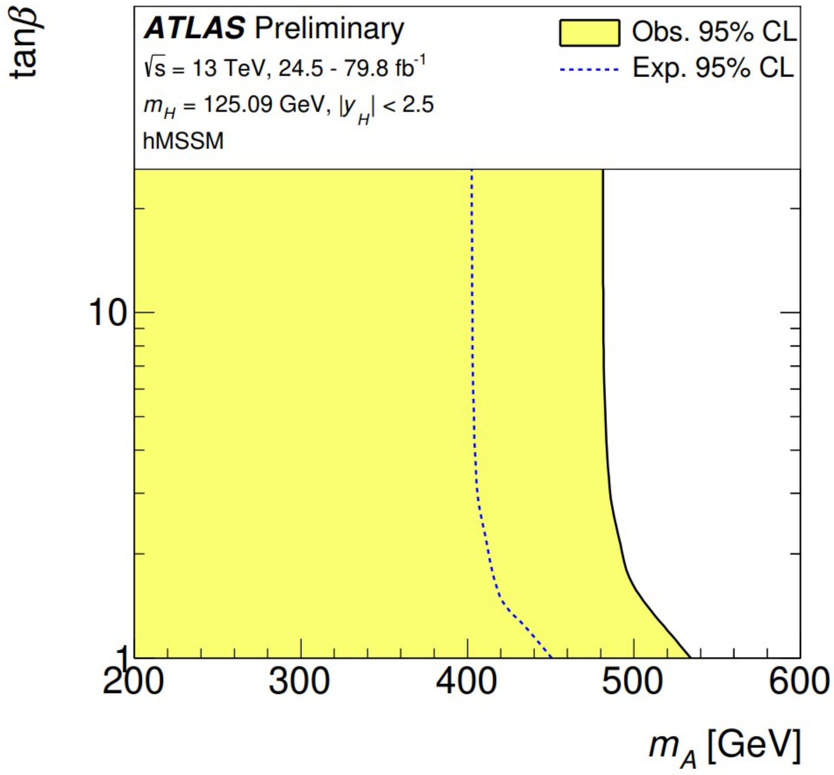

ATLAS

Regions up to 530 GeV in mA and tan β
in the hMSSM excluded

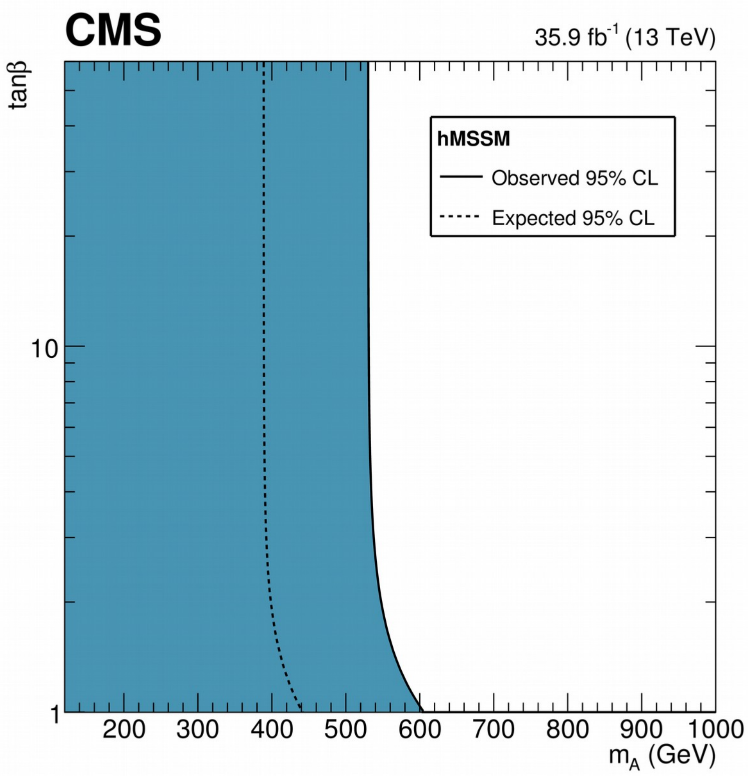

CMS

Regions up to 600 GeV in mA and tan β
in the hMSSM excluded

BSM Higgs

ATLAS

H+ → tau nu (HIGG-2016-11)	https://link.springer.com/article/10.1007/JHEP09(2018)139
H+ → tb (HIGG-2017-04)	https://link.springer.com/article/10.1007/JHEP11(2018)085
H++ → W+W+ (HIGG-2016-09)	https://link.springer.com/article/10.1140/epjc/s10052-018-6500-y
H++ → multilepton (EXOT-2016-07)	https://link.springer.com/article/10.1140%2Fepjc%2Fs10052-018-5661-z
H+ → WZ (EXOT-2016-11)	https://www.sciencedirect.com/science/article/pii/S0370269318307901?via=ihub

CMS

H+ → tau nu (HIGG-2016-11)	https://cds.cern.ch/record/2640359
H+ → tb lep. (HIG-18-004)	https://cds.cern.ch/record/2667222
H+ → WA (HIG-18-020)	https://cds.cern.ch/record/2667217
H++ → W+W+ leptonic (SMP-17-004)	https://arxiv.org/abs/1709.05822
H+ → WZ leptonic (SMP-18-001)	https://arxiv.org/abs/1901.04060
H+ → WV semi-leptonic boosted (SMP-18-006)	http://cds.cern.ch/record/2665482

BSM Higgs

H+ → tb leptonic: results

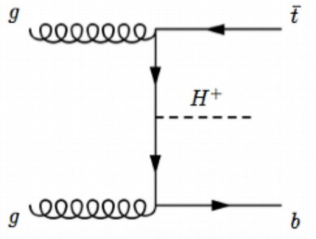

No excess observed in all categories → 95% CL upper limits set on charged Higgs production cross sections times branching ratio

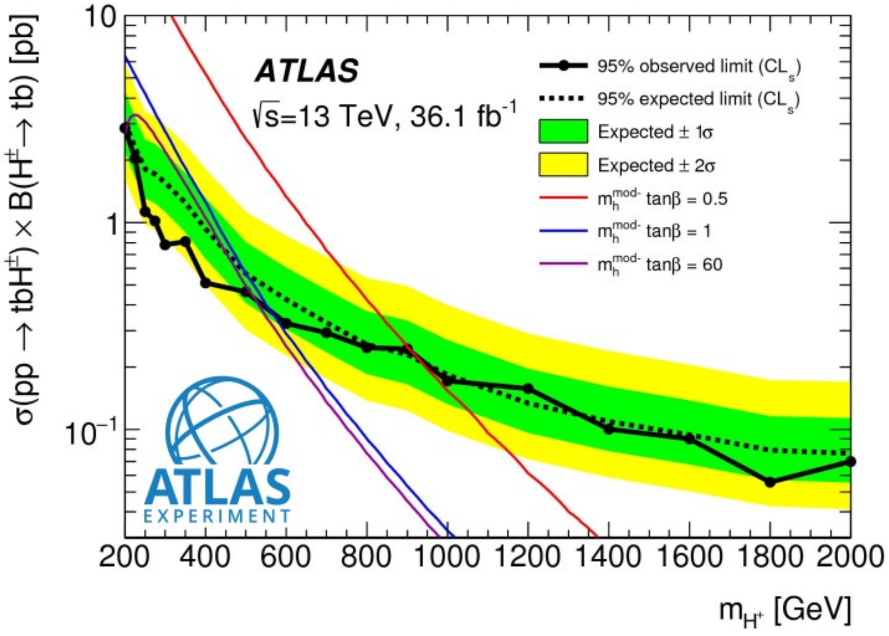

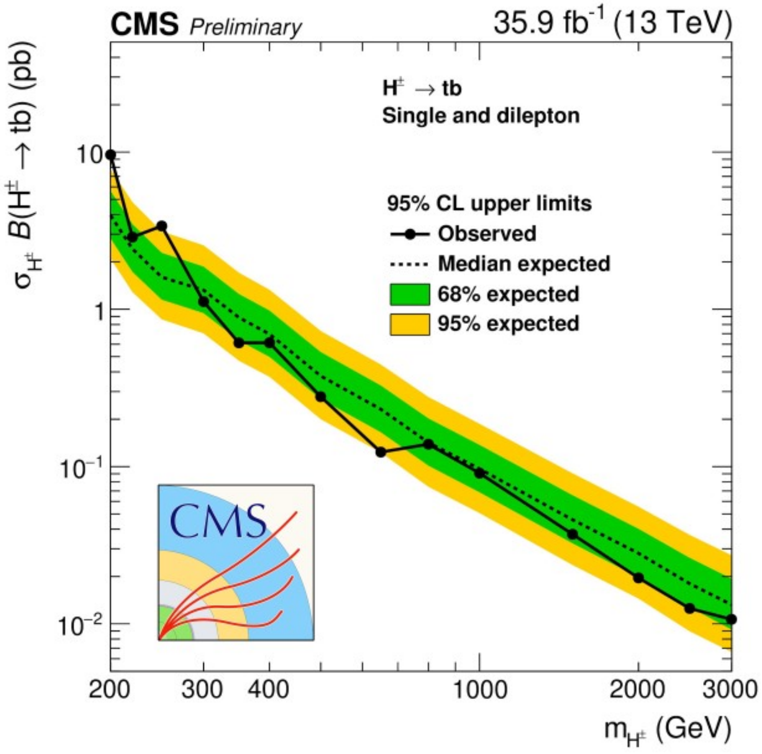

Jan Eysermans at LHCP 2019

BSM Higgs

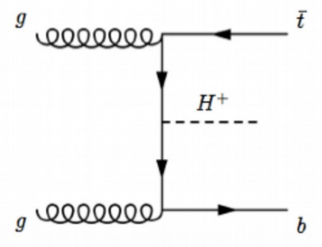

H+ ⟶ τν: results

No excess observed in all categories → 95% CL upper limits set on charged Higgs production cross sections times branching ratio

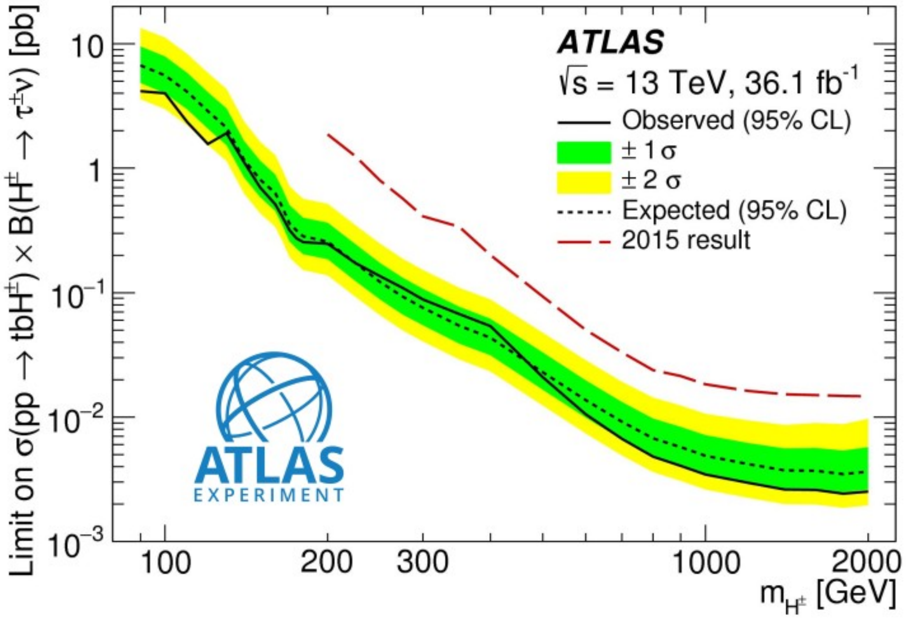

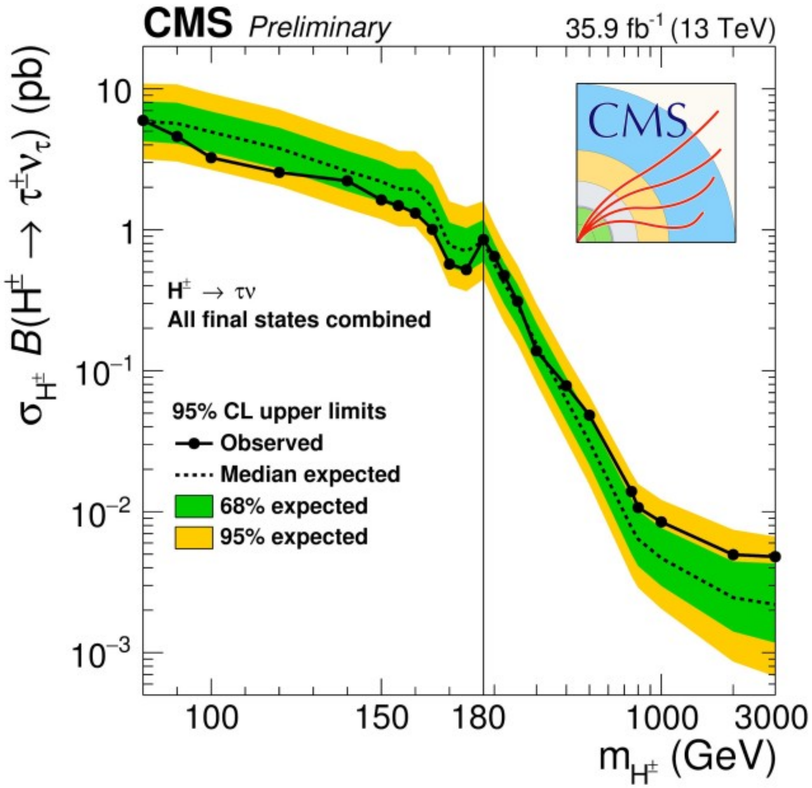

Jan Eysermans at LHCP 2019

ATLAS Higgs combination

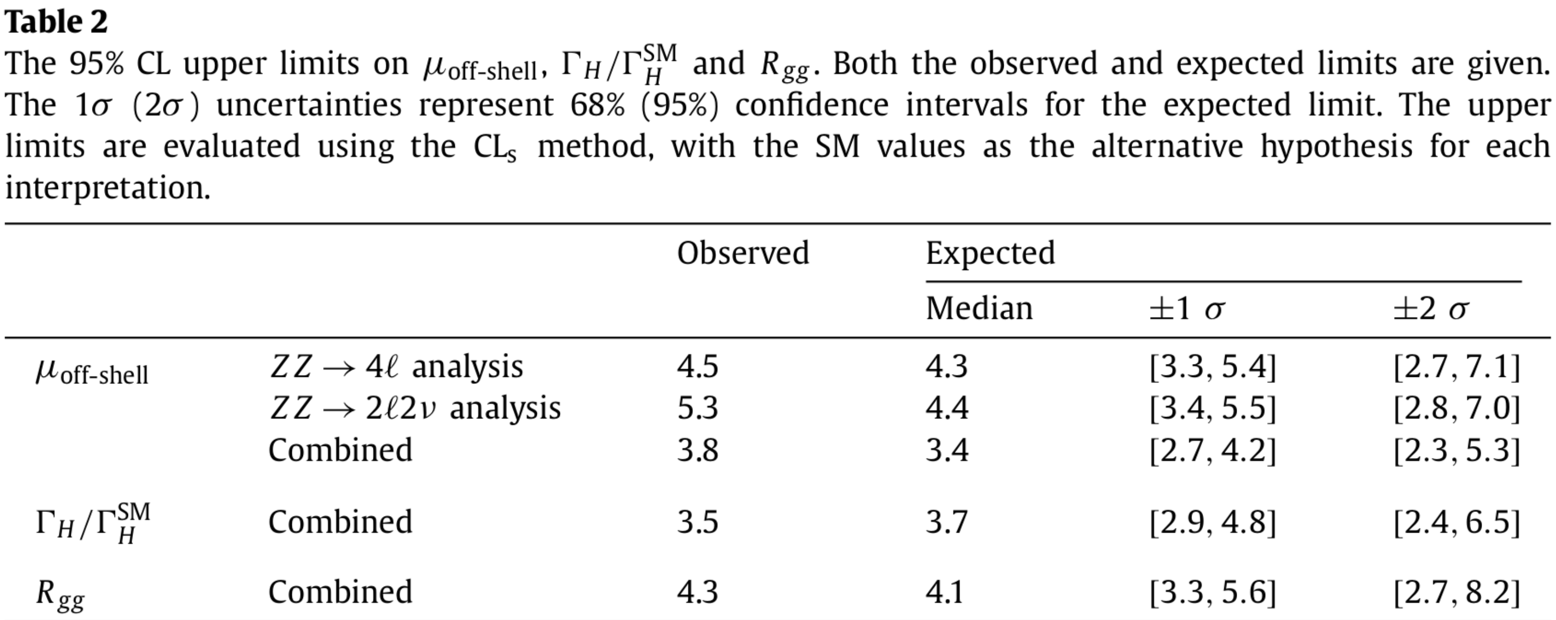

Table 2

The 95% CL upper limits on $\mu_{\text{off-shell}}$, $\Gamma_H/\Gamma_H^{\text{SM}}$ and R_{gg}. Both the observed and expected limits are given. The 1σ (2σ) uncertainties represent 68% (95%) confidence intervals for the expected limit. The upper limits are evaluated using the CL_s method, with the SM values as the alternative hypothesis for each interpretation.

		Observed	Expected		
			Median	$\pm 1\ \sigma$	$\pm 2\ \sigma$
$\mu_{\text{off-shell}}$	$ZZ \to 4\ell$ analysis	4.5	4.3	[3.3, 5.4]	[2.7, 7.1]
	$ZZ \to 2\ell 2\nu$ analysis	5.3	4.4	[3.4, 5.5]	[2.8, 7.0]
	Combined	3.8	3.4	[2.7, 4.2]	[2.3, 5.3]
$\Gamma_H/\Gamma_H^{\text{SM}}$	Combined	3.5	3.7	[2.9, 4.8]	[2.4, 6.5]
R_{gg}	Combined	4.3	4.1	[3.3, 5.6]	[2.7, 8.2]

$$\downarrow$$

$$R_{gg} = \mu^{\text{ggF}}_{\text{off-shell}}/\mu^{\text{ggF}}_{\text{on-shell}}$$

Constraint of κ_λ from single Higgs measurements

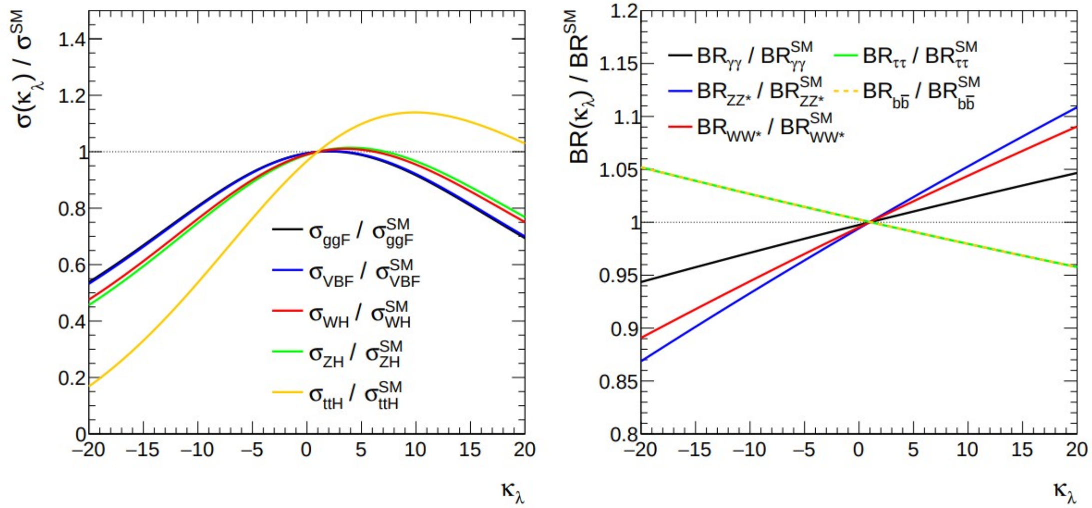

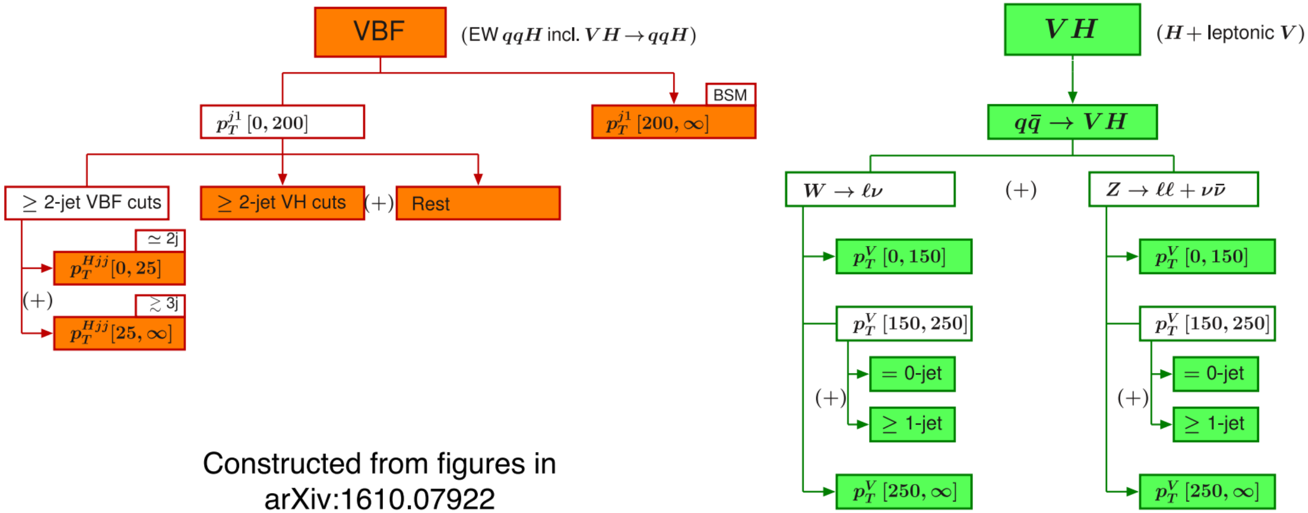

Constructed from figures in
arXiv:1610.07922

Figure 3: Schematic diagram of the $VBF + V(\text{had})H$ (left) and $V(\text{lep})H$ (right) STXS regions. p_T^{Hjj} is the p_T of the Higgs boson plus two jets system, p_T^V is the p_T of the vector boson V in the VH production mode, p_T^{j1} is the p_T of the jet with the highest p_T. In the VH, $H \to b\bar{b}$ analysis, the separation in jet number of the p_T^V [150, 250] region in the VH production mode has been ignored, merging the 0 and the ≥ 1 jet regions. The diagrams are obtained from Ref. [14].

Di-Higgs cross-section

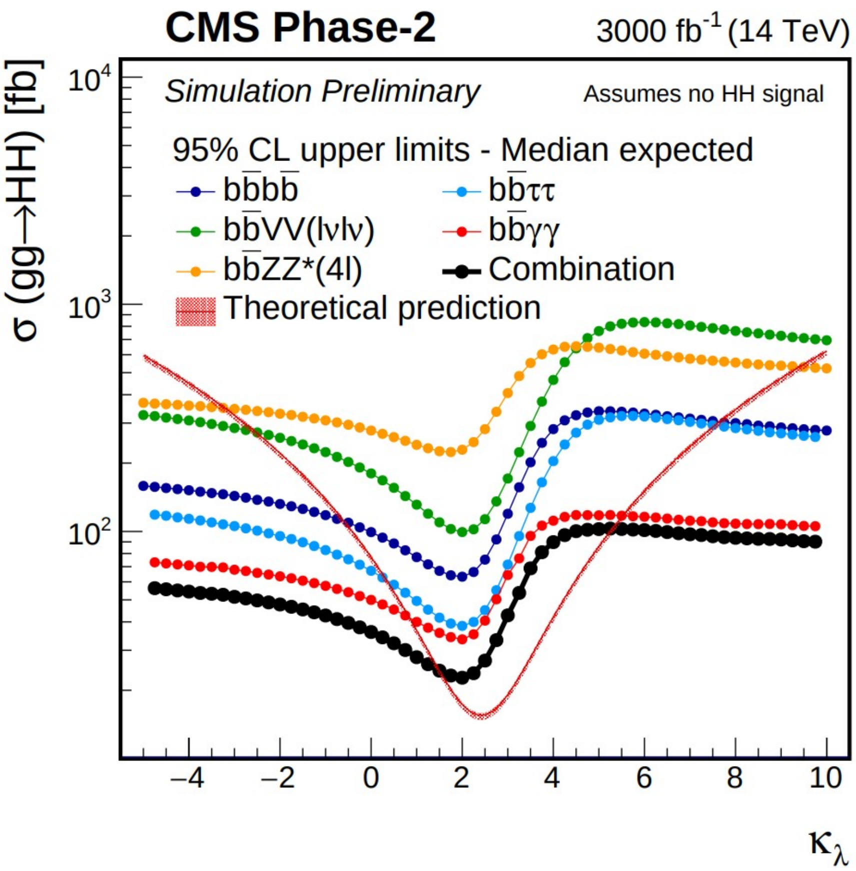

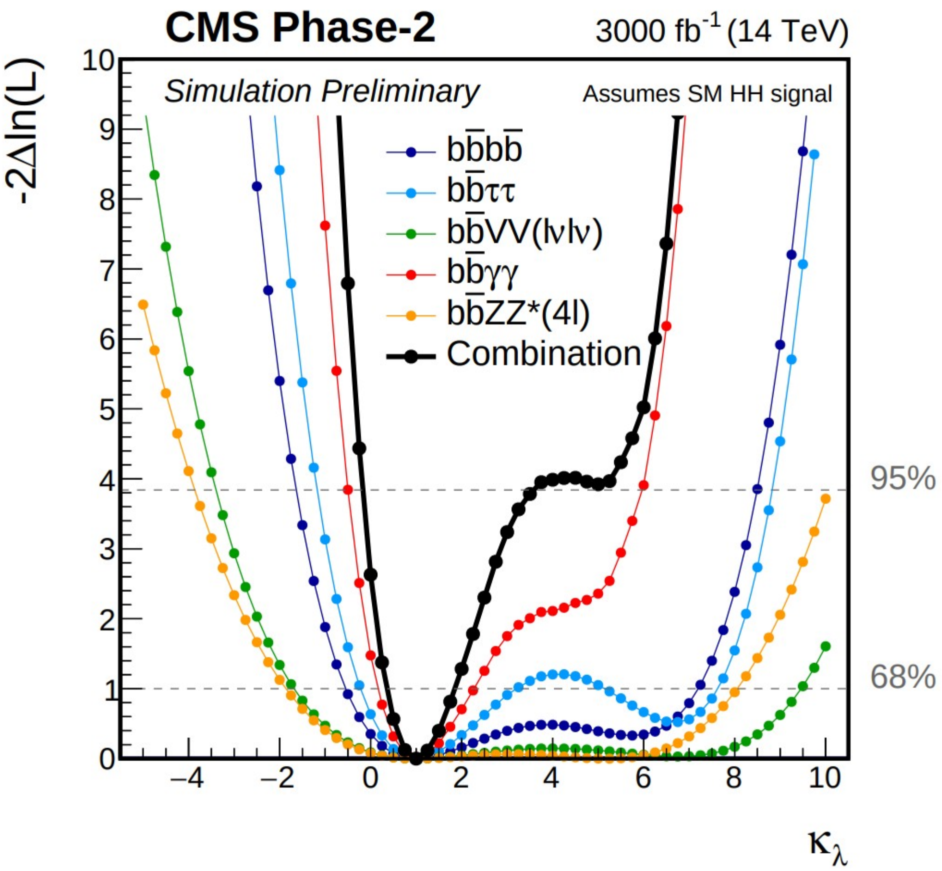

Coupling modifiers: “kappa”

$$\boxed{\sigma \cdot B(i \to H \to f) = \frac{\sigma_i \cdot \Gamma_f}{\Gamma_H} = \frac{\sigma_i^{SM} \cdot \Gamma_f^{SM}}{\Gamma_H^{SM}} \cdot \left(\frac{\kappa_i^2 \kappa_f^2}{\kappa_H^2}\right)}$$

$$\kappa_i^2 = \frac{\sigma_i}{\sigma_i^{SM}} \qquad \kappa_f^2 = \frac{\Gamma_f}{\Gamma_f^{SM}} \qquad \kappa_H^2 = \frac{\sum \Gamma_f}{\sum \Gamma_f^{SM}}$$

Production **Decay** **Total width**

- Not “physical parameters”
- Introduced to parameterize possible deviation from SM